The Thesis Committee for Jeremy Scott Slaugenwhite
Certifies that this is the approved version of the following thesis:

Mass Transport Deposit and Turbidite Interaction in the Mio-Pliocene Gulf of California: Fish Creek-Vallecito Basin, Salton Trough

APPROVED BY
SUPERVISING COMMITTEE:

Supervisor:

Ronald Steel

David Mohrig

Cornel Olariu

Mass Transport Deposit and Turbidite Interaction in the Mio-Pliocene Gulf of California: Fish Creek-Vallecito Basin, Salton Trough

by

Jeremy Scott Slaugenwhite, B.S.

Thesis

Presented to the Faculty of the Graduate School of

The University of Texas at Austin

in Partial Fulfillment

of the Requirements

for the Degree of

Master of Science in Geological Sciences

The University of Texas at Austin

May 2015

Dedication

To my wonderful wife and children. Thank you for your patience and unwavering support.

Acknowledgements

Many thanks to Sarah Bateman, David Conwell, Anthony McGlown, Michael Cloos, and Michelle Gevedon for all of your help in the field. Thank you David Mohrig, Whitney Behr, and Mark Cloos. I could not have completed this work without your assistance, comments, and suggestions. Thank you Cornel Olariu for all of your mentorship.

And thank you Ron Steel. I could not have chosen a better advisor.

Abstract

Mass Transport Deposit and Turbidite Interaction in the Mio-Pliocene Gulf of California: Fish Creek-Vallecito Basin, Salton Trough

Jeremy Scott Slaugenwhite, M.S. Geo. Sci.

The University of Texas at Austin, 2015

Supervisor: Ronald Steel

Mass transport deposits represent a significant component of modern and ancient deep-water depositional systems. However, geophysical data lack the resolution needed to identify meso-scale (meters to tens of meters) interactions between mass transport deposits and the underlying and overlying sediment. An exposed section of supra-detachment rift basin sedimentary deposits containing subaerial and subaqueous debris flows and coarse-grained turbidites provides an opportunity to examine both the variability related to debris flow emplacement and the unique type of debris flow known as a sturzstrom.

The Fish Creek – Vallecito Basin, part of the larger Salton Trough region of southern California, contains a late Miocene to Pliocene stratigraphic section that records the opening of the rift basin, marine flooding by the Gulf of California, and the arrival of the Colorado River. The lower Split Mountain Group debris flow (up to 50 m thick) was deposited subaerially and was extensive enough to partially cover the previously deposited alluvial fans. At this time it is likely that the subaerial basin floor had subsided

below sea-level, much like the floor of the Salton Sea today. Breaching of the basin walls then led to a rapid marine incursion into an already deep basin, such that the lower debris flow was immediately and conformably overlain by gypsum, mudstones, and coarse-grained Lycium member turbidites of the Imperial Group. A second major debris flow (up to 45 m thick), this one a subaqueous flow, severely deformed, scoured, and truncated the underlying Lycium member turbidites, and profoundly impacted the routing and deposition of the overlying Wind Caves member turbidites that signal the arrival to the basin of the Colorado River. Each of the turbidite successions thus follows an event of catastrophic mass transport.

This thesis describes and documents the variable meso-scale erosion of the underlying turbidite deposits by the younger debris flow, the impact of variable upper debris flow surface bathymetry on subsequent turbidite deposition and connectivity, and links these findings to observations made by other workers studying similar deep-water deposits in outcrop and in seismic-reflection data. Building on the efforts of previous workers, this thesis also describes the characteristics of the subaerial lower and subaqueous upper sturzstroms, investigates emplacement mechanism implications of micro-scale features, and provides the first paleogeographic reconstruction of the basin during the time of subaerial to marine transition and the arrival of the Colorado River into the region.

Table of Contents

List of Figures

Introduction

SALTON TROUGH AND FISH CREEK – VALLECITO BASIN

The Salton Trough, the northern-most part of the Gulf of California rift basin, is a half-graben formed as a result of middle Miocene (~12 to 14 Ma) regional crustal extension, crustal thinning, and sedimentation. Focused extension in a long, straight zone that paralleled the existing Miocene continental margin created a single rift basin and led to the detachment of Baja California from North America and the development of the Gulf of California (Winker and Kidwell, 1996; Abbott et al., 2002; Dorsey et al., 2011). Unlike the southern expression of the rift basin, the Gulf of California, the present-day Salton Trough is a sub-sea-level non-marine depression bounded by the Peninsular Ranges to the west and the Mojave Desert ranges to the east. The Colorado delta plain to the south cuts the basin off from the rest of the Gulf of California (Winker, 1987). Tectonically the fault-bounded Salton Trough is separated from the Peninsular Ranges by the Elsinore, San Felipe, and San Jacinto faults, and from the Mojave Desert ranges by the San Andreas Fault (Dorsey et al., 2011).

Miocene extension and subsidence, controlled by the San Andreas Fault to the east and the now-inactive West Salton detachment fault to the west, and potentially numerous smaller synthetic normal faults in-between, created a paleotopography of small, tilted blocks and linked basins separated by some uplifted and tilted Cretaceous plutons and associated metamorphic rocks (Abbott et al., 2002; Dorsey et al., 2007). Progressive marine inundation from the south began ~13 Ma, and likely reached the northernmost part of the Salton Trough at San Gorgonio Pass by 6.5 Ma (Winker and Kidwell, 1996). The arrival of the Colorado River 5.3 Ma (Dorsey et al., 2007) triggered the building of a large delta that dominated sedimentation through to the present day, and

created the barrier that separates the non-marine Salton Trough from the rest of the marine Gulf of California.

The Fish Creek – Vallecito Basin (Fig. 1), located within Anza-Borrego Desert State Park in the Colorado Desert of southern California, is one such small supra-detachment basin created by the paleotopography related to extension of the western Salton Trough. Here a 5.5-km-thick package of late Miocene to early Pleistocene sediment was deposited on the hanging wall of the oblique, dextral-normal West Salton detachment fault (Kerr, 1984; Winker, 1987; Kerr and Kidwell, 1991; Winker and Kidwell, 1996; Abbott et al., 2002; Dorsey et al., 2007, 2011). Early subaerial rift-related coarse clastic sedimentation gave way to marine sedimentation as marine water abruptly entered the basin ~6.3 Ma (Dorsey et al., 2011). Soon after, the first evidence of Colorado River-derived sands appears in the basin, and the remaining basin history is controlled by the development and progradation of the Colorado River delta and its associated deepwater slope and basin floor sediments.

A transition from extension to dextral strike-slip tectonics beginning 1.1 to 1.3 Ma resulted in transpressive deformation, uplift, and erosion that has exposed more than 20 m.y. of Miocene to Pleistocene depositional history (Winker, 1987; Dorsey et al., 2011). Dextral strike-slip movement along the San Andreas fault has also translated the Salton Trough sediments to the northwest relative to North America over the past ~1 Ma (Dorsey et al., 2011). As a result, the now-exposed strata in the Fish Creek – Vallecito Basin is a high-resolution record of the basin's entire history: from the subaerial deposition of thick alluvial fans linked to tectonic extension and basin subsidence, to catastrophic basin wall failure, debris flow deposition, and sudden marine water incursion, and finally to the progradation of a delta built by the Colorado River.

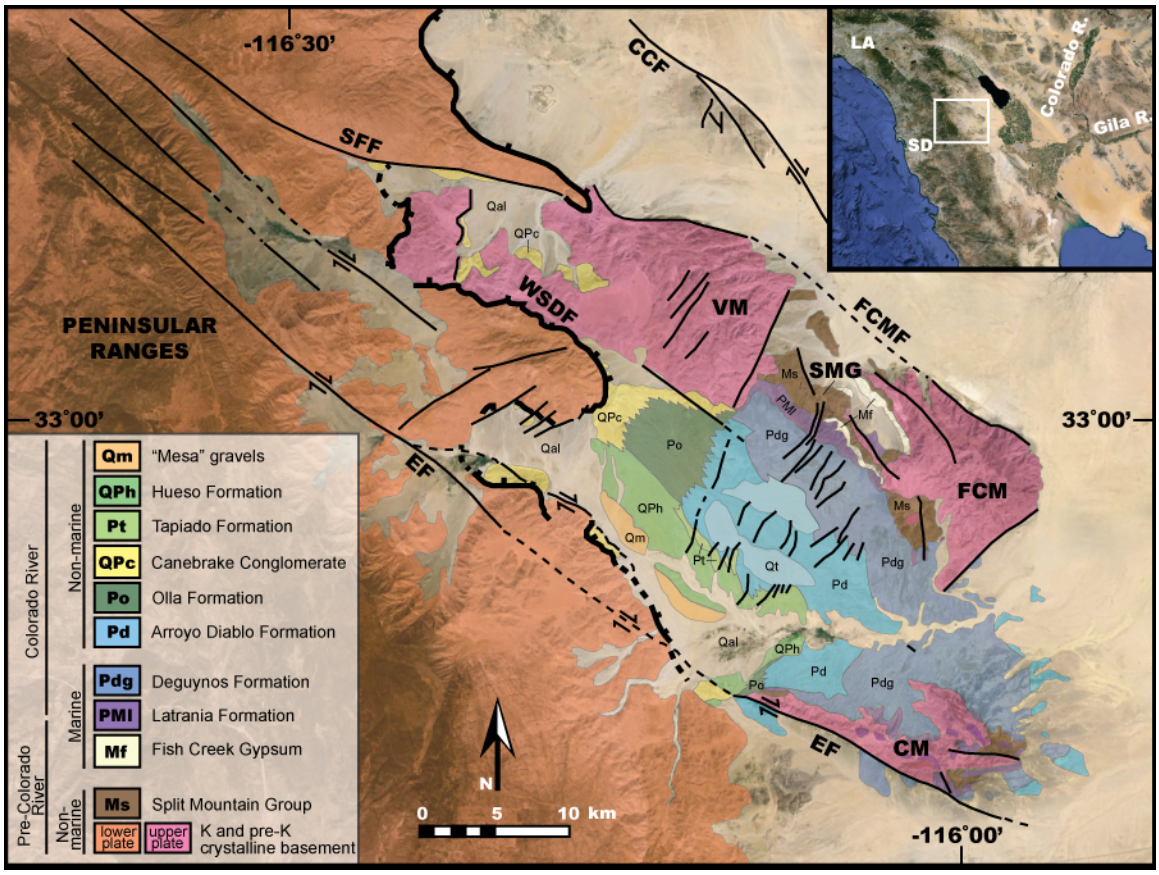

Figure 1. Geologic map of the Fish Creek – Vallecito Basin in southern California. Modified from Winker (1986) and Dorsey et al. (2007).

Of particular interest within the Fish Creek – Vallecito Basin stratigraphy are the deposits that bracket the sudden incursion of marine water into the basin. Much of the early history of the basin is dominated by the deposition of a ~400 m thick alluvial fan succession that records the onset and dominance of regional extension. Resting conformably on the alluvial fans is a ~45 m thick megabreccia debris flow deposit that marks the transition between subaerial and subaqueous deposition and emphasizes growing topography, subsidence outpacing sediment infilling, and the creation of a relatively deepwater sub-basin in this area. A pure layer of marine gypsum was initially and rapidly deposited on top of the megabreccia and in places directly on the alluvial

fans, before giving way to a thick and spectacular succession of locally fed, coarse-grained turbidites. The unstable alluvial slopes and basin walls would collapse a second time to form a fast, far travelling subaqueous debris flow that again is closely related in space and time to the last major step in the basin's evolution – the arrival of the Colorado river.

The megabreccia debris flows combined with the abundant lateral and vertical facies changes seen in deposits during this phase of the basin's history are evidence for unstable slopes and variable paleotopography that influenced turbidite deposition in this tectonically active extensional rift basin. The exposed rocks in the Fish Creek – Vallecito Basin provide an opportunity to investigate on a meso-scale the complex interactions between debris flows and underlying and overlying turbidites, the main subject of this thesis. The basin also allows for a detailed investigation of a unique type of megabreccia debris flow or rock avalanche, the sturzstrom.

STURZSTROMS

Geologist Albert Heim investigated the aftermath of a singularly devastating 1881 rock avalanche in Elm, Switzerland that buried the village and took 115 lives. Ten million cubic meters of crushed slate dropped 600 m, and then flowed 2.23 km as a dry mass moving at an estimated speed of 180 km/hr. An eyewitness reported that the dry mass flowed like a torrential flood, or a boiling stew. Upon inspection, Heim noted that the debris flow still showed some of the original mountainside stratigraphy, and, like a jigsaw puzzle, the broken pieces might be put back together. Heim called this unique rock avalanche deposit a sturzstrom – German for "fall stream" (Shreve, 1968; Hsü, 1975; Abbott, 1996). In his review of rockfall-generated debris flows, Hsü (1975) proposed that

the term sturzstrom be adopted and defined as "as a stream of very rapidly moving debris derived from the disintegration of a fallen rock mass of very large size; the speed of a sturzstrom often exceeds 100 km/hr, and its volume is commonly greater than $1x10^6$ m^3."

Characteristics

Since Heim's work at Elm, numerous other deposits that share a distinct set of characteristics have been identified in the modern and ancient rock record (Shreve, 1968; Hsü, 1975; Kerr, 1984; Cruden and Hungr, 1986; Winker, 1987; Kerr and Abbott, 1996; Hewitt, 1999; Abbott et al., 2002; Wassmer et al., 2004). Each begin as a large (> $1x10^6$ m^3) mass of falling rock that, after reaching the more gentle slopes below their scarp and source area, flow at high speed and travel greater distances than would be predicted for other types of landslides or debris flows.

Sturzstroms are unsorted and unstratified breccia of angular grains ranging in size from silt to boulders (Fig. 2), and have been reported to show both normal and inverse grading among the finest fraction of matrix. It is common, however, for the largest clasts to gradually increase in size with height above the sturzstrom base, but abruptly coarsen at the top of the flow as the largest shattered boulders often armor the surface of the deposit. Sturzstroms can be matrix-supported and/or grain-supported, and a switch between the two can occur vertically within the same deposit. The debris provenance is from local bedrock, and the composition at a single sample site is often monolithologic. Sturzstroms often are marked by compositional zoning, where the matrix is closely related to the clasts it surrounds (Fig. 2 B). The clasts and associated matrix often form the jigsaw-puzzle fabric reported by Heim.

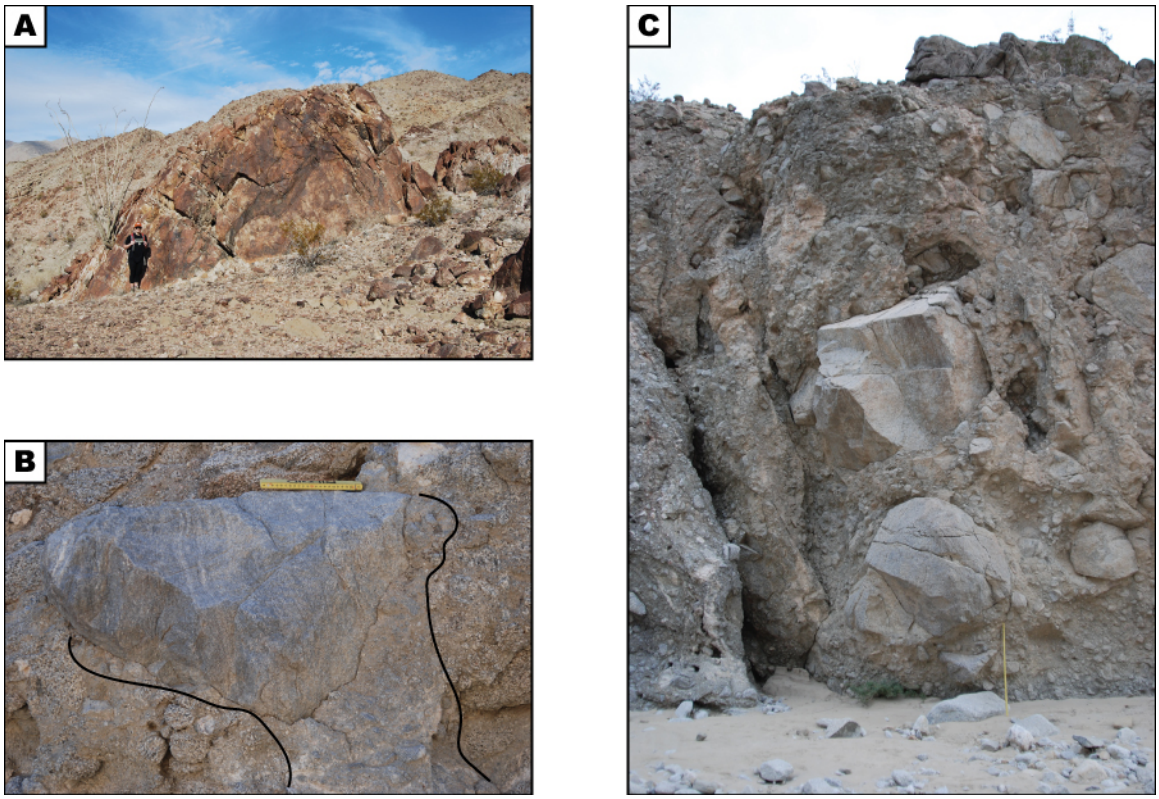

Figure 2. Fish Creek – Vallecito Basin sturzstroms. (A) Large clast at top of upper megabreccia west of Oyster Shell Canyon #1. (B) Boulder clast and compositional zoning in matrix, lower megabreccia in east wall of Split Mountain Gorge. (C) Lower megabreccia in east wall of Split Mountain Gorge.

Hsu (1975) noted that the outer geometry and internal structure of sturzstroms are similar to those of lava flows or glaciers. Sheet-like, lobate deposit morphology is common, and aerial extents are rarely less than 2 km^2 and can exceed 40 km^2. Often there is evidence that the flow was able to run-up on opposing slopes or over high ground and irregular topography. Where a sturzstrom was not able to overtop an obstacle, the flow often thickens against impact slopes. Many sturzstroms terminate in moraine-like ridges along the edges of the deposit, often with parallel subsidiary ridges toward the axis of the deposit. A hummocky top surface is common, often due to the presence of transverse

corrugations or ridges that run perpendicular to the axis of the slide on top of the deposit. The transverse ridges may curve on either side of the deposit axis to meet the lateral moraine-like ridges tangentially. The distal edge of a sturzstrom may display a low rim and steep scarp, with evidence that the lower portion of the fallen rock mass has become the distal end of the deposit. As evidenced by the two megabreccia debris flows found in the Fish Creek – Vallecito Basin, sturzstroms can be deposited subaerially and subaqueously.

Emplacement Mechanism

The emplacement mechanism which can explain the set of flow observations and deposit features, chiefly to resolve why sturzstroms have a much longer run-out and a much lower coefficient of friction than what should be expected, is still a matter of debate. Legros (2002) conducted a review of hypotheses proposed to explain the mobility of long-runout landslides. Many theories involve fluidizing mediums such as air, water, water vapor, volcanic gasses, or a dry suspension of fine particles. Shreve (1968), in his study of the Blackhawk landslide, proposed that landslides could flow on top of a compressed air layer trapped under the flow. Other workers invoked water-saturated bases (Johnson, 1978; Voight and Sousa, 1994), or lubrication by vapor pressure created by heated water within and near the basal shear zone (Habib, 1975; Goguel, 1978; De Blasio, 2008). Hsü (1975) hypothesized that dispersive forces generated by fine, powder-sized particles alone, without the aid of a supporting fluid, could be responsible for the fluidization of large rock avalanches. Other workers have proposed granular flow models requiring no fluid medium. These include acoustic fluidization (Melosh, 1979), mechanical fluidization (Davies, 1982; Campbell et al., 1995; Straub, 2001), and passive

transport on top of a thin layer of shear-induced melting (Heuberger et al., 1984; Masch et al., 1985; Legros et al., 2000; Takagi et al., 2007; Spray, 2010; Weidinger et al., 2014).

MASS TRANSPORT DEPOSIT / TURBIDITE INTERACTIONS

In the Fish Creek – Vallecito Basin, unstable basin walls of crystalline igneous basement rock and associated metamorphics twice collapsed to form large, far travelling sturzstroms. The younger of the two, the upper megabreccia, entered marine water and was emplaced over a thick package of Lycium member turbidites. Accordingly, the basin provides an excellent location to investigate the variable interactions between Mass Transport Deposits and the overlying and underlying strata.

Mass Transport Deposits (MTD) and Mass Transport Complexes (MTC) – single-event submarine debris flows and amalgamations of debris flows at a scale recognizable in seismic data, respectively – are a significant contribution to deep-water deposition in modern and ancient basins. MTDs and MTCs, in rare cases of otherwise low supply to the margin, can represent as much as 70% of the entire slope and basin floor deposition (Wynn et al., 2000; Weimer and Shipp, 2004; Pickering and Corregidor, 2005; Moscardelli et al., 2006; Butler and McCaffrey, 2010; Mulder and Etienne, 2014; Ogata et al. 2014b). In addition to their abundance, these submarine debris flows may also significantly modify existing slope and basin bathymetry through the evacuation of the failed sediment and their erosive power during flow. Once emplaced, MTDs and MTCs create new bathymetry on their surfaces that may reorganize sediment pathways and influence subsequent sediment deposition. MTD and MTC are general terms for a variety of mass-transport related, cohesive, gravity-driven sediments that include slides, slumps, and debris flows deposits (Weimer and Shipp, 2004; Mulder and Etienne, 2014).

Following Moscardelli et al. (2006), the terms MTD and MTC in this work will be inclusive of the several varieties of gravity-induced slope and basin deposits, and will exclude turbidity current-driven turbidites.

Hydrocarbon Systems

While MTCs are not reservoir targets, they may act as important regional seals. MTCs are also a risk factor for deep-water hydrocarbon exploration and development, as they are often associated with rapid changes in porosity and permeability. Frequently occurring shallow MTCs can be significant drilling hazards and may impact field development planning (Weimer and Shipp, 2004; Moscardelli et al., 2006).

Through erosion and the bathymetric controls they place on subsequent sedimentation, MTCs may greatly influence the hydrocarbon system. They have the power to significantly erode underlying sediments leading to the truncation of reservoir and/or seal facies (Moscardelli et al., 2006). Later deposition of sandstone reservoir facies on top of irregular MTC surfaces can be impacted in several ways: (1) the sediment failure that triggered mass movement of sediment may create significant accommodation in the sediment-evacuated zone (Hackbarth and Shew, 1994; Shultz et. al., 2005; Armitage et al., 2009) that can serve as turbidity current pathways or sites of sediment accumulation; (2) the debris flow may create erosional remnants or other obstacles which redirect turbidity currents (Kastens and Shor, 1985; Pickering and Corregidor, 2005; Armitage et al., 2009); (3) irregular bathymetry may create depressions on the MTC surface that induce sediment ponding (Shor and Piper, 1989; Pickering and Corregidor, 2000; Shultz et al., 2005; Armitage et al., 2009).

Seismic data, Outcrops, and Integrated Studies

One particular challenging aspect of the study of MTCs in deep-water systems is the constraint placed on their analysis by the resolution of seismic-reflection data. The minimum resolvable vertical resolution of petroleum-industry seismic-reflection data is ~30m (Armitage et al., 2009). The lack of meso-scale resolution (meters to tens of meters) makes it impossible to recognize the majority of internal debris flow structures (Ogata et al., 2014). A lack of resolution may also prohibit thorough investigation into the myriad ways MTDs interact with substrata on multiple scales, insight into the depositional geometries and connectivity of overlying sandy reservoir facies, and the determination of whether an irregular MTD surface is a depositional feature, a product of later erosion, or some combination of the two (Armitage et al., 2009).

The study of ancient MTCs in outcrop suffers no minimum resolution issue and could therefore be used to link meso-scale field observations to the information gained in seismic studies. While outcrop examples may be smaller two-dimensional views of MTCs, and therefore less representative of the much larger debris flow deposit, they do offer the opportunity to study the internal architecture and structure of the deposits directly and in detail (Weimer and Shipp, 2004; Butler and McCaffrey, 2010; Dakin et al. 2013). As Ogata et al. (2014) notes, outcrop studies allow for multi-scale analysis at microscopic to cartographic / geophysical resolutions. Through the study of outcrop analogs to deep-water systems, deficiencies inherent in both approaches may be overcome to provide a more complete picture of how MTCs modify substrata and influence later sediment deposition.

Given the significance of MTDs and MTCs in deep-water systems, it is surprising to find relatively few investigations which attempt to integrate large-scale seismic data and meso-scale outcrop analysis (Lucente and Pini, 2003; Pickering and Corregidor,

2005; Callot et al., 2008a, 2008b; Armitage et al., 2009; Butler and McCaffrey, 2010; Festa et al., 2010a, 2010b, 2012; Ogata et al., 2012a; Ortiz-Karpf et al., 2015). The lack of an integrated approach in the study of submarine debris flows may lead to insufficient knowledge of their meso-scale features and the inability to fully recognize implications at the seismic-scale (Ogata et al., 2014).

Erosion caused by MTC Emplacement

Recent work on MTCs utilizing seismic-reflection data provides evidence that debris flows can cause significant erosion and entrainment of underlying sediment. Erosion by debris flows can be thought of to occur in two ways: (1) entrainment of non-lithified sediment, or (2) erosion of lithified substratum through plucking and/or the scouring of the substratum by clasts or blocks that are part of the debris flow (Dakin et al., 2013). This can result in tens of meters or more of erosion into the substrata.

The basal surfaces of MTCs are variable in the degree of erosion and the geometry of the surface. While some MTC basal surfaces imaged through seismic-reflection data are planar and show little evidence of erosion, many show significant erosion and the removal of up to 200 m of underlying sediment. Basal surfaces may also have a stair-step profile where, from one side of the debris flow to another, the decollement may be at different depths (Weimer and Shipp, 2004). The distal end of MTCs has also been reported to be variable. On a smooth surface they may appear to have simply frozen into place, or imbricate thrusts may form within the MTC if local bathymetry is encountered. If there is insufficient contraction of the MTC to create thrusting, lateral pressure ridges may form and be expressed at the top surface of the flow (Weimer and Shipp, 2004).

Moscardelli et al. (2006) used seismic data to document significant erosional surfaces beneath MTCs off the coast of Trinidad. These include steep erosional edges of the debris flows up to 250 m in relief, and deep linear grooves or megascours that are more than 30 m deep and are similar to those reported by other workers (McGilvery and Cook, 2003; Posamentier and Kolla, 2003; Ortiz-Karpf et al., 2015). Such megascours may be distinctive features of debris flows and may be common elements of their basal erosional surfaces (Posamentier and Kolla, 2003). The creation of these lineations has been attributed to the scraping or gouging of blocks or clasts transported by the flow (Weimer and Shipp, 2004). Where sea-floor topography acts to confine the flow, erosion of the underlying sediments may be the greatest. Differences between the axial and peripheral parts of the MTC may also be linked to flow confinement control over the degree of basal incision, the presence of syndepositional structures, and the overall deposit geometry and thickness.

Dakin et al. (2013) investigated deep-marine siliciclastic outcrop exposures in the Middle Eocene deep-marine Ainsa Basin, Spanish Pyrenees, and found that erosional channel-like features created by subaqueous debris flows were able to remove ~35m of the underlying sandy submarine-fan deposits. The debris flow deposits that fill the evacuated areas often contain disaggregated and floating sandstone turbidite blocks or rafts that may have been sourced locally from the underlying submarine-fan deposits. Ortiz-Karpf et al. (2015) report ~250m to ~500m of MTD erosion into underlying sediment, while only ~100m to –200m of the evacuated spaced is filled with the megaclast-bearing debris flow.

Accommodation created by MTC Emplacement

MTCs can, through their alteration of slope gradients and equilibrium profiles, modify available accommodation space, disrupt established sediment pathways, impact sediment storage and bypass on the slope, and influence subsequent turbidite deposit distribution and geometry at multiple scales. The upper MTC surface is often irregular, and reflects the bathymetry present after erosion and MTC emplacement. Sediments delivered to the basin are then deposited on this surface, often as channel-levee complexes, overbank deposits, sheet sands, prograding clinoforms, or hemipelagic sediments (Weimer and Shipp, 2004). Bathymetry created by MTCs significantly controls the distribution and overall architecture of overlying deposits (Moscardelli et al., 2006; Armitage et al., 2009; Mulder and Etienne, 2014).

MTCs create accommodation through the removal of sediment from their source area (collapse scar accommodation), the creation of obstacles or ridges in channels which deflect turbidites, and the creation of irregular bathymetry that allow turbidites to pond in depressions. Ponding on the irregularly shaped MTD surface can create local, lateral compartmentalization of turbidites, and at a large enough scale could serve to isolate entire depositional packages resulting in large-scale compartmentalization (Shor and Piper, 1989; Pickering and Corregidor, 2000, 2005; Armitage et al., 2009; Mulder and Etienne, 2014). The creation of accommodation space through erosion and irregular bathymetry can lead to the accumulation of coarse-grained sediments in areas typically associated with the bypass of such sediments (Olafiranye et al., 2013).

Much of the accommodation created by MTCs is a product of their irregular top surface, which is often linked to their internal structure generated during flow and emplacement. Olafiranye et al. (2013), in a study of three dimensional seismic-reflection data in offshore Angola, identified two types of depositional relief and accommodation

creation on the upper surface of MTDs: (1) tens of meters of relief created by the buckling of the upper MTD surface during emplacement, and (2) up to several hundreds of meters of relief created by protruding megaclasts on the MTD upper surface. This relief can persists for several kilometers along strike and results in the creation of mini-basins that greatly impact the thickness of overlying deposits. Moscardelli et al. (2006) show in their seismic study of MTCs on the deep-marine margin of eastern offshore Trinidad that the thickness of an overlying turbidite levee-channel system is greatest along the axial trace of the underlying MTC, and attribute this to excess accommodation space in the erosive channel left underfilled by the MTC during flow, erosion, and deposition.

MTCs can also significantly alter established sediment pathways on the slope and basin floor. Through the incomplete filling of the available space created by the erosion of substrata, they may significantly alter bathymetry and create accommodation where there was once none or very little. Ortiz-Karpf et al. (2015) reported that erosion and changes in bathymetry associated with the emplacement of a large MTC in the southern Magdalena Fan, offshore Colombia, primed the system for submarine channel avulsion and lead to a significant change in sediment routing and deposition. The MTC flowed adjacent to a major established channel-levee complex, and incompletely filled the space created by erosion. As the levee built out over a thin ridge of intact substrata and encountered the sharp erosional surface created by the MTC, the levee over-steepened, became unstable, and collapsed. The breach in the levee led to the avulsion of the channel-levee complex, which then flowed on top of the MTC and into the newly created accommodation space. The irregular MTD surface bathymetry, primarily created by protruding megaclasts transported by the flow, influenced the subsequent deposition and evolution of the avulsion lobe.

As a supplement to the use of seismic-reflection data as described above, other workers have used outcrop studies to investigate MTC-created accommodation space. Pickering and Corregidor (2005) investigated Middle Eocene confined basin-floor submarine fan outcrops in the south Spanish Pyrenees and showed that MTCs can stack to create significant seafloor bathymetry (~35m) which influences turbidity current flow and turbidite depositional morphology. Armitage et al. (2009) describe the architectural evolution of sandy turbidites deposited on the irregular surface of a MTD as seen in outcrop exposures in the Cretaceous Magallanes foreland basin of southern Chile. They found that the initial sandstone beds deposited on the MTD surface pinch out and lap onto the relative topographic highs present on the surface. Smoothing of the MTD surface and reduction of bathymetric relief due to progressive sedimentation results in diminished confinement and a transition to more laterally continuous, sheet-like sand deposits. Thus in this instance the lateral continuity of the reservoir-scale sandstone-rich facies is principally controlled by the irregular surface bathymetry of the MTD. Work done by Butler and McCaffrey (2010) in the Italian Apennines shows that post-depositional internal deformation of an MTD can also impact sand body geometries on top of the MTD. Ortiz-Karpf et al. (2015) describe an irregular MTD top surface with bathymetry created largely by protruding ~50-250m thick megaclasts.

MTD / Turbidite Interaction in the Fish Creek – Vallecito Basin

This previous work on MTCs utilizing both seismic-reflection data and outcrop analogs demonstrates the ability of debris flows to erode tens of meters or more into the substrate and to create significant accommodation space above the MTC surface. They may rearrange sediment pathways and create bathymetry favorable to the deposition of

significant thicknesses of reservoir facies. These common MTC features may have significant implications for the local hydrocarbon reservoir system yet remain undetectable in all but the highest resolution seismic data.

The uplift and erosion that has taken place in the Fish Creek – Vallecito Basin over the previous ~1 m.y. has exposed the deep-water deposits of a tectonically active narrow rift basin. The Fish Creek – Vallecito Basin can therefore be added to the relatively small list of locations that provide outcrop evidence of the complex interactions between debris flows and the underlying and overlying turbidites, and may be used as an analog for other rift basin deepwater systems.

Thesis Objectives

STURZSTROMS

The Fish Creek – Vallecito Basin provides the opportunity to study two well exposed and vertically dissected sturzstroms. Steep erosion by the local drainage systems results in many locations in the basin that afford clean and uninterrupted exposures of the flow interiors, and therefore the basin may be better suited for sturzstrom study than other, better known sturzstroms (e.g. Blackhawk, Frank, Elm). Building on the efforts of previous workers (particularly the work of Kerr, 1984), this paper will attempt to:

- Document the differences between the upper and lower sturzstroms, especially those attributable to subaerial vs. subaqueous emplacement
- Investigate micro-scale features of the sturzstroms and their implications for emplacement mechanisms
- Delineate the aerial extent of both sturzstroms, and compare to associated turbidite, evaporite, and alluvial fan facies and rapid facies changes
- Reconstruct the basin at it was during the time of subaerial to marine transition

MTD / TURBIDITE INTERACTION

The younger of the Fish Creek – Vallecito sturzstroms flowed over the basin slope and floor, interrupting the deposition of a thick succession of sandy turbidites. To support the basins use as an outcrop analog of other deep-water systems studied through seismic-reflection data, this paper will attempt to:

- Describe and document the meso-scale variability in the younger MTD erosion of underlying turbidite deposits
- Investigate the variable bathymetry created on the upper MTD surface and the impact that it had on subsequent turbidite deposition, architecture, and connectivity
- Link the Fish Creek – Vallecito findings back to the observations made by other workers studying similar deep-water deposits in outcrop and seismic-reflection data

Tectonic Setting and Stratigraphy of the Fish Creek – Vallecito Basin

The Fish Creek – Vallecito Basin, located within the Anza-Borrego Desert State Park in the Colorado Desert of southern California, is a tectonically controlled rift basin and part of the larger Salton Trough, the northernmost extension of the Gulf of California. Exposed in the basin is a 5.5 km-thick package of late Miocene to early Pleistocene sediment that records its complete history (Fig. 3). Deposition associated with the onset of rifting and extensional tectonics, punctuated by spectacular basin wall collapse, abruptly gave way to deep-water facies due to continued subsidence and a sudden filling of the basin by marine water. Soon after, appeared the first sediments sourced from the continent's interior, marking the arrival of the Colorado River into the region. The remaining depositional history is one of shallowing linked to the building and progradation of the Colorado River delta and its associated deepwater margin, and the eventual transition to subaerial and lacustrine delta plain environments.

TECTONIC HISTORY AND BASIN BOUNDARIES

The Fish Creek – Vallecito Basin (Fig. 4) was formed as a result of extension in the Salton Trough region from 8.0 +/- 0.4 Ma to ~0.95 Ma. During this time, crustal extension and subsidence were controlled by low-angle slip on the West Salton detachment fault to the west and the strike-slip San Andreas Fault to the northeast (Axen and Fletcher, 1998; Dorsey et al., 2011). It is likely that a number of synthetic and antithetic normal faults existed to the east of the current western end of the West Salton detachment fault, giving rise to the apparent segmentation of the Fish Creek – Vallecito Basin into sub-basins as suggested by a late Miocene stratigraphic succession replete with

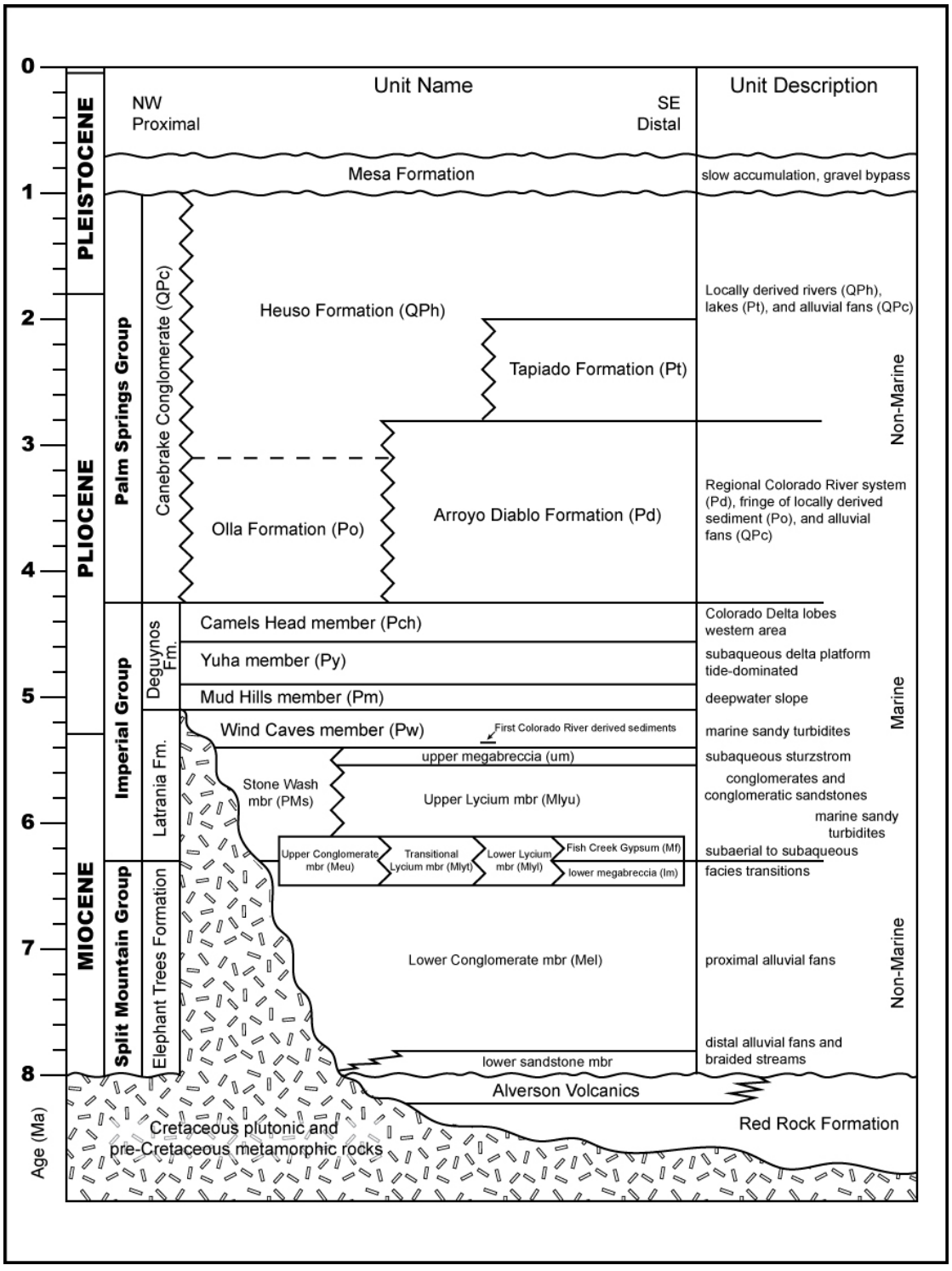

Figure 3. Fish Creek – Vallecito Basin stratigraphic column. Modified from Winker (1986) and Dorsey et al. (2007).

rapid facies changes and steep basin margins. By early Pliocene, coinciding with the arrival of the Colorado River to the basin, there is evidence that the sub-basin morphology and paleobathymetry had been mitigated through extensive sediment deposition resulting in a more contiguous Salton Trough depocenter and margin. During this time, dextral movement along the San Andreas Fault steadily translated the Fish Creek – Vallecito Basin as part of the larger Salton Trough region to the northwest relative to the North American plate. Slip on the West Salton detachment fault terminated ~1.1– 1.3 Ma and led to strike-slip movement along the modern Elsinore, San Felipe, and San Jacinto faults and the uplift responsible for exposing the Fish Creek – Vallecito Basin stratigraphy (Dorsey et al., 2011).

The Fish Creek – Vallecito Basin is bounded to the west by the Peninsular Ranges, to the north-northwest by the Vallecito Mountains, to the east-southeast by the Fish Creek Mountains, and to the south by Coyote Mountains. Early in the basin's history it is likely that now-buried basement exposures were present within the basin, as discussed further below.

FISH CREEK – VALLECITO BASIN STRATIGRAPHY

Thickness and stratigraphic nomenclature

The total thickness of the exposed Miocene to Pleistocene section in the Fish Creek – Vallecito Basin is ~5,500 m and encompasses ~7 M.y. of depositional history – from the coarse clastic alluvial material deposited during the initial extension to the unconformity on top of the Colorado River deltaic, fluvial, and lacustrine deposits caused

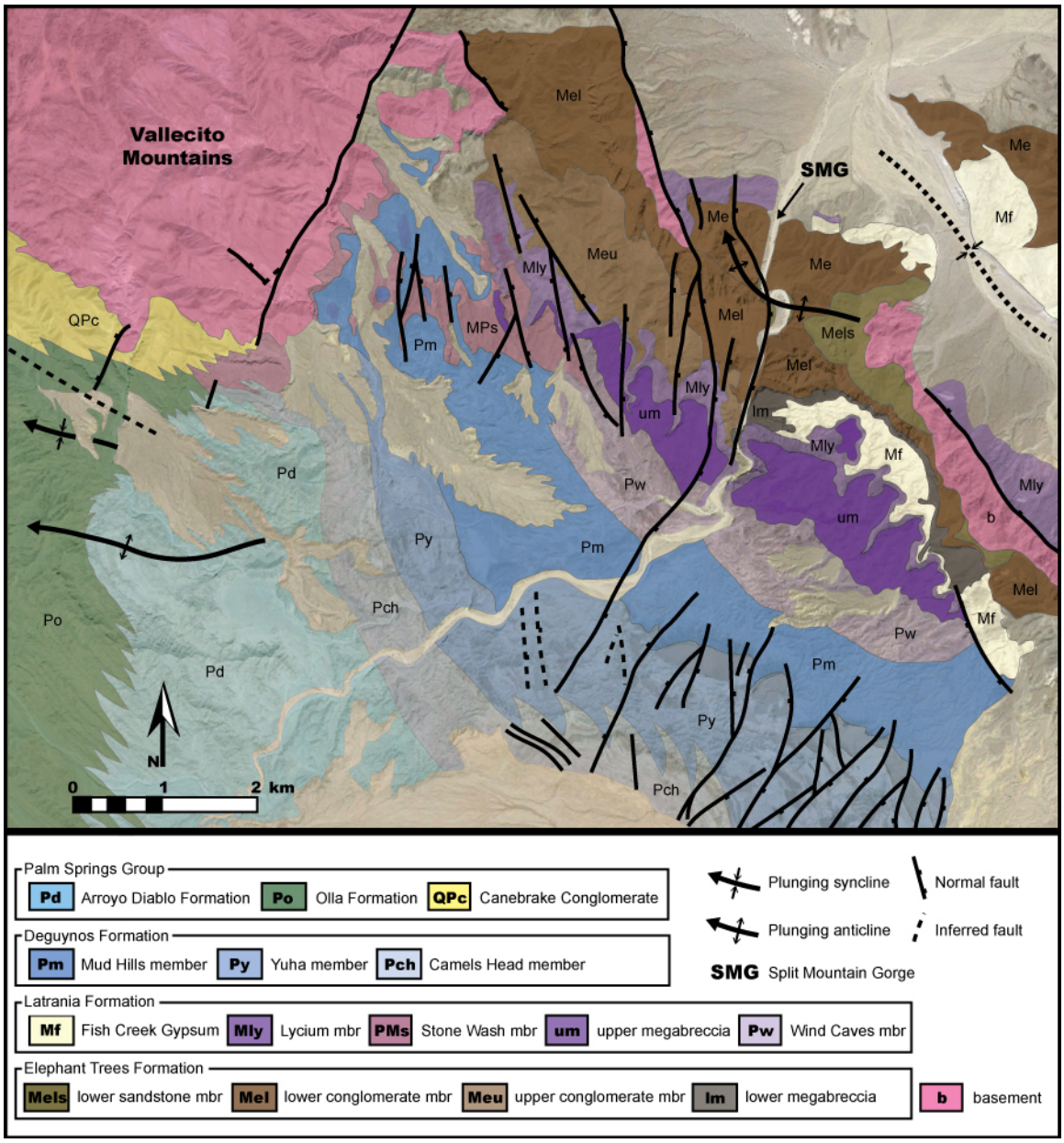

Figure 4. Geologic map of the Split Mountain Gorge area of the Fish Creek – Vallecito Basin. Modified from Winker (1986) and Dorsey et al. (2007).

by regional uplift over the past ~1 m.y. (Dorsey et al., 2011). The stratigraphic nomenclature used in this paper broadly follows that of Dorsey et al. (2011), which had incorporated work from Woodard (1963), Winker (1987), Winker and Kidwell (1996),

and Cassiliano (1999). In addition, formation members of Winker (1987) that highlight lateral facies changes will be included as appropriate. As Kerr and Abbott (1996) point out, many of the formal stratigraphic units, especially within the marine Imperial Group, are lateral facies equivalents or are otherwise contemporaneous to other units.

Basement

To the west of the Fish Creek – Vallecito Basin and forming the basement of the Miocene – Pleistocene sequence are the Peninsular Ranges, a suite of metamorphic rocks intruded by the Peninsular Ranges Batholith. The protolith of the greenschist to amphibolite grade metamorphic rock is thought to have been Paleozoic to Jurassic interbedded sediments and volcanics. The plutons of the Cretaceous Peninsular Ranges Batholith are dominantly tonalite, but range in composition from granite to diorite (Kerr, 1984; Winker, 1987).

Bounding the basin to the northwest are the Vallecito Mountains, plutonic rocks chiefly made up of quartz diorite with minor, localized diorite and quartz monzonite. Dikes of tonalite, aplite, and pegmatite are also present. The Fish Creek Mountains to the southeast are similar in composition to the Vallecitos, but contain a significant amount of gneiss, biotite schist, and pegmatite. To the south of the basin are the greenschist-grade metamorphic rocks of the Coyote Mountains, which are dominated by marble in the east and by biotite schist in the west. Amphibolite, gneiss, quartzite, and intrusions of quartz diorite, granodiorite, and pegmatite occur locally (Kerr, 1982, 1984; Winker, 1987). These critical compositional differences have been used by many workers to determine the sediment source area for much of the locally derived pre-marine rocks in the basin.

Pre- and Early Extension

The oldest deposits in the Fish Creek – Vallecito Basin are the nonmarine Red Rock Formation sandstone and the 22–14 Ma Alverson volcanics (Ruisaard, 1979; Kerr, 1982; Winker and Kidwell, 1996; Dorsey et al., 2011). These rocks were deposited before rift-related extension in the Salton Trough region.

The Cretaceous tonalite that forms the base of the section is overlain by the thin (~0–40 m) reddish pebbly sandstone of the Red Rock Formation. The red sandstone is unconformably overlain by a southeast-thickening (~0–200 m) pale tan distal alluvial fan and axial braided stream sandstone (Dorsey et al., 2007). Kerr (1984) and Winker and Kidwell (1996) had included both of these sandstones in the Red Rock Formation. Due to the stratigraphic relationship with the Alverson volcanics, however, assigning the pale tan sandstone to the Red Rocks Formation would suggest that it is older than 22–14 Ma. Due to the conformable nature of the contacts above the pale tan sandstone in the Split Mountain Gorge area (Fig. 5), Dorsey et al. (2007) has assigned it to the lower Elephant Trees Formation and determined an age of 8.1 ± 0.4 Ma for the base of the thickest part of the tan sandstone member. This age therefore corresponds to the base of the Split Mountain Group, and marks the beginning of strong extension and basin formation linked to an established and active West Salton detachment fault.

Split Mountain Group - Elephant Trees Formation

The Elephant Trees Formation of the Split Mountain Group contains at its base the lower distal alluvial fan and axial braided stream sandstone member described above, and the thick alluvial fan facies of the conglomerate member. The lower sandstone member of the Elephant Trees Formation rests on Cretaceous tonalite and is conformably overlain by the conglomerate member. East of Split Mountain Gorge, the lower sandstone

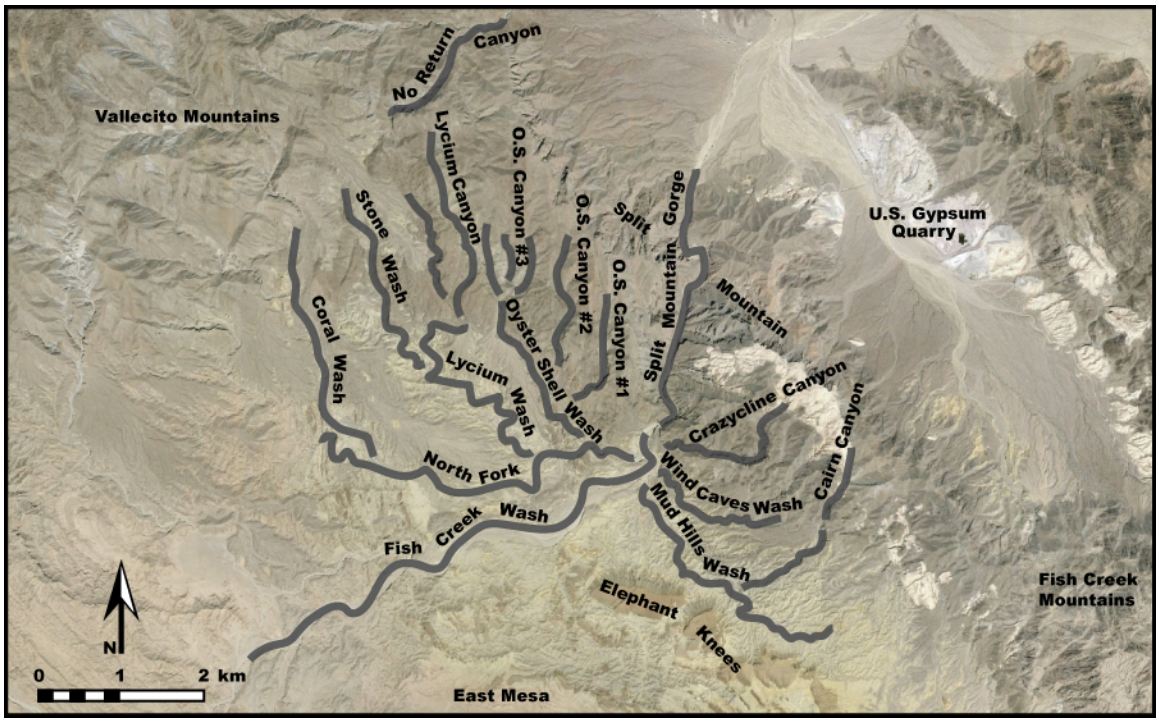

Figure 5. Map of drainages, features, and landmarks in the Split Mountain Gorge area of the Fish Creek – Vallecito Basin. Modified from Winker (1986).

member is estimated to be 150–200 m thick (Fig. 6 A, furthest Me in photo). In other parts of the basin, the lower sandstone member is thin to absent, or transitions laterally into the conglomerate member (Dorsey et al., 2007, 2011).

The alluvial fan facies of the conglomerate member of the Elephant Trees Formation consists of thickly but very well-bedded conglomerates (mainly subaerial debris flows) interstratified with conglomeratic sandstones, some of which are stream deposits (Kerr, 1984; Winker and Kidwell, 1996). It is monomictic, with clasts primarily made up of quartz diorite similar to what is found in the Vallecito Mountains (Kerr, 1984) and without the biotite schist and gneiss so prevalent in the Fish Creek Mountains. The conglomerate member extends ~6.5 km from the southeastern flanks of the Vallecito Mountains to just east of Split Mountain. It achieves a maximum thickness of ~450 m

just west of Split Mountain Gorge. On the eastern edge of the Vallecito Mountains the unit is ~360 m thick, and thins east of the gorge toward the Fish Creek Mountains, reaching ~70-75m in Cairn Canyon and ~30m between Boundary Mountain and Red Rock Canyon, and pinches out ~6km southeast of Split Mountain Gorge before reaching Red Rock Canyon (Kerr, 1982; Kerr, 1984; Winker, 1987; Winker and Kidwell, 1996).

Progradation of the alluvial fan lobes from the Vallecito Mountains is suggested by an up-section increase in bed thickness and maximum clast size, the eastward-thinning geometry, mainly northeastward directed paleocurrents, and a clast composition consistent with a Vallecito Mountain and possibly a Peninsular Range source. In addition, east-west oriented exposures in Split Mountain Gorge of individual conglomerate beds can be traced for ~1 km, while north-south exposures are not laterally continuous (Kerr, 1984; Winker and Kidwell, 1996). Winker and Kidwell (1996) place the proximal end of the conglomerate member at No Return fault, where it terminates fairly abruptly against the Vallecito Mountains basement rock, and interpret the down-to-the-east fault as syn-depositional with the Elephant Trees Formation.

Winker (1987) described lower and upper conglomerate members in the study area (Mel and Meu fanglomerates, respectively). The red, thickly bedded lower conglomerate member forms the steep walls of Split Mountain Gorge, and in this location can be compared to the less resistant, more thinly bedded, green to tan upper conglomerate member (Fig. 6 B). Northwest of Split Mountain Gorge, the upper conglomerate unit overlies the lower conglomerate unit between Oyster Shell Canyon #1 and the gorge. It laterally grades into green, gypsum-bearing, relatively thin-bedded coarse sandstones, debris-flow beds, and sparse reddish beds. Winker called the upper conglomerate unit laterally equivalent to his transitional unit (MP1t) of the Lycium member and possibly to the Fish Creek Gypsum exposed on the eastern side of the gorge.

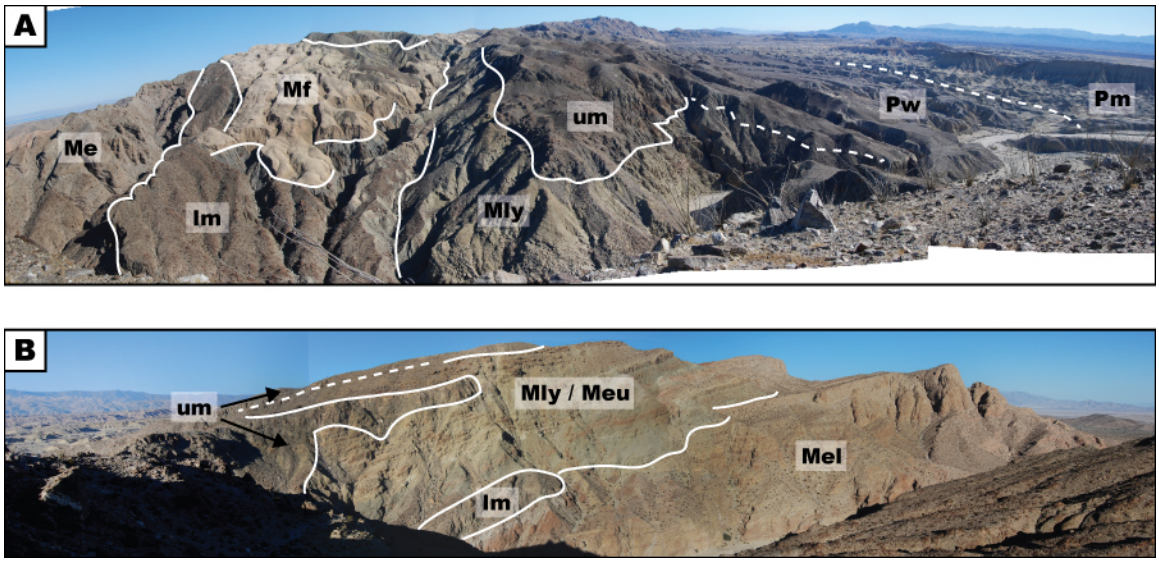

Figure 6. Panoramic photos of the Split Mountain Gorge east wall (A) and west wall (B).

The vertical transition from the upper conglomerate member to the Lycium turbidites can be gradational, as is the case in the west wall of Split Mountain Gorge, or sharp. Where the contact is sharp, predominantly to the northwest of the gorge, the upper conglomerate unit contains a series of distinct red beds within its top ~5 m. It is clear that the two conglomerate units are separated based on the larger transition that occurred in the basin at the time: alluvial fan conglomerates, sands, and gypsum deposited after the first major sturzstrom event and appearance of marine water (the upper conglomerate unit), and the alluvial fan conglomerates deposited before this transition (the lower conglomerate unit).

Split Mountain Group - Lower Megabreccia

The Split Mountain Group lower megabreccia [also referred to as the lower boulder bed (Winker, 1987) or the Split Mountain sturzstrom (Kerr and Abbott, 1996; Abbott et al., 2002)] is a mass transport deposit exhibiting nearly all of the features that would suggest its classification as a sturzstrom. The rock seems to have been shattered

in-situ (Fig. 7 A), with little evidence of turbulent flow, mixing, or widespread dispersion of clasts (Kerr, 1984; Kerr and Abbott, 1996; Abbott et al., 2002). It is a chaotic breccia of shattered and comminuted plutonic bedrock, exhibiting jigsaw-puzzle fabric on many scales. Where the megabreccia locally includes clasts that are visually different from neighboring clasts, or where broken clasts include veins of pegmatite, these clasts and surrounding matrix are clearly separable into distinct compositional domains (Fig. 7 A). Intact veins of pegmatite within a clast can be followed as separate domains of matrix that often connect to adjacent vein-bearing clasts.

The megabreccia is extremely poorly sorted, and includes essentially an entire range of clast sizes – from silt included in the finest matrix fraction to truck-sized boulders at the top of the flow (Fig. 18 B). It is matrix-supported, especially near the base, but locally may be clast-supported in the upper portions of the deposit. Clasts are angular to sub-rounded, and the sturzstrom is inversely graded in the coarsest fraction of the deposit (Fig. 8). The size of boulders increases toward the top of the deposit, with the very largest boulders (a few in excess of 5 m) located on the hummocky top surface of the deposit. Abbott et al. (2002) attributes this inverse grading to a "ball-mill effect," in which the shattered plutonic clasts in the lower portions of the flow were subjected to greater shear stress and numerous repeat collisions, and therefore were reduced to ever-smaller grain sizes during flow and emplacement. The largest clasts, riding on top of the flow, were spared the most violent comminution and survived relatively intact. Kerr and Abbott (1996), however, report that the minimum and median macroscopic grain size decreases up-section, while max clast diameter increases up-section. The above explanation of the inverse grading is unconventional (in the literature) but perhaps is consistent with compositional and textural features suggesting that little mixing occurred within the flow, that clasts did not move upward in the flow during its downslope

Figure 7. Lower megabreccia matrix characteristics. (A) Lower megabreccia clasts and matrix showing compositional domains, with matrix characteristics closely associated with adjacent clasts. (B) Typical lower megabreccia matrix.

movement (i.e., it moved with so-called 'plug' flow), and that the matrix is genetically related to the larger clasts which it surrounds. The conventional explanation would be that dispersive stress in the flow had greater impact on clasts with larger surface area, causing these clasts to slowly move higher in the flow (Fisher, 1971; Hampton, 1975, 1979; Walker, 1975; Middleton and Hampton, 1976; Nemec and Steel, 1984).

The megabreccia is nearly uniformly monomictic, with a quartz diorite clast lithology identical to that of the subjacent alluvial fans and the Vallecito Mountains to the north – northwest. There is general consensus that the Vallecito Mountains are the basement source for the megabreccia plutonic rocks (Kerr, 1984; Winker, 1987; Winker and Kidwell, 1996; Abbott et al., 2002; Shirvell, 2006; Dorsey et al., 2011).

Angular, very poorly sorted, fine to medium-grained sands comprise the matrix (Fig. 7 B). Its overall olive gray color is a reflection of the abundant biotite in the matrix (Kerr, 1984; Kerr and Abbott, 1996). Locally the color of the matrix is found to reflect the composition of the clasts it surrounds. The biotite and feldspar grains are unaltered and the matrix is devoid of clay minerals, which may suggest an unweathered source (Kerr, 1984).

Kerr and Abbott (1996) and Abbott et al. (2002) conducted geochemical analysis of lower megabreccia clasts and matrix samples 1 m away, and found them to be essentially identical. They cite this as evidence for the lack of mixing that occurs during sturzstrom emplacement. They next compared the chemistry of the megabreccia matrix fine fraction to that of the muds above and below the megabreccia. The megabreccia matrix was found to lack any phyllosilicate minerals (smectite, illite, kaolinite) that would have been formed during chemical weathering. The matrix was instead similar to the chemical compositions of representative samples of tonalites from the Peninsular Ranges batholith. This was taken as evidence that the megabreccia matrix was created

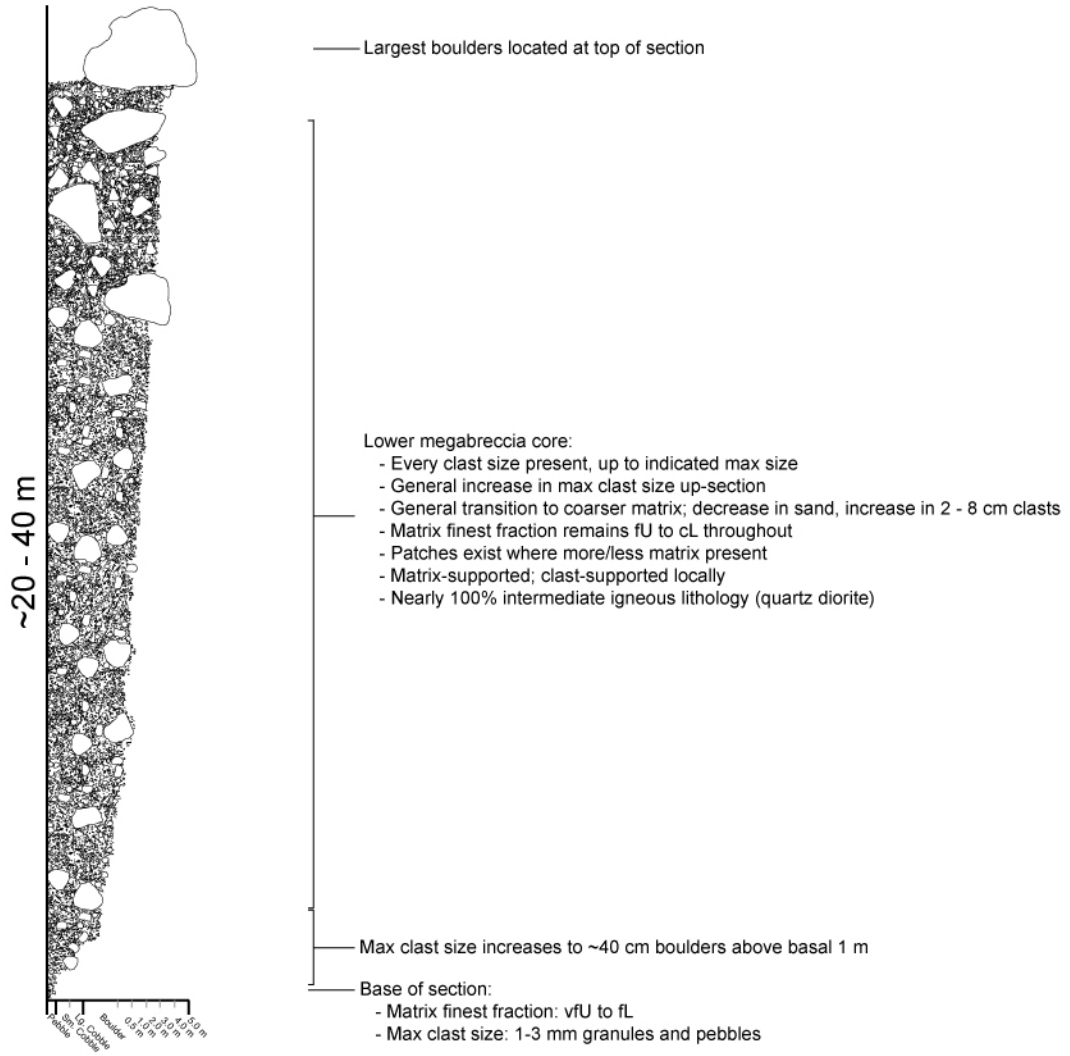

Figure 8. Schematic lower megabreccia section.

during transport, and did not undergo chemical weathering processes prior to the event that triggered the sturzstrom. While the Vallecito Mountains have been widely cited as the source location for the lower megabreccia, this evidence supports the interpretation that a Peninsular Ranges source is reasonable as well.

Kerr (1982, 1984) reported westward dipping, imbricated clay and crushed rock seams within the lower megabreccia that were not seen by this worker. The seams are asymmetrically folded, with the east limb dipping at a steeper angle than the west limb. As Winker (1987) points out, this deformation of the clay seams infers a southeast transport direction consistent with the Vallecito Mountains as a source area for the flow. Long pulverized white streams of pegmatite were observed, although their tendency to rise upward in the inferred down-flow direction as observed by Abbott et al. (2002) could not be verified.

It is typically ~45 m – 50 m thick, but increases to ~180 m thick against the Fish Creek Mountains. Its general uniform thickness can be seen in the prominent 5.2 km-long northeast-facing cliff that it forms from the entrance to Split Mountain Gorge in the north to the Fish Creek Mountains in the south (Kerr, 1984; Winker, 1987). Kerr and Abbott (1996) estimate the megabreccia deposit has a volume of 3.3×10^8 m^3 +/- 50% and a total run-out of 12.2km: 5.2km from the Vallecito Mountains to Split Mountain Gorge, then 4.2km to the base of the Fish Creek Mountains, then an additional 1.6km after it was deflected to the northeast by the Fish Creek Mountains.

In Split Mountain Gorge, the top ~20m of alluvial fan deposits that directly underlie the sharp basal contact of the lower megabreccia are chaotically deformed (Fig. 9 C) (Winker, 1987; Kerr, 1984). It is unlikely that the emplacement of lower megabreccia caused the disruption in the alluvial fan, as small sediment-filled channels can clearly be seen to cut into the deformed alluvial fan deposits below the contact with the lower megabreccia in the west wall of the gorge (Fig. 9 B). The disturbed alluvial fan deposits possibly represent smaller forerunner debris flows preceding the larger lower megabreccia event, and Kerr and Abbott (1996) refer to them as a separate sturzstrom deposit, the Red and Gray Sturzstrom. No field evidence was found to suggest that the

disturbed alluvial fan deposits exhibit the attributes of a sturzstrom, and it is possible that the uppermost fan debris flows were simply mobilized by precursors to the big event that created the lower megabreccia.

Along with its stratigraphic position on top of the subaerial Elephant Trees Formation alluvial fans, other features suggest that the lower megabreccia was emplaced subaerially as a high-velocity, non-turbulent laminar flow. The megabreccia has a sharp, undulatory basal contact across the underlying alluvial fans (Fig. 9 A). As described above, the lower megabreccia did not disturb the substrate, but rather abraded it as it cut across the ground. While there is no evidence of the wholesale entrainment of underlying subaerial alluvial fan sediments by the lower megabreccia, the small stream channels on top of the alluvial fan deposits were clearly truncated by the sturzstrom. Boulders that had at one time protruded from the upper surface of the alluvial fan were cleanly abraded, grooved, and decapitated by the overriding flow (Kerr and Abbott, 1996; Abbott et al., 2002).

The aerial extent of the megabreccia at the time of deposition may have been limited to the deepest parts of the basin (Fig. 13). It abruptly pinches out to the northwest, and the last vestige of it can be seen in the west wall of Split Mountain Gorge. To the southeast, where it is not deflected by the Fish Creek Mountains, it pinches out between Boundary Mountain and Red Rock Canyon. The megabreccia is entirely absent to the north – northeast of the Split Mountain Anticline, including in the vicinity of the U. S. Gypsum quarry (Winker, 1987).

The lower megabreccia is overlain by a thick deposit evaporite, the Fish Creek Gypsum (Fig. 6 A), though small lenses of sandstone or mudstone are present locally. These lenses of clastic deposits between the lower megabreccia and the gypsum are the upper conglomerate sandstone member (Meu) and the transitional Lycium unit (MP1t) of

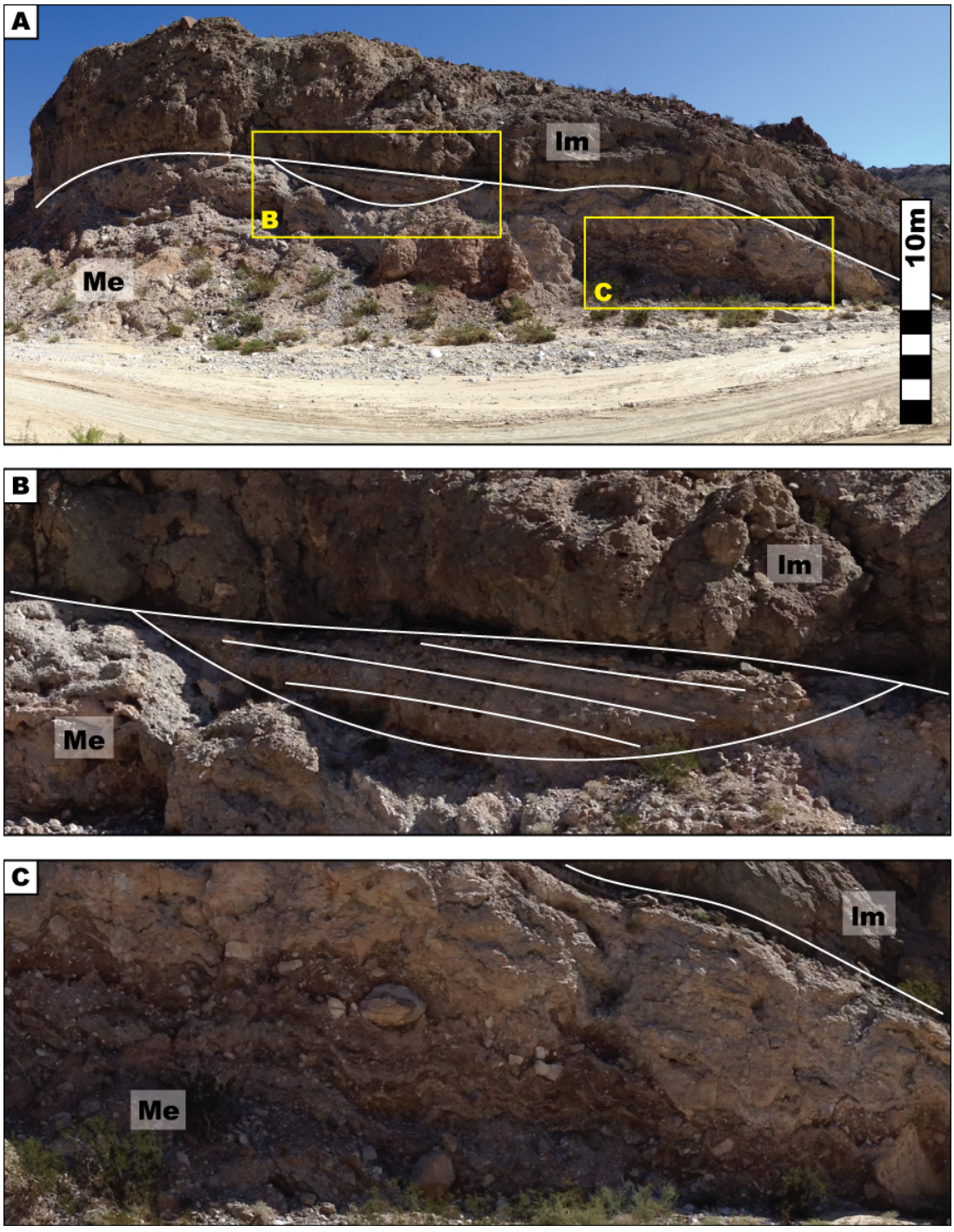

Figure 9. Lower megabreccia contact with Elephant Trees Formation alluvial fans in the east wall of Split Mountain Gorge. (A) Sharp, undulatory contact. (B) Channel cut into the deformed alluvial fan deposits. (C) Deformed alluvial fan deposits below the lower megabreccia contact.

Winker (1987), present in the Split Mountain Gorge west wall and east wall respectively. These units are also described by Kerr and Abbott (1996) and Abbott et al. (2002) as greenish subaqueous fan-delta mudstones and sandstones. Abbott et al. (2002) also mentions that the upper surface of the lower megabreccia is in some locations covered with 15cm-thick lenses or discontinuous layers of thinly bedded, medium to very coarse grained plutonic rock detritus sandstone inferred to be a subaerial fallout cap.

Imperial Group - Latrania Formation - Fish Creek Gypsum

The Fish Creek Gypsum is a ~60 m thick deposit of nearly pure calcium sulfate (>90%-95% $CaSO_4$; 35% anhydrite, 65% gypsum) that is largely free of terrigenous clastic sediment. A few thin interbedded claystones appear within the base and top, but are rare in the bulk of the deposit (Dean, 1996; Abbott et al., 2002). It is the oldest evidence for marine incursion into the western Salton Trough and the Fish Creek – Vallecito Basin (Winker and Kidwell, 1996).

Prior to a study by Dean (1996), a marine origin for the gypsum had been uncertain due to its stratigraphic position between the nonfossiliferous, nonmarine alluvial fans of the Elephant Trees Formation and the lower megabreccia below, and the marine Lycium Member turbidites above (Winker and Kidwell, 1996). Sulfate isotope ratios, the presence of calcareous nannofossils in claystones within the Fish Creek Gypsum, and a more detailed understanding of the stratigraphic relationships between transitional facies in the basin have confirmed that the evaporite deposit is of marine origin. Dean (1996) found terrestrial spores and pollen within the upper conglomerate unit (Meu) defined by Winker (1996) and within the basal claystone beds of the gypsum deposit, suggesting an initial terrestrial – fluvial influence. Clay interbeds within the

middle and top of the gypsum deposit contain a marine fossil assemblage similar to what is present in the overlying Imperial Formation, requiring an association with, and a close proximity to, a normal salinity marine environment. Dean (1996) saw this as evidence that terrestrial – fluvial input became less important as marine waters encroached the basin.

Lamination is the only primary sedimentary features preserved in the gypsum. Clay-bearing 1-2 mm-thick dark grey laminae with calcite and biotite impurities alternate with purer 0.25-0.5 cm-thick white laminae. Dean (1996) interpreted these laminations as varves related to storm activity, where the white laminae represent periods of intense brine concentration and the dark laminae represent storm-induced brine freshening and increased clastic input. The wavy character of the laminations suggests they formed in an intermediate energy regime such as intertidal, subtidal, and lagoonal environments. Such environments do correspond to the paleobathymetric estimates for the overlying turbidites, as we will see later.

The Fish Creek Gypsum is interpreted to have been subaqueously precipitated from shallow marine waters in a restricted shallow-water basin. In many locations (likely representing the periphery of the basin at the time) the gypsum occurs between two shallow water transitional marine facies, the upper conglomerate (Meu) and the transitional marine sandstone unit (MPlt) of Winker (1987). Two facies are present within the gypsum. The first is interbedded with upper conglomerate siltstones and claystones that indicates that precipitation occurred within the bottom sediments in shallow marine water at initial stage of brine concentration. The second facies represents the bulk of the deposit, pure and with little clastic sediment, i.e. it is thought to have precipitated out of the water column in a shallow water embayment. This facies laps out in sharp contact over all underlying sediment present at the time (Dean, 1996).

Dean (1996) reports that the thickest portion of the deposit was originally located in the northwest-trending wash (the location of the U.S. Gypsum company quarry) and adjacent western portion of the eastern synclinal limb of the Split Mountain Anticline. The deposit pinches out near northern entrance of Split Mountain Gorge, where it interfingers with the transitional alluvial fan / turbidite facies. The bulk of the deposit conformably overlies the lower megabreccia. Where the megabreccia is absent, the gypsum is in direct contact with the upper conglomerate of the Elephant Trees Formation alluvial fan and, over a vertical distance of a few meters, may be interbedded with ripple-laminated green micaceous sandstone and siltstone (Winker, 1987; Dean, 1996).

Imperial Group - Latrania Formation - Lycium Member

Overlying the Split Mountain Group subaerial deposits is a ~ 75m-thick section of locally derived ("L-suite") Latrania Formation marine mudstones, turbidites, grain-flow sandstones, and boulder-bearing sandstones (Kerr and Abbott, 1996; Bateman, 2015). The majority of the Lycium Member deposits are medium to thin-bedded, coarse-grained sediment-gravity flows (Fig. 10), with graded beds and bioturbated tops, and other abundant trace fossils (Winker, 1987; Winker and Kidwell, 1996). Proximal to source, roughly fringing the Vallecito Mountains near the Peninsular Ranges, the Lycium member becomes more conglomeratic. Northwest of Split Mountain Gorge, Lycium Member channelized, coarse-grained turbidites often contain numerous ~1-2 m diameter rounded boulders. Further to the southeast, near Cairn Canyon, the package thins and becomes finer grained and very thinly bedded.

Figure 10. Lycium member turbidites in the east wall of Lycium Canyon. Upper megabreccia lie at the top of the turbidite cliff.

The Lycium Member is in sharp, irregular contact with the underlying deposits, which can be either the Fish Creek Gypsum, the lower megabreccia, or the coarse sandstones associated with the upper conglomerate of the Elephant Trees member (Dorsey et al., 2007, 2011). According to Winker (1987), between Split Mountain Gorge and Oyster Shell Canyon #1 the Lycium Member interfingers with and grades laterally into the alluvial fans of the Elephant Trees Formation. Such stratigraphic nomenclature, however, tends to become less meaningful as all of the stratigraphic units discussed thus far are traced back to their proximal positions near the Vallecito Mountains. Northwest of Split Mountain Gorge, the entire section conformably vertically transitions from the clearly nonmarine conglomerate of the Elephant Trees Formation through subaqueous conglomeratic debris flows and boulder-bearing turbidites that could arguably be called part of the Lycium Member, and into the marine mudstones of the Mud Hills member (Dorsey et al., 2011). According to Dorsey et al. (2011), this conformable transition

northwest of Split Mountain Gorge indicates a conformable relationship between the lower megabreccia, the gypsum, and the marine turbidites within the gorge.

The lateral facies variability present in the Lycium Member can be seen in the work done by Winker (1987), Winker and Kidwell (1996), and Bateman (2015) where it has been subdivided into lower, upper, and transitional submembers. The thin-bedded turbidites of the lower submember (Mlyl) overlie the Fish Creek Gypsum. The lower sub-member grades proximally into the transitional member (Mlyt), and more proximally into the upper conglomerate of the Elephant Trees Formation (Meu). The green colored transitional member is present at Split Mountain Gorge as the fine-grained base of the turbidite succession. The upper sub-member (Mlyu) includes the thick channelized turbidites that crop out in Split Mountain Gorge and Lycium Canyon.

The Lycium Member is overlain, cut into, and often deformed by the upper megabreccia. Where the upper megabreccia is not present, the member grades vertically and proximally into thick, amalgamated conglomerates and conglomeratic sandstones of the Stone Wash Member. Proposed by Winker (1987), the Stone Wash Member (Mps) is present to the northwest of Split Mountain Gorge and represents the most proximal marine facies of the Lycium member and lowermost "L-suite" component of the Wind Caves member. It pinches out against the Vallecito Mountains basement rock to the west-northwest. In the vicinity of Coral Wash, west of the gorge and abutting the Vallecito Mountains basement rock, an assemblage of oysters, echinoids, and corals can be found on top of the Stone Wash Member (Winker and Kidwell, 1996). The conglomerates closest to the Vallecito Mountains retain a monomictic clast lithology, but those further away are polymictic and contain metamorphic clasts not present in the Vallecito Mountains.

Imperial Group - Latrania Formation - Upper Megabreccia

The upper megabreccia is similar to the lower megabreccia, and exhibits all of the qualifying attributes of a sturzstrom. It differs from the lower megabreccia in clast composition, and due to its subaqueous emplacement over unconsolidated or semi-lithified sediment, in the way that it deforms and disrupts the sub-stratum.

The upper megabreccia is an unsorted, chaotic, polymictic breccia (Fig. 11) containing clasts of granodiorite, tonalite, granite, pegmatite, and an assortment of metamorphic rocks including mica and biotite schist, biotite gneiss, and marble. Like the lower megabreccia, clast range from silt to boulder size, and the dark gray to olive matrix takes on the composition of surrounding clasts. In places it has jigsaw-puzzle fabric, compositional zoning, and abundant streaks of white comminuted pegmatite. Geochemical analysis reported by Kerr and Abbott (1996) and Abbott et al. (2002) confirms that little mixing took place during the flow, though the uppermost meter or so in the Gorge shows a normally graded sandstone top, indicating turbulence during the waning stages of sturzstrom emplacement. Due to the polymictic nature of the upper megabreccia, workers have proposed as the source the Fish Creek Mountains to the east – southeast, or a now-buried basement block to the south – southwest (Winker and Kidwell, 1996). The upper megabreccia attains a maximum thickness of ~40 m at the southern entrance to Split Mountain Gorge, and thins to the northwest and southeast.

In the southeast near Cairn Canyon, the upper megabreccia overlies the thin, fine-grained Lycium Member package. In the area of Split Mountain Gorge, the upper megabreccia occurs between the thick turbidites of the Lycium and Wind Caves members. Further northwest it overlies proximal Lycium Member facies and is in turn overlain by the conglomerates of the Stone Wash Member. As the upper megabreccia moved across the basin floor, it incorporated large tabular rip-up clasts of the underlying

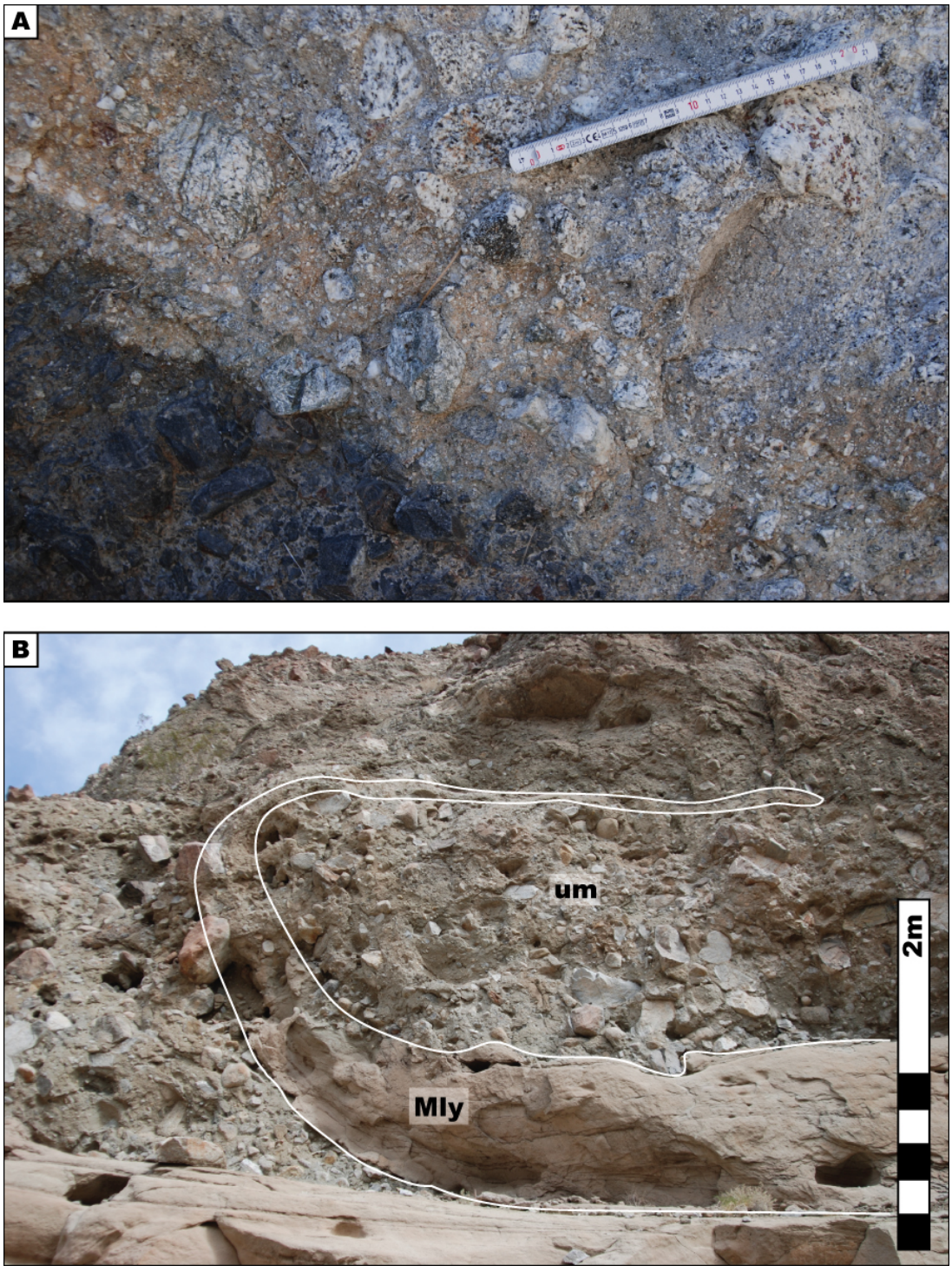

Figure 11. Upper megabreccia characteristics. (A) Typical upper megabreccia matrix with compositional zoning. (B) Lycium member turbidite incorporated into the base of the upper megabreccia in Oyster Shell Canyon #2.

turbidites (Fig. 11 B), or injected megabreccia lobes deep into the sediment that resulted in spectacular deformation of the turbidites on multiple scales (Fig. 25). The folded and deformed Lycium Member turbidites can best be seen in Split Mountain Gorge and Crazycline Canyon (Fig. 10). Winker (1987) measured axial orientations of several folded turbidites and found them to be preferentially oriented to the northeast-southwest with no preferential sense of overturning.

In multiple locations, the upper megabreccia grades/fines upwards and is topped by a ~1-2 m-thick cap of coarse sandstone (Fig. 19). This normally graded turbidity current cap confirms a subaqueous emplacement of the upper megabreccia and suggests that the flow produced a turbulent, sandy wake on its upper surface prior to coming to rest.

As Winker and Kidwell (1996) observed, the upper megabreccia has a slightly more extensive distribution than the lower megabreccia. This could be attributed to the filling in of local bathymetry or sub-basins by the Lycium Member post lower megabreccia emplacement but prior to the upper megabreccia flow. Similar incremental smoothing of paleobathymetry may have occurred throughout the basin's history.

Imperial Group - Latrania Formation - Wind Caves Member

The Wind Caves Member turbidites are significant because they mark the earliest influx of Colorado River derived "C-suite" sediments. The base of the Wind Caves Member begins with "L-suite" turbidites similar to those of the Lycium Member. The fine-grained, well-rounded, hematite-coated quartz sand that marks the arrival of the Colorado River in the basin occurs ~5 – 10 m above the contact with the underlying upper megabreccia (Winker and Kidwell, 1996; Dorsey et al., 2007, 2011; Cloos, 2014).

The remainder of the member is a ~200 m thick package of "C-suite" turbidites that occasionally alternates with minor, thin, locally derived "L-suite" turbidites. Towards the northwest, the Wind Caves Member laterally grades into the Stone Wash Member.

Unlike the "L-suite" sedimentation that was sourced from nearby and local drainage systems and generated fans, fan-deltas and deepwater fans, the Wind Caves member was a product of much more distant drainage (Colorado River) and represents southward-prograding submarine-fan lobes that occurred at the base of a northerly deepwater continental slope that now extended eastwards along strike to the Salton Sea area. The Wind Caves Member was fed with sediment, by-passed through the deepwater slope from the Colorado River shelf that now straddles the primitive Gulf of California. The Wind Caves Member was likely only a small part of a larger, eastward-extending submarine fan complex. Winker and Kidwell (1996) note that the bedding thickness decreases and the sediment becomes more fine-grained up-section and laterally, and suggest that these changes may be due to enlargement of the fan as the local sub-basin was progressively filled. It is likely that the upward fining is simply the normal upward transition to the muddy deepwater slope. As is typical of deepwater margins, basin-floor sands pass up to slope muds and eventually to shelf sands, all within basinward-migrating clinoforms (Steel and Olsen, 2002; Johannessen and Steel, 2005). This southward march of the new shelf margin clinoforms (coeval Yuha-Mud Hills-Wind Caves) is consistent with sediment by-pass and delivery of sands to deeper parts of the basin to the south once the local paleobathymetry was smoothed by sediment deposition.

Imperial Group - Deguynos Formation - Mud Hills, Yuha, and Camels Head members

The Mud Hills Member is a ~700 m-thick package of regionally extensive deepwater slope claystones and siltstones. The middle and upper portion of the slope succession in the vicinity of Fish Creek Wash has conspicuous rhythmic banding that has been interpreted as decadal Colorado river flood cycles on the deepwater slope driven by El Nino forcing (Steel pers. comm., 2015). The Yuha and Camels Head members, fossiliferous shallow-marine sands of the prograding Colorado River delta, overlie these marine rhythmites (Winker, 1987; Winker and Kidwell, 1996; Dorsey et al., 2011).

Palm Springs Group

The deepwater margin slope and delta deposits of the Imperial Group give way to Colorado River and coeval locally derived fluvial sediments (Arroyo Diablo Formation and Olla Formation), basin margin alluvial fan conglomerates (Canebrake Conglomerate), lacustrine mudstone and sandstones (Tapiado Formation), and transitional locally derived fluvial sandstones and conglomerate (Hueso Formation) of the Palm Springs Group (Winker, 1987; Winker and Kidwell, 1996, Dorsey et al., 2011).

AGE OF FISH CREEK – VALLECITO BASIN SECTION

Based on stratigraphic, paleomagnetic, and micropaleontologic analysis presented by Dorsey et al. (2007) and Dorsey et al. (2011), the Fish Creek – Vallecito Basin section ranges in age from ca. 8.0 ± 0.4 Ma at the base of the Elephant Trees Formation to 0.95 Ma at the top of the Hueso Formation. The age of the oldest conglomerate in the Split

Mountain Group is ca. 7.4 Ma, which at a minimum marks the beginning of strong extension in the region and movement on the West Salton detachment fault. Based on the conformable nature of the contacts within the Elephant Trees Formation, however, Dorsey et al. (2011) believe that deposition of the lower sandstone member likely coincides with tectonic activity starting ca. 8.0 ± 0.4 Ma.

The lower megabreccia was emplaced between 6.57 Ma and 6.27 Ma. The oldest marine deposits in the basin, at the base of the Lycium member turbidites, are ca. 6.3 Ma and similar in age to other latest Miocene marine deposits found in the Salton Trough and Gulf of California region (Dorsey et al., 2007). The upper megabreccia between 5.89 Ma and ~5.33 Ma, and sands from the Colorado River first appear in the Wind Caves Member at 5.33 Ma.

SUBSIDENCE HISTORY AND PALEOBATHYMETRY

Dorsey et al. (2011) presented a detailed subsidence analysis of the Fish Creek – Vallecito Basin from ca. 8.0 Ma to 0.95 Ma that showed four stages of subsidence history: (1) a long period of moderate subsidence from 8.0 Ma to 4.5 Ma; (2) 1.4 m.y. of more rapid subsidence through 3.1 Ma; (3) a return of moderate subsidence through 0.95 Ma; and (4) rapid ~6.0 mm/yr uplift since 0.95 Ma.

Based on similarly-aged marine deposits that conformably overlie nonmarine deposits in a ~600 km-long belt stretching from the Gulf of California to the northern Salton Trough, Dorsey et al. (2011) suggested that regionally integrated extension along an established Pacific–North America plate boundary replaced the local extension present in the Fish Creek – Vallecito Basin and other Salton Trough sub-basins, and caused unification and integration of extension that resulted in the widespread marine flooding of

the entire Salton Trough region at ca. 6.3–6.5 Ma. However, due to the moderate and relatively constant subsidence rate in the Fish Creek – Vallecito Basin from ca. 8.0 to 4.5 Ma, the marine incursion at 6.3 Ma was unlikely the result of an increase in subsidence (the rate of landscape drowning at 6.3 Ma was far greater than could be achieved by any rate of subsidence), nor is there clear evidence of a large-scale late Miocene change in global sea level. The likely solution here is that prior to marine incursion, the early extension on the West Salton Detachment System with its capping sub-basins had already subsided below sea level.

Dorsey et al. (2007) and McDougall (2008) conducted a paleobathymetric analysis based on benthic foraminifers from outcrops along the Fish Creek Wash. Due to the rarity of benthic foraminifers in the Lycium member turbidites, both workers contend that initial deposition occurred in inner neritic depths (< 40 m), but it is possible, as the turbidite succession is far thicker than 40m, that the shallower forams were brought in by the turbidity currents from a shallower shelf. They report that benthic fauna becomes more abundant and diverse above the upper megabreccia during deposition of the Wind Caves member turbidites, suggesting increased water depths (150–500 m), and that a gradual decrease in water depths and salinity begins with the lower Mud Hills member.

The dramatic "deepening" postulated by Dorsey et al. (2011) preceding Fish Creek – Vallecito Basin marine flooding and deposition of Lycium member turbidites was instead caused by marine infiltration through a sill breach or other catastrophic breach into an already topographically deepened landscape (Fig. 12). If the appearance of marine water in the Fish Creek – Vallecito Basin is viewed in this context, the difficulties in reconciling paleobathymetric estimates with a preferred smooth subsidence curve encountered by Dorsey et al. (2011) and leading to the preferred selection of inaccurate "minimum" paleodepths (Fig. 12 A) become irrelevant.

If this paleobathymetric analysis is considered along with evidence that the (sub) basin was already topographically deep at the time of significant marine incursion, and that all "c-suite" sedimentation was part of the southward-advancing Colorado River deepwater margin, contradictions between paleobathymetry and stratigraphic facies can also be rectified (Fig. 12 B). Irrespective of the presence of shallow water microfossils and lack of deepwater benthic foraminifers, the very thick Lycium member turbidites likely require water depths of at least 150 m. The turbidity currents responsible for Lycium member deposition must also have carried shallow water microfossils. That the deepwater slope upon which the Mud Hills member was deposited was found to have shallowed is a natural result of the prograding Colorado River margin.

PALEOCURRENTS AND PROVENANCE

In general, paleocurrents in the Fish Creek – Vallecito sediments are controlled by provenance. Locally sourced "L-suite" sediment deposited in the Miocene, prior to the arrival of the Colorado River to the basin, flowed from west-southwest to east-northeast. This sediment was sourced from the exposed Peninsular Ranges and Vallecito Mountains basement rock. The Pliocene "C-suite" sediments were delivered to the basin via the Colorado River, which entered the basin from the north. Colorado River-derived sediments flowed from the north-northwest to the south-southeast, parallel to the basin axis (Winker and Kidwell, 1996). Paleocurrent relationship to the overall geography of the basin is therefore straightforward: "L-suite" sediment sourced from the basin margins flowed into the basin orthogonal to the basin margins, and "C-suite" sediment sourced from the Colorado River flowed into the basin much like the present-day Colorado River flows into the Gulf of California.

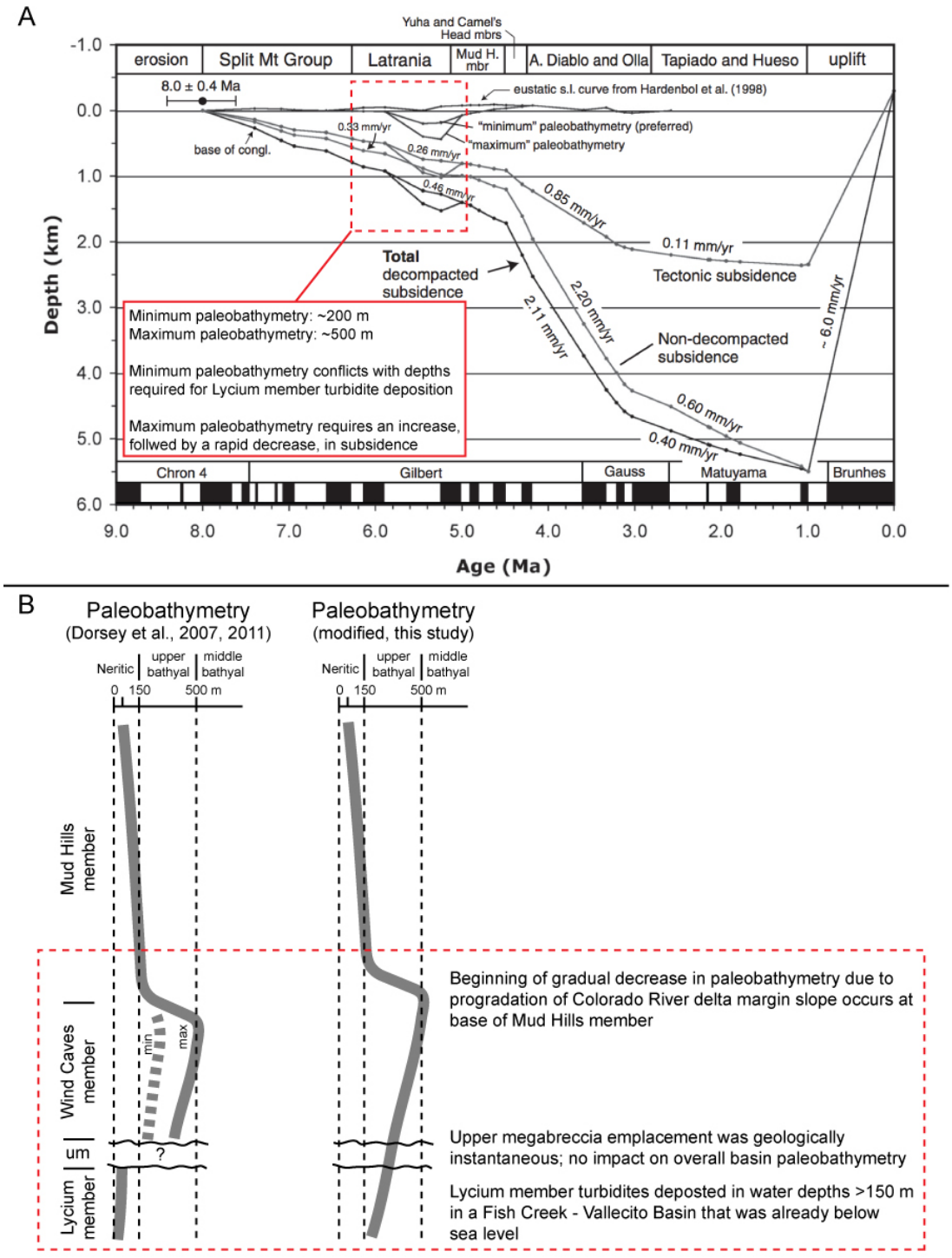

Figure 12. Fish Creek – Vallecito Basin subsidence curve (A) and paleobathymetry (B) modified from Dorsey et al. (2007, 2011) to address inconsistencies between paleobathymetry and sediment facies.

Red Rock Formation

The braided stream deposits of the Red Rock Formation are an exception to the general paleocurrent relationships discussed above. Kerr (1984) determined a northward paleoflow for the Red Rock Formation, and Winker and Kidwell (1996) proposed that paleocurrent directions might have been controlled by the orientation of bedrock paleovalleys.

Split Mountain Group – Elephant Trees Formation

Kerr (1984) and Winker (1987) report dominant east-northeast paleocurrent directions on a northeast paleoslope for the conglomerate alluvial fans of the Elephant Trees Formation based on trough foresets, channel axes, and lineations.

Split Mountain Group – lower megabreccia

The lower megabreccia attribute most widely used to determine paleoflow and sediment source is clast lithology, which points to the Vallecito Mountains as the likely location of the sturzstrom's origin. Kerr (1984) and Abbott et al. (2002) also used groves and striation on decapitated stones, and imbricated clay and crushed rock seams to infer emplacement from the west.

Imperial Group – Latrania and Deguynos formations

Based on paleocurrent data from the locally derived "L-suite" Lycium Member turbidites and the Stone Wash Member conglomerates, Winker (1987) and Winker and Kidwell (1996) determined that the dominant transport direction was toward the east-northeast. They found that Latrania Formation deposition is intimately linked to the

underlying Elephant Trees Formation alluvial fan deposits, as evidenced by the time-transgressive and gradational intervening contact.

The source, and therefore the flow direction, of the upper megabreccia are debated. Based on lithological composition, the metamorphic rock-rich basement of the Fish Creek Mountains to the southeast appear to be the most likely choice. Abbott et al. (2002) were convinced of this, and chose to call the upper megabreccia the Fish Creek Sturzstrom. Analysis of fold axes in the disturbed underlying Lycium Member turbidites in Crazycline Canyon by Winker (1987) revealed preferred axial orientations to the northeast-southwest but no consistent sense of overturning. If the axial orientations were perpendicular to the flow direction, a northwest flow direction would suggest a Fish Creek Mountain source. However, it is conceivable that the axial orientations are parallel to the flow direction, which would point to a northeast or southwest source area. As Winker (1987) outlined, a west – southwestern source for the upper megabreccia would require (1) a now buried exposure of basement rock to the south of the Vallecito Mountains; or (2) a Vallecito Mountain source that included metamorphic roof pendants which have subsequently been entirely removed by erosion. Both of these options are entirely plausible.

Paleocurrent data from the "C-suite" sediments of the Latrania Formation Wind Caves Member and the Deguynos Formation Yuha and Camels Head members show a strong and abrupt shift in sediment transport to the south based on cross-stratification, ripple foresets and crests, and sole marks measured by Winker and Kidwell (1996).

Palm Springs Group – Arroyo Diablo and Olla formations

Foresets in trough cross-stratified delta plain paleochannels of the Pliocene of the Arroyo Diablo and Olla members show predominantly southerly paleocurrent directions with considerable scatter attributed to meandering fluvial system (Winker and Kidwell, 1986).

Methods and Results

METHODS

Measured Sections

To investigate the attributes and flow characteristics of the Fish Creek – Vallecito Basin megabreccia deposits, and to determine the ways in which these mass transport deposits (1) scoured and eroded underlying turbidites; (2) created bathymetry on their top surfaces that acted as turbidity current conduits; and (3) impacted the lateral continuity of adjacent sandstone beds, 10 vertical sections were measured through deposits that crop out over 6 km (Fig. 13).

Because of the macro-scale chaotic homogeneity of the megabreccia, a detailed investigation of their attributes, from matrix fabric to vertical trends in clast size, was done utilizing a combination of field observations and image analysis. Measured sections were created by importing outcrop images at multiple scales into Adobe Illustrator, where individual clasts ranging in size from pebbles to boulders were manual selected and outlined. Rather than relying on necessarily interpretive in-the-field drawings, the author believes that this method best represents the character of the megabreccia. Measured section locations were chosen to document changes seen in the proximal vs. distal and axial vs. edges of both the lower and upper mass transport deposits.

To better constrain the paleogeographic reconstruction of the Fish Creek – Vallecito Basin at the time of marine incursion, the extent of stratigraphic units from the top of the Elephant Trees Formation alluvial fan to the base of the Wind Caves Member, inclusive of lateral facies changes, were further refined based on the investigations of previous workers (e.g. Kerr, 1984; Winker and Kidwell, 1986; Winker, 1987; Winker and Kidwell, 1996; Abbott et al., 2002; Dorsey et al., 2007, 2011).

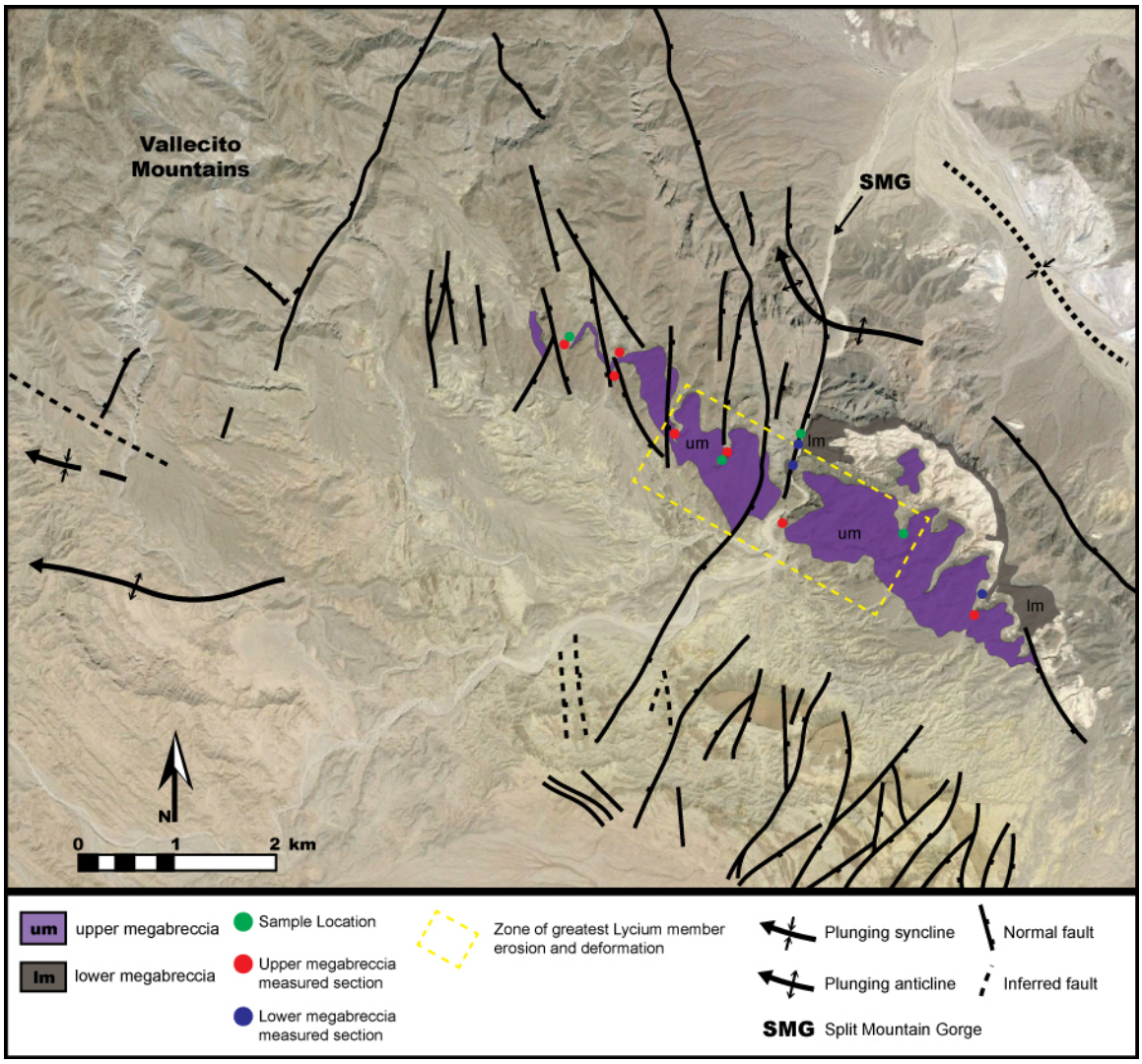

Figure 13. Extent of outcropping lower and upper megabreccia, with measured section locations, sample locations, and zone of greatest Lycium member erosion and deformation.

Locations of MTD / turbidite interactions were mapped and documented in measured sections and in panoramic images. These macro-scale outcrop observations were then linked to MTD / turbidite interactions documented at the seismic scale.

Sample Collection and Thin Sections

Few of the previous investigations into sturzstrom deposits have included thin section analysis. Of those that have, e.g. Masch et al. (1985) and Legros et al. (2000), the main focus has been on the small zone of basal contact between the megabreccia and underlying deposits. None have reported on samples taken meters above the base or at the fringes of the flow. The numerous accessible outcrops of the subaerially and subaqueously emplaced Fish Creek – Vallecito Basin sturzstroms provides an opportunity to add to our micro-scale understanding of the characteristics and flow mechanics of these deposits.

Nine matrix and matrix + clast samples were collected from ~1-5 m above the base of the deposits or from tongues injected into underlying turbidites: 5 samples of the lower megabreccia from Split Mountain Gorge, and 4 samples of the upper megabreccia from Lycium Canyon, Crazycline Canyon, and Oyster Shell Canyon #1 (Fig. 13). The samples were selected for their ability to capture a range of sturzstrom features: (1) apparently "normal" matrix that, to the naked eye, contain no fabric; (2) altered "smeared" clasts that flow around other clasts and include sandy matrix injections; and (3) matrix containing compositionally zoned and partitioned crushed rock streaks visible due to contrasting lithologies.

RESULTS

Mass Transport Deposits

Outcrop Characteristics

Both the subaerially emplaced lower megabreccia and the subaqueously emplaced lower megabreccia are homogeneously chaotic (Figs. 14, 15, and 22). There is little to no

difference between outcrops of lower megabreccia, or between outcrops of upper megabreccia. Each respective deposit contains a suite of characteristics that identifies it as a sturzstrom, more or less randomly dispersed throughout the flow, and generally independent of the total thickness of the deposits at a particular location. The lower and upper megabreccia do differ from one another in significant ways, however, primarily in clast lithology and the manner in which the sturzstrom impacted the substrate and influenced later deposition on top of them.

Lower Megabreccia

The lower megabreccia clast lithology is nearly 100% quartz diorite. It is extremely poorly sorted, and taken as a whole contains essentially an entire range of clast sizes, from fine biotite flakes in the matrix finest fraction to truck-sized boulders that ride on top of the flow. It is generally matrix-supported, but patches exist where more or less matrix is present and in these locations the lower megabreccia can nearly be considered clast-supported. The matrix is composed of igneous rock fragments, quartz, feldspar, mica, and biotite.

Utilizing the well-exposed cliff face in the east wall of Split Mountain Gorge as a representative deposit location, the lower megabreccia has the following characteristics from its base to its top (Figs. 14 and 15). Where exposed, the basal 4 cm of the deposit contains clasts that are, at maximum, granule and pebble-sized suspended in a matrix of vfU to fL sand. The actual contact with the underlying alluvial fans is a 0.5 to 1.0 cm thick zone of white, friable powder likely significantly altered in the time since original deposition by meteoric water and the streams that cut the canyon exposures. Rarely underlying this contact are decapitated alluvial fan clasts that clearly had once protruded

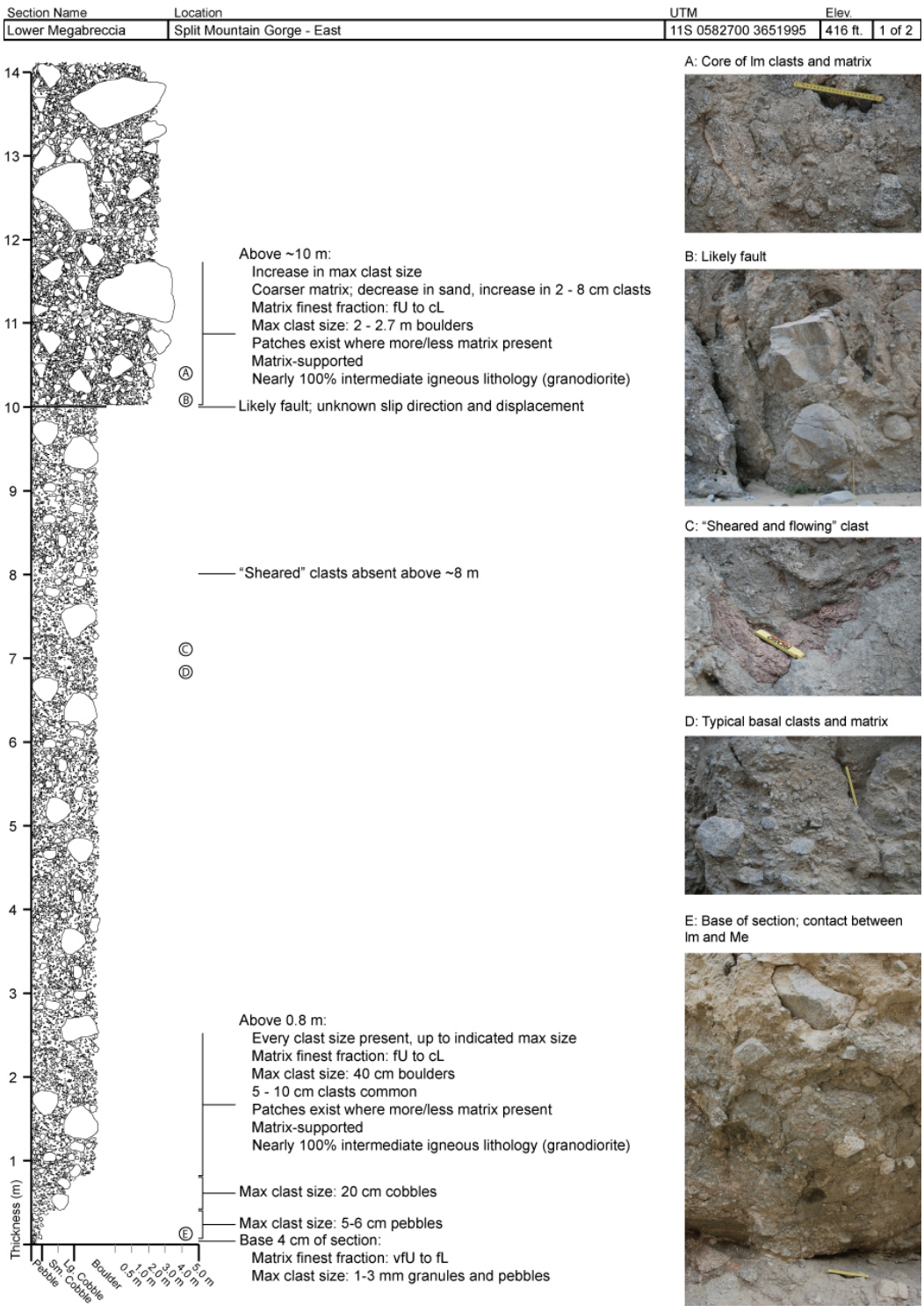

Figure 14. Lower megabreccia measured section from east wall of Split Mountain Gorge. Base of section.

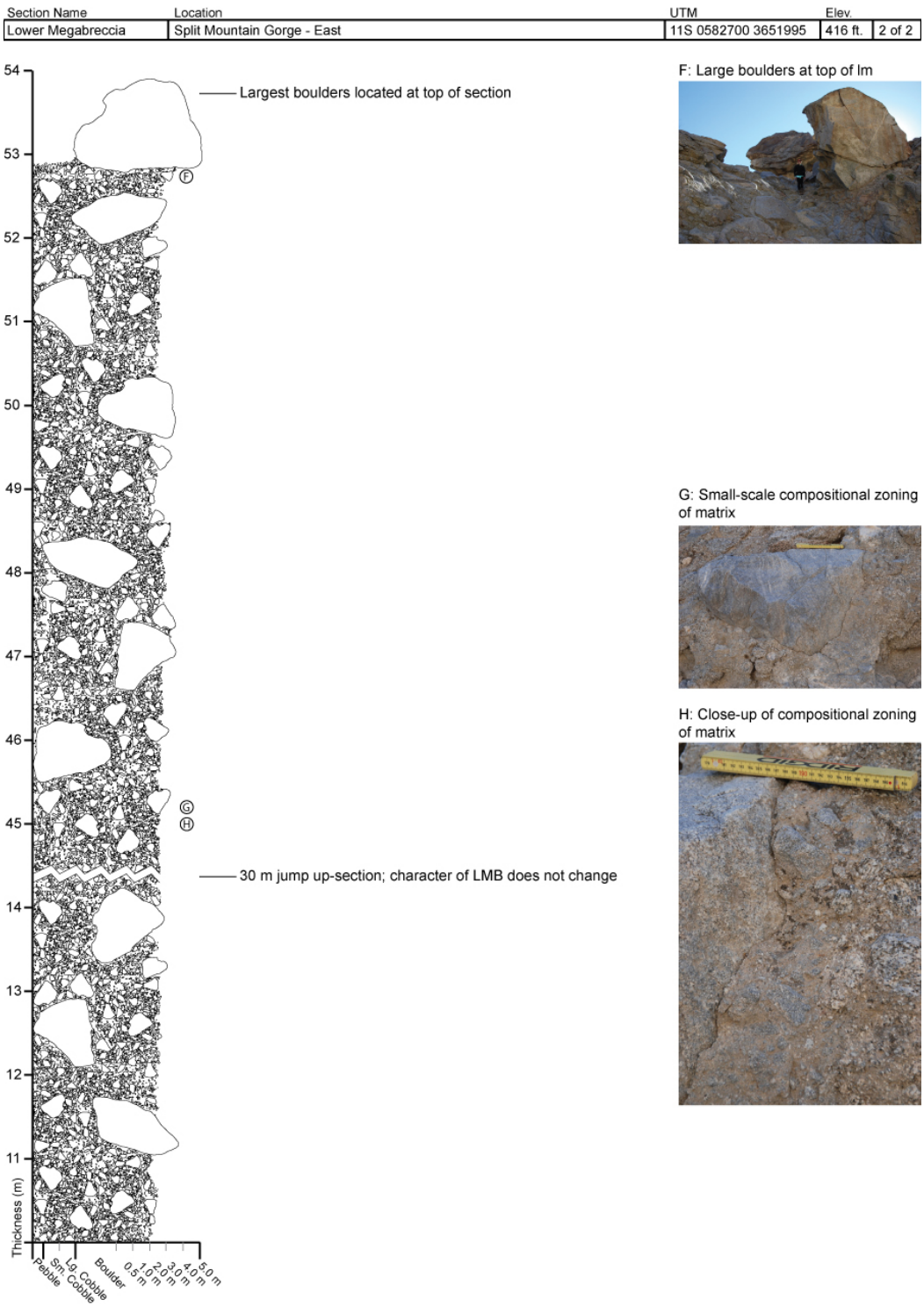

Figure 15. Lower megabreccia measured section from east wall of Split Mountain Gorge. Top of section.

above the fan surface but were violently abraded into a sharp contact by the overriding sturzstrom flow.

Within the lowest meter of the deposit, the maximum clast size rapidly increases to 20 cm cobbles. Above the first meter, the deposit remains matrix-supported, the matrix finest-fraction increases to fU to cL sand, maximum clast size increases to ~40 cm boulders, and ~5 - 10 cm clasts are common. Above this point and through the bulk of the deposit, across several tens of meters, there is a gradual coarsening of the deposit. While the matrix finest-fraction remains fU to cL sand, the maximum clast size increases to ~2 – 3 m boulders and clasts ~2 – 8 cm in size become common. At the top of the deposit, boulders as large as 8 m protrude from the top surface of the megabreccia (Fig. 18 B).

Where pegmatitic veins are present within clasts, or where clasts are visually distinct from surrounding clasts, a jigsaw-puzzle fabric and compositional zoning in the form of crushed rock streams are readily apparent (Figs. 15 G and H, and 17). Also present in these circumstances is abundant compositional zoning within the matrix, where the matrix composition is intimately related to the composition of the adjacent clast from which it was derived. The basal ~8 m of the deposit contain enigmatic “smeared” clasts (Fig. 17). They are conspicuously visible in the lower megabreccia due to their markedly distinct fabric and deep red color. They occur in discrete elongate patches ~ 10 cm – 2 m in length that are roughly aligned horizontally in what would be the flow orientation of the deposit. The clasts themselves have a stretched lineation fabric and flow around more competent clasts. Often fine megabreccia matrix has been injected into the clasts. The clasts have clearly been altered, and while a post-depositional change cannot entirely be ruled out, a possible explanation given their characteristics and relationships to surrounding material is that these clasts represent a lithology that was more susceptible to

alteration by the shear stresses and heat present within the flow. These clasts were altered in the minutes it took the lower megabreccia to flow and then come to rest. The microscopic features of these clasts are discussed in the Results and Discussion sections of this thesis.

The lower megabreccia is ~53 m thick in Split Mountain Gorge. It is impossible to determine thickness in other outcrops within the study area as the base of the lower megabreccia is not exposed elsewhere. Kerr (1984) and Winker (1987) report a typical thickness of ~45 m – 50 m, which seems likely based on field observations and minimum incomplete measured section thicknesses. The northwestern-most extent of the lower megabreccia is within Split Mountain Gorge, where a small patch is exposed in the gorge's western wall. To the southeast, the deposit thickens as it came into contact with and was deflected by the Fish Creek Mountains.

The lower megabreccia is best exposed in Split Mountain Gorge and Cairn Canyon, and these locations provide the best exposures of the deposit's contact with underlying and overlying units. In Split Mountain Gorge, the lower megabreccia lies in sharp, somewhat undulatory contact with the underlying alluvial fan debris flow deposit and intervening small stream channels. Stratigraphic position, sharp erosive contact with underlying deposits, and lack of evidence of the incorporation of underlying sediment suggests that at least where it is exposed the lower megabreccia was deposited subaerially. In Split Mountain Gorge the megabreccia is overlain either by the Fish Creek Gypsum or by the distinct green-colored transitional Lycium member turbidites. Exposed in Cairn Canyon is a previously undocumented coarse sand facies that is present between the lower megabreccia and the gypsum (Fig. 16). This ~2 m thick facies is distinct from the Lycium member, and fills and pinches out against irregular top surface highs of the lower megabreccia. Individual beds are ~ 2 – 4 cm thick, fine upward from very coarse

sand and granules to fine sand and silt, and are inclined. The facies appear to be thin, laterally accreting, fluvial sheet sands. The sand beds near the top of the deposit alternate with thin beds of gypsum before giving way entirely to the gypsum at the top of the deposit.

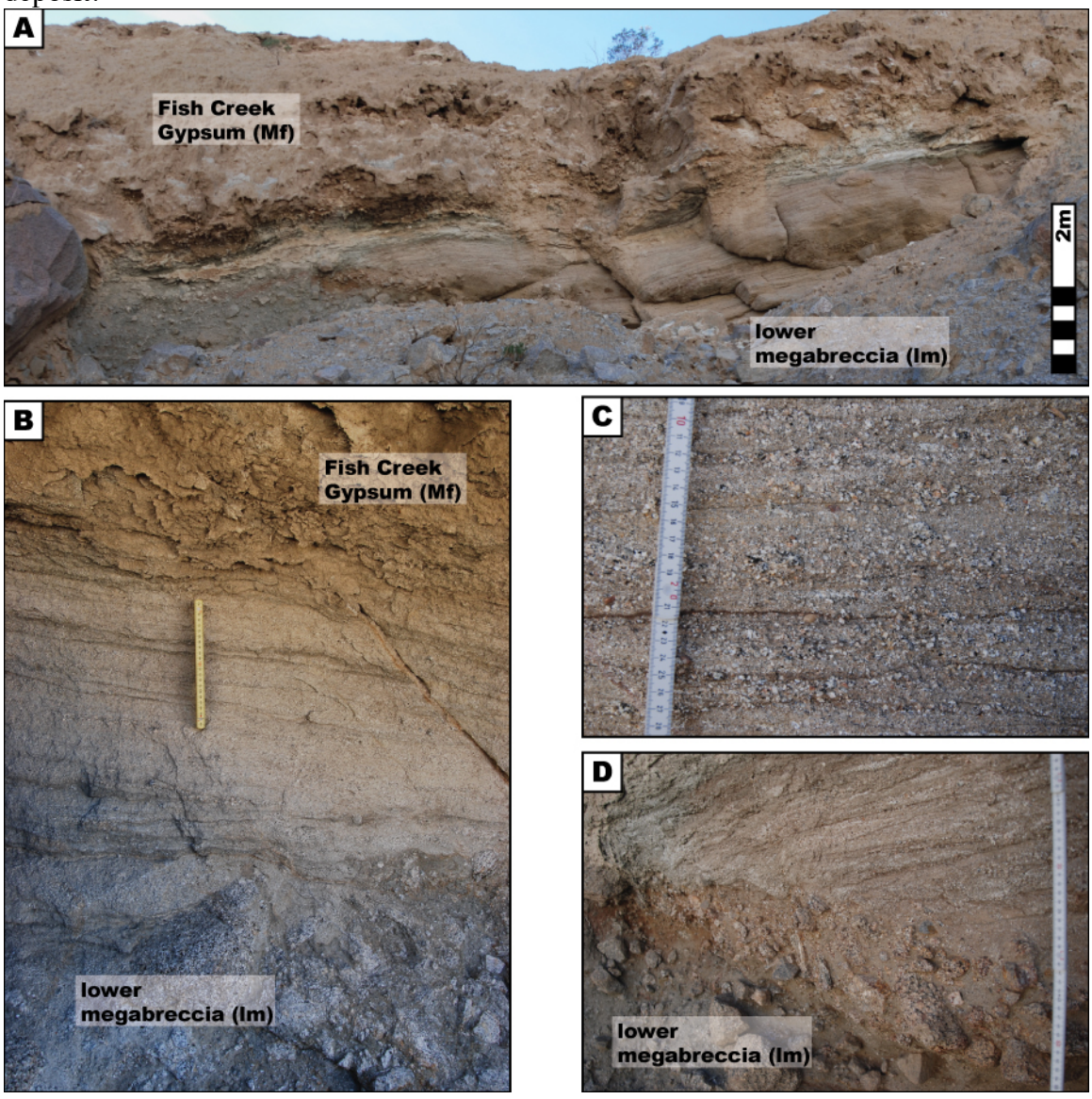

Figure 16. Coarse sand facies between the lower megabreccia and the Fish Creek Gypsum in Cairn Canyon. (A) Sand onlaps and pinches out against the lower megabreccia. (B) Transition from lower megabreccia to sand to gypsum. (C) Detail of sand facies. (D) Inclined beds.

Upper Megabreccia

The upper megabreccia forms the westward-dipping slope of Split Mountain and is present to the northwest and southeast of Split Mountain Gorge and is exposed throughout the study area. Like the lower megabreccia, the upper megabreccia is chaotically homogeneous and varies little from one outcrop to the next. However, it differs significantly from the lower megabreccia in lithologic composition and in the manner in which it interacted with the substrate over which it flowed. Significant amount of metamorphic clasts, including gneiss and biotite schist, along with the quartz diorite common to both megabreccia deposits, makes compositional zoning and jigsaw-puzzle fabrics easy to identify (Fig. 17). The deposit is matrix-supported at its base, and approaches clast-supported in some locations near the top of the flow.

The characteristics of the upper megabreccia base vary from location to location in the study area. Near the southern entrance to Split Mountain Gorge and in the Oyster Shell Canyons area, tabular rip-up clasts of Lycium member turbidites are incorporated into the base of the megabreccia. The entire upper megabreccia from base to top is exposed in Oyster Shell Canyon #3 (Fig. 20). Here there is minimal erosion of the deposit into the underlying turbidites and incorporation of rip-up clasts. The basal 2 m contains abundant 5 – 20 cm clasts in a fU sandy matrix. The maximum clast size increases to ~1 – 1.5 m above the basal 2 m of the deposit. In Lycium Canyon a full range of clast sizes, from granules to cobbles are present, with a maximum clast size ~10 – 15 cm in a cL to mU matrix. The base of the upper megabreccia at the entrance to Cairn Canyon contains a population of ~0.5 m clasts in a mL sandy matrix. Occasionally there are anomalously large ~1.5 m clasts included in the base. Approximately 15 m from base the average maximum clast size increases to ~1 m in a slightly more coarse cL to mU sandy matrix.

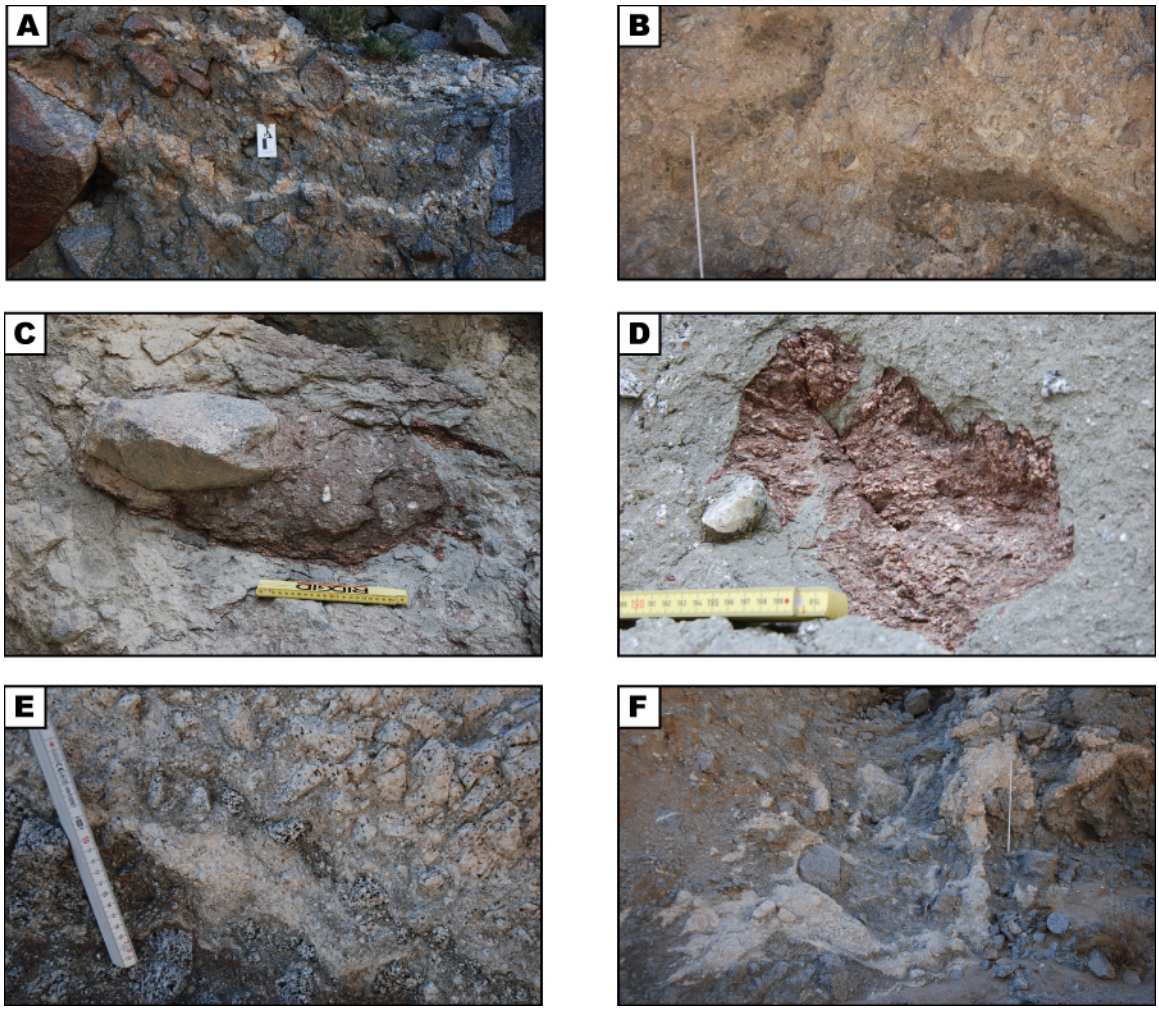

Figure 17. Megabreccia features. (A) Crushed rock streamers and jigsaw-puzzle fabric in the upper megabreccia. (B) Compositional zoning. (C) "Smeared" clast in lower megabreccia. (D) "Smeared" clast detail. (E) Compositional zoning and matrix / clast relationship in lower megabreccia. (F) Comminution of a pegmatite dike in the lower megabreccia.

Like the lower megabreccia, extremely large boulders often cap the upper megabreccia. The largest boulder in the study area is located in Wind Caves wash, just southeast of Fish Creek wash, and is well over 10 m in diameter. Where the overlying deposits have not been removed by erosion, such as exposures in Fish Creek wash and Oyster Shell Canyon #3, the upper megabreccia is capped by a ~1 – 2 m thick deposit of

clean, fining-upward sand (Fig. 19). This sandy cap is interpreted to have been deposited by turbidity currents generated by the violent emplacement of the deposit after the main body of the upper megabreccia had come to rest. Stratigraphic position between two undeniably marine sandstone deposits, the variable erosive contact with underlying deposits, the turbulent sand that caps the deposit, and incorporation of underlying turbidite rip-up clasts suggests that the lower megabreccia was emplaced subaqueously.

The upper megabreccia is ~40 m thick within Split Mountain Gorge, where it is thickest, and thins to the northwest and southeast. It is ~15 – 20 m thick in Oyster Shell Canyon #2, ~ 10 – 15 m thick in Oyster Shell Canyon #3, and < 10 m thick at its northwestern most extent at Lycium Canyon. Within Lycium Canyon the upper megabreccia is seen to also thin laterally to ~1 m at the edge of the deposit, perhaps as multiple fingers of debris flows that minimally inject into the underlying turbidites (Fig. 21 A). To the southeast, in Crazycline Canyon the upper megabreccia is ~10 – 20 m thick, and in Cairn Canyon it is ~ 10 – 15 m thick. In many locations within the field area, however, it is difficult to determine the thickness of the upper megabreccia. The top of the deposits is highly undulatory, and the base often penetrates the underlying turbidites. This results in mounds of upper megabreccia exposed in canyon walls with no clear indication of how much of the deposit is actually exposed.

Where the deposit is thinnest to the northwest, in the vicinity of the southern entrance to Lycium Canyon, the megabreccia loses characteristics that classify it as a sturzstrom, and instead appears to be more akin to a subaqueous debris flow. In these locations where the lateral flanks of the deposit is exposed, the range of clasts becomes almost bi-modal: ~5 – 15 cm clasts are common, the matrix contains pebbles ~1 – 2 cm along with fine to coarse sand, and intermediate clast sizes are not present (Fig. 21 B). The matrix characteristics become more homogeneous and lack any genetic connection

with adjacent clasts. It is clear that a significant portion of the matrix is comprised of sand from the underlying turbidites. Other evidence of compositional zoning or jigsaw-puzzle fabrics is absent. The core of the deposit further into Lycium Canyon, even at one quarter the thickness of the exposed upper megabreccia in Fish Creek Wash, still retains all of the characteristics of a sturzstrom.

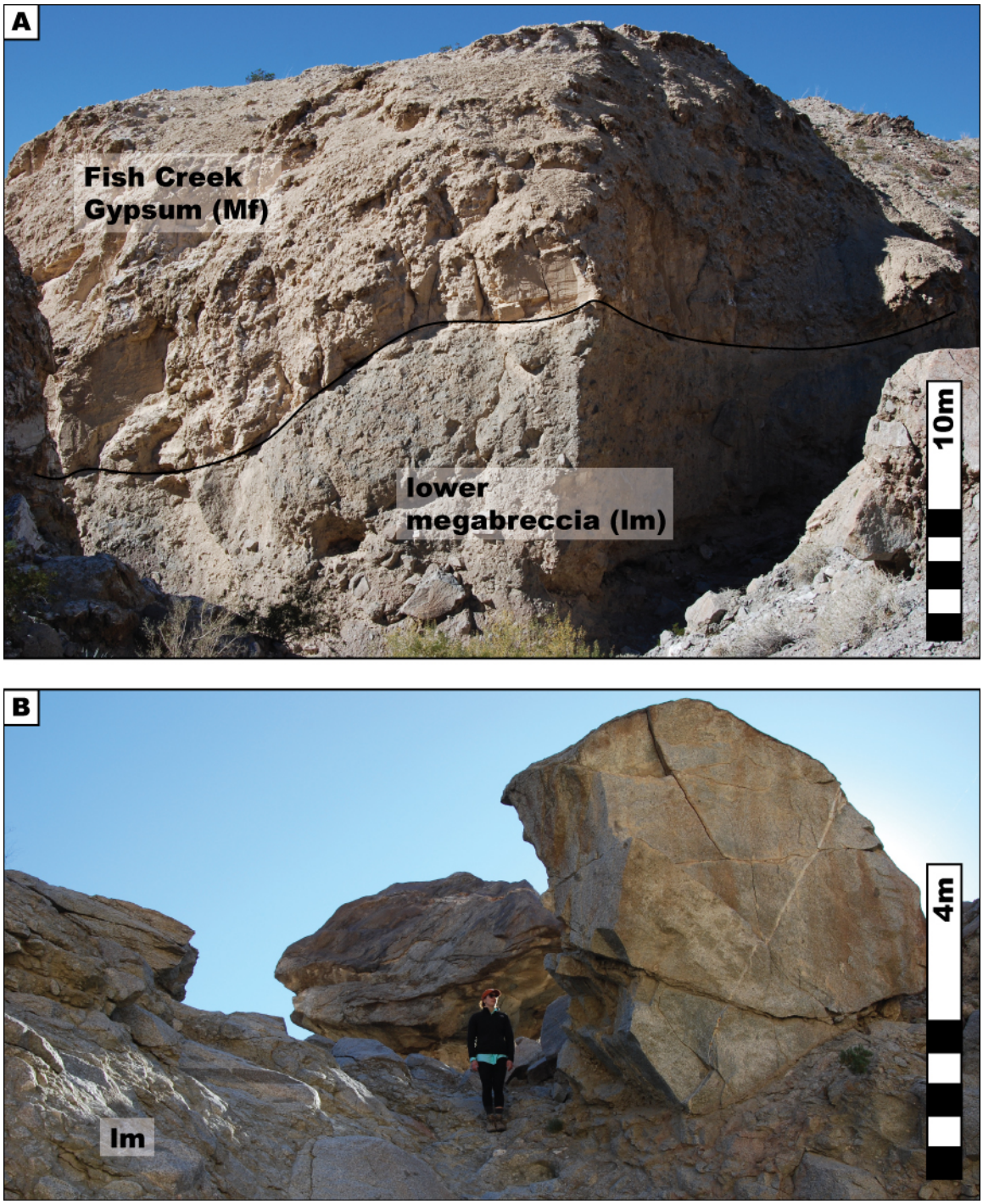

Figure 18. Megabreccia top characteristics. (A) Fish Creek Gypsum deposited on the irregular lower megabreccia top surface in Cairn Canyon. (B) Large boulders cap the lower megabreccia in Split Mountain Gorge.

Figure 19. Megabreccia top characteristics. (A) Fining-up sands cap the compositionally zoned upper megabreccia at the southern entrance to Split Mountain Gorge. (B) Upper megabreccia compositional zoning and fining-up sand cap near Oyster Shell Canyon #3.

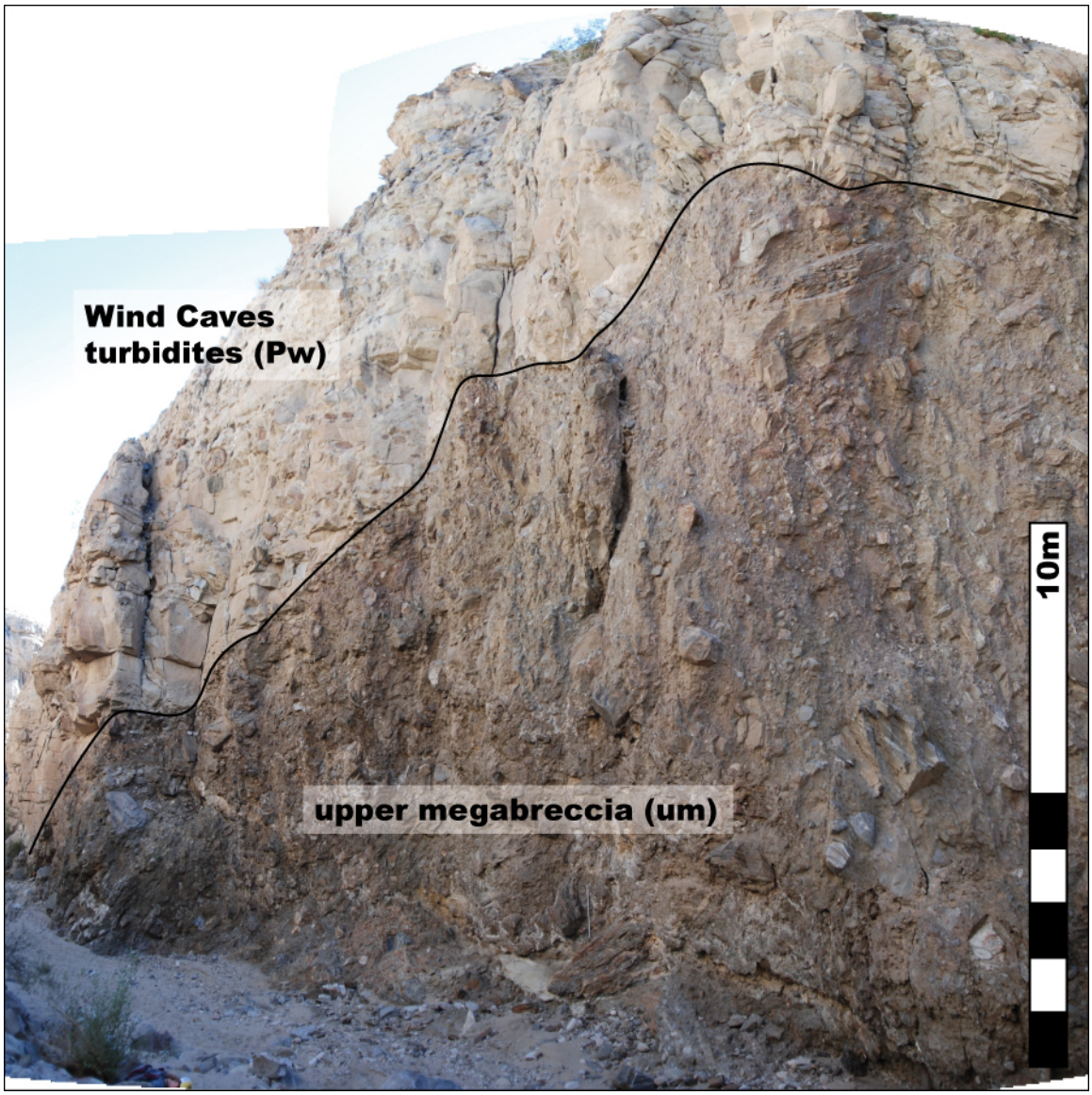

Figure 20. Megabreccia top characteristics. Bathymetric relief on the upper megabreccia top surface in Oyster Shell Canyon #3.

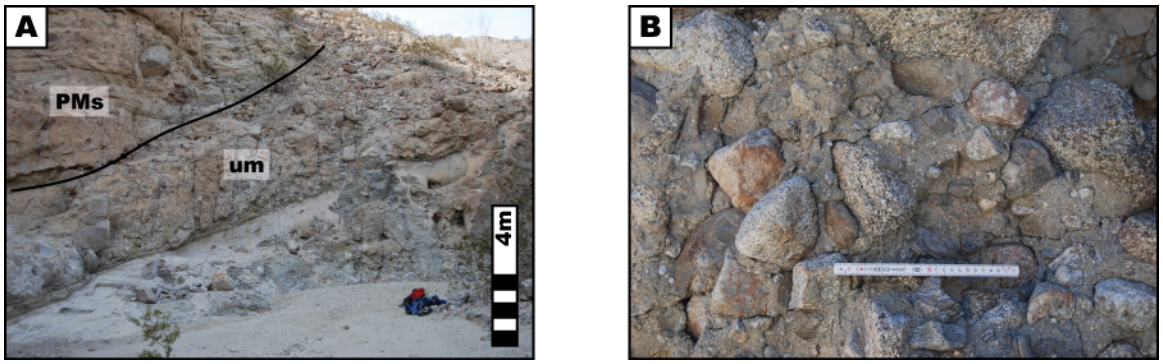

Figure 21. Upper megabreccia in Lycium Canyon. (A) Edge of upper megabreccia, transformed into a debris flow. (B) Debris flow texture.

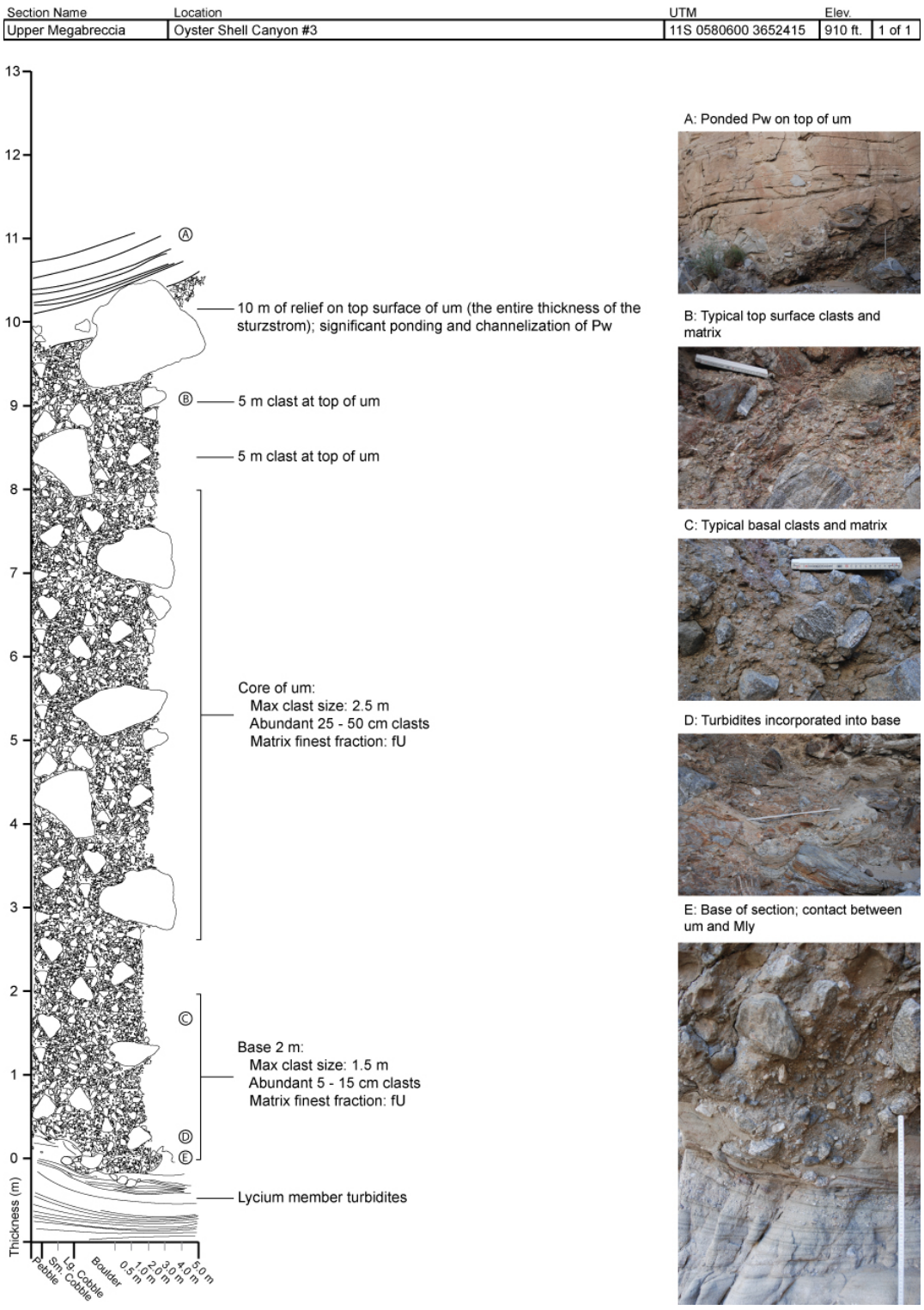

Figure 22. Upper megabreccia measured section in Oyster Shell Canyon #3.

Microscopic Characteristics

Three thin sections are presented: a "smeared" clast from the lower megabreccia in Split Mountain Gorge (Fig. 23 A), the matrix of an upper megabreccia tongue containing a crushed pegmatite streamer that was injected into the Lycium member turbidites in Oyster Shell Canyon #1 (Fig. 23 B), and the matrix of the ~1 – 2 m thick distal edge of the upper megabreccia in Lycium Canyon that showed no visible fabric in hand samples (Fig. 23 C). The texture and fabric visible in thin section suggest that both Fish Creek – Vallecito Basin sturzstroms could be considered cataclasites. This is remarkable for two reasons: (1) cataclasites are generally thought to occur in fault rocks, not rock avalanches; and (2) despite having flowed in two different fluid mediums (air and water), both sturzstroms display the features of a cataclasite.

The "smeared" clast from the lower megabreccia in Split Mountain Gorge (Fig. 23 A) shows incipient mica coalescence and complete mica coalescence into shear planes. The shear planes correspond to zones of greatest brecciation and comminution of the more competent angular quartz, feldspar, and lithic fragments. Abundant hematite is also found within the shear planes. With the exception of the mica, there is no preferred orientation of grains of individual fragments. While abundant, the plastic deformation of the mica is subordinate to the fracturing seen in the mineral grains and lithic fragments. The mica, once coalesced into a distinct foliation, could accommodate shear – resulting in sliding on the phylosillicate laminae and the brecciation of everything else. Mica grains not yet aligned are kinked as if frozen in the process of alignment.

The "smeared" clasts contain much more chlorite than other samples taken from the lower and upper megabreccias. It is clear that the foliation is related to sturzstrom flow and emplacement, but the mineralogy need not be. This particular clast could have started out rich in chlorite. However, it is intriguing to think that biotite could have been

altered to chlorite during the sturzstrom flow and emplacement. As will be discussed later in the thesis, it is likely that temperatures within the flow would have been high enough to cause such alteration. Whether there would have been enough time, however, remains unknown.

With the exception of those taken from the distal edge of the deposit in Lycium Canyon, all of the upper megabreccia samples, including the upper megabreccia sample from Oyster Shell Canyon #1 (Fig. 23 B), show evidence of extensive oxidation. In these dark zones, chlorite has been altered to hematite, and the mica + oxides coalesce in zones where the matrix is most crushed. Coupled with alteration occurring along fractures of potassium feldspar grains, it is possible that hot water, incorporated during flow and produced as a result of frictional heating, produced the alteration present in the upper megabreccia samples. Of course, it is also possible that the alteration occurred at the source area prior to the failure that produced the upper megabreccia, either at the West Salton detachment fault or an associated synthetic fault. That the alteration occurs along fractures within grains, and such fractured grains would have surely been preferentially disaggregated during the violent emplacement event that was responsible for the great comminution of all of the grains, suggests that alteration occurred during the sturzstrom event.

Additional evidence that alteration may have occurred during the event can be seen in samples taken from the distal edge of the upper megabreccia in Lycium Canyon (Fig. 23 C). Individual mineral grains and lithic fragments of quartz + feldspar in this sample are larger and more pristine. Little to no chlorite is present, and there is little evidence of alteration. If alteration occurred at the source area, we would not expect upper megabreccia in this location to look any different. If diagenetic alteration is responsible, there is no reason why this location should have been spared.

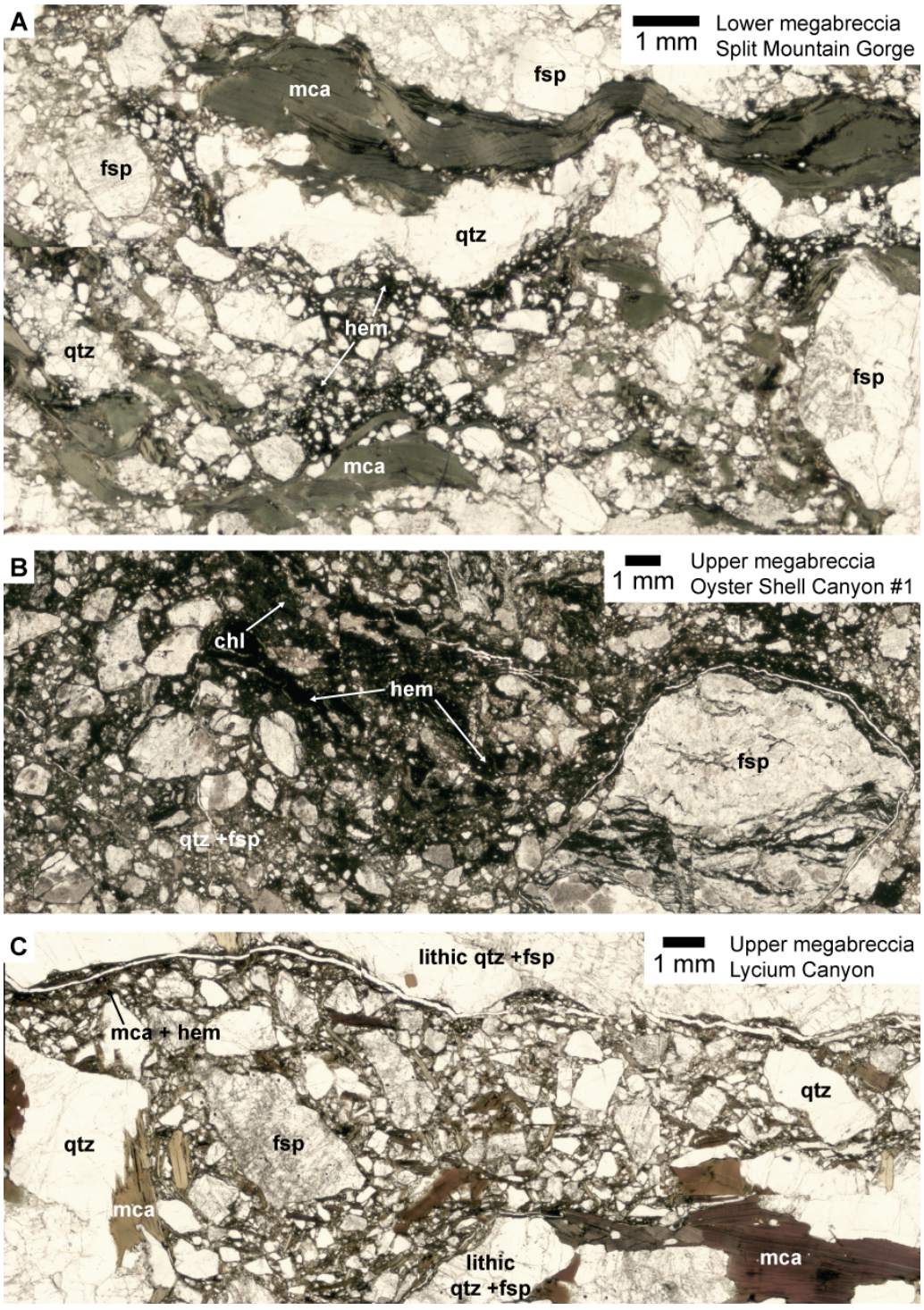

Figure 23. Thin sections of (A) lower megabreccia "smeared" clast in Split Mountain Gorge; (B) penetrating tongue of upper megabreccia in Oyster Shell Canyon #1; and (C) distal edge of upper megabreccia in Lycium Canyon.

Mass Transport Deposit and Turbidite Interaction

Basal Erosion and Deformation

Unlike the lower megabreccia, where any abrasive erosion associated with debris flow emplacement is difficult to quantify due to little evidence of underlying sediment incorporation, the upper megabreccia contains examples of significant erosion into underlying Lycium member turbidites. The degree of erosion and subsequent deformation of the turbidites does vary over the study area, however (Fig. 28). There is little erosion of the thin package of muddy Lycium member turbidites in the southeastern-most part of the field area near Cairn Canyon. Northwest of this location, just southeast of Split Mountain Gorge in the aptly named Crazycline Canyon, the upper megabreccia severely deforms the underlying sandy turbidites along a ~1.5 km length of the canyon (Fig. 24 A). Significant but unquantifiable erosion occurred at the interface between the two units as seen in the abundant truncated turbidite beds, and deformation of the turbidites into tight folds is common to depths >10 m. In Split Mountain Gorge, multiple tongues of upper megabreccia penetrate 30 m or more into the Lycium turbidites. These tongues caused >30 m of folding in the sandy turbidites and ~20 m of the transitional Lycium member to thrust into stacked horses (Fig. 25).

In other northwestern locations, such as Oyster Shell Wash #2, both erosion without deformation and erosion with significant deformation occurred. In one exposure, the upper megabreccia has clearly removed at least 10 m of Lycium turbidites and incorporated some of the sand along a shear plane ~10 – 15 m in length (Fig. 26). Further into the canyon, the upper megabreccia penetrates, deforms, and folds ~10 m of the turbidites (Fig. 24 B).

There is correlation between the thickness of the upper megabreccia and the degree of deformation seen in the underlying turbidites (Fig. 28). Upper megabreccia

penetration into the Lycium and the resulting deformation is at a maximum in an area centered on Split Mountain Gorge. Similarly, the upper megabreccia is ~40 m thick at Split Mountain Gorge, and ~20 m thick in adjacent canyon exposures to the northwest and southeast. It may also be that the degree of deformation is linked to the facies of the turbidites. The most deformation occurs in >0.5 – 1 m thick beds of sandy Lycium turbidite facies. Proximal conglomeratic facies (e.g. Stone Wash member) and distal muddy facies (e.g. distal Lycium member) are rarely deformed. The weight of the megabreccia over thick sandy turbidites may have resulted in the overpressure of interstitial fluid, making deformation more likely.

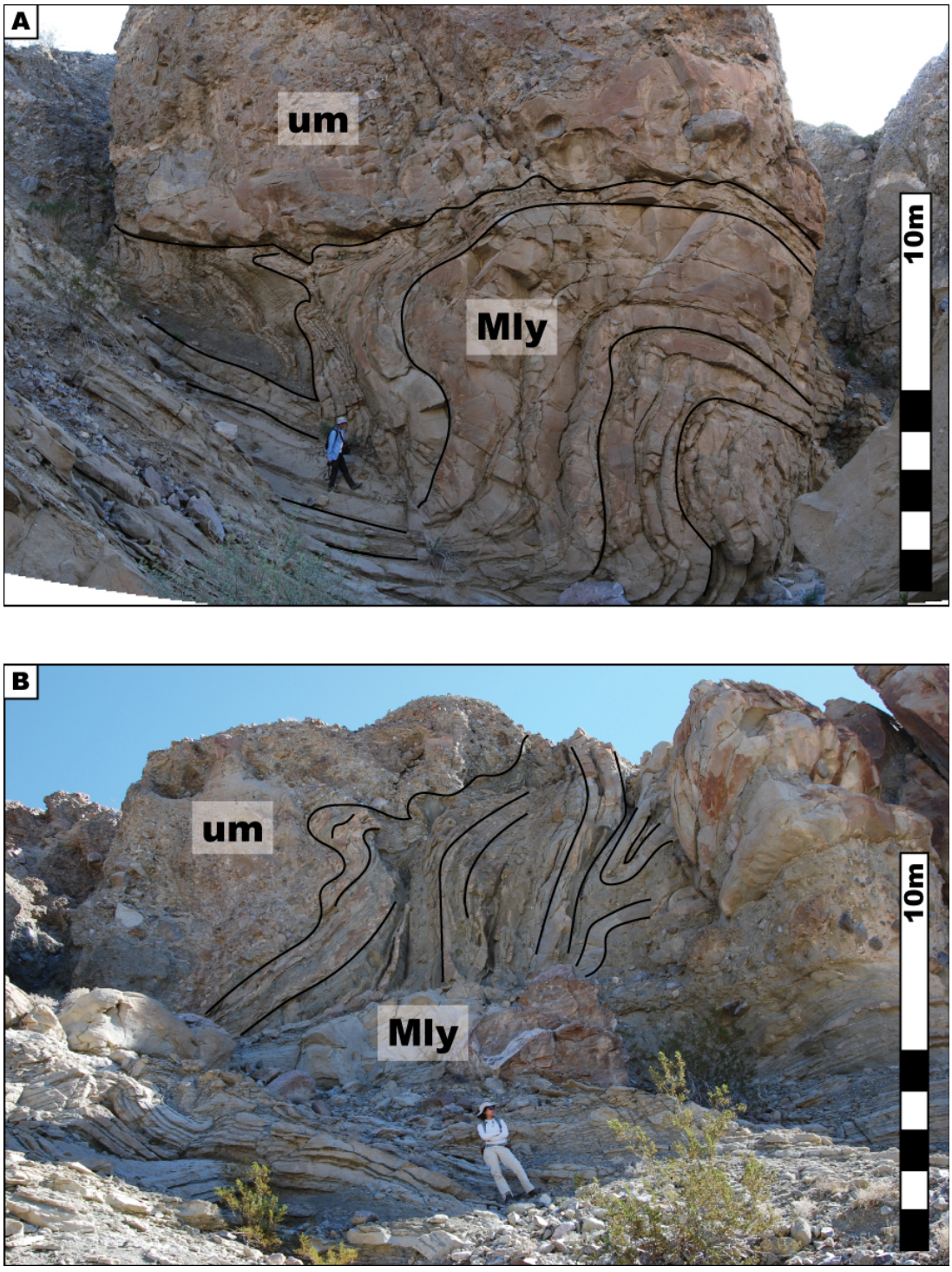

Figure 24. Upper megabreccia basal characteristics. (A) Eroded and folded Lycium member turbidites in Crazycline Canyon. (B) >10 m fold in the Lycium member turbidites in Oyster Shell Canyon #2.

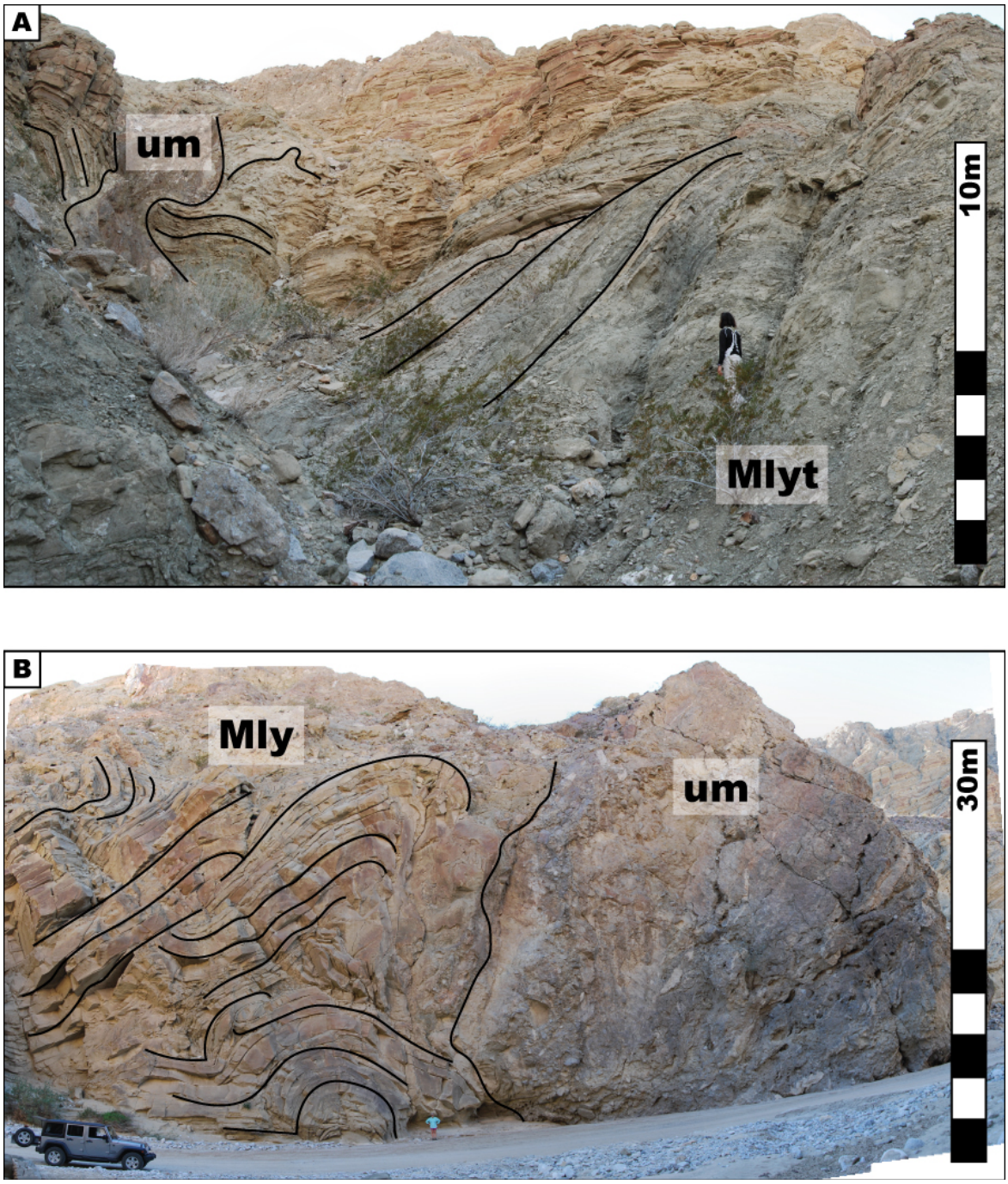

Figure 25. Upper megabreccia basal characteristics. (A) Injection of upper megabreccia into Lycium member turbidites in Split Mountain Gorge resulted in thrusts and imbricate horses in the green Lycium transitional member. (B) Injection of upper megabreccia caused ~30 m of Lycium member turbidites to fold in Split Mountain Gorge.

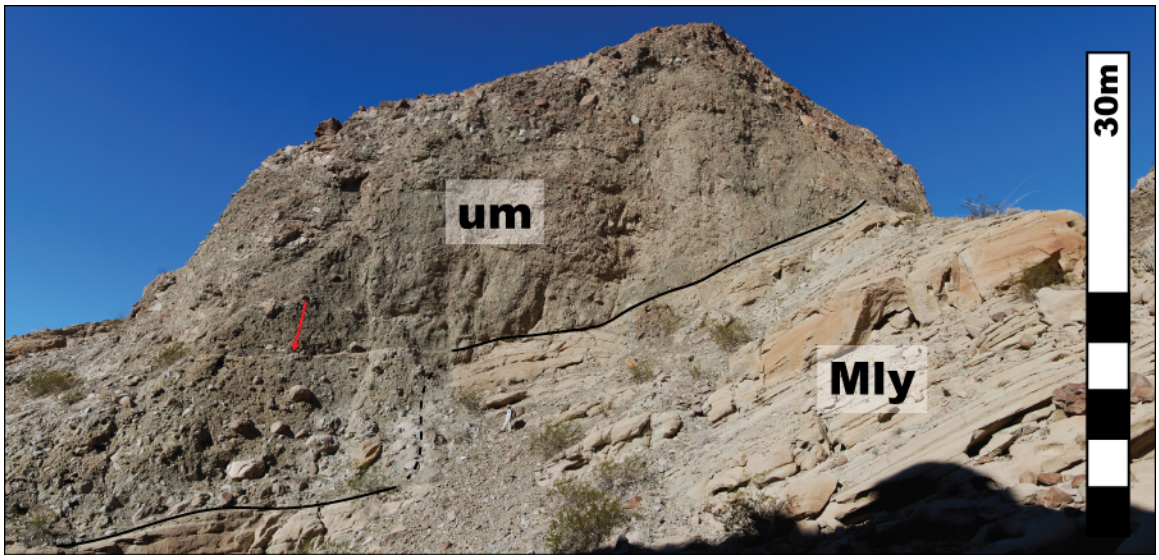

Figure 26. Sharp erosional contact between Lycium member turbidites and the upper megabreccia in Oyster Shell Canyon #2. Red arrow points to a streak of sand incorporated into the upper megabreccia.

MTD-related Paleobathymetry

Evidence for paleobathymetry created by the lower megabreccia can be seen in Oyster Shell Canyon #1. Here the lower megabreccia is not exposed, and may be absent entirely. However, this location is at the very least on the proximal edge of the debris flow (it is just northwest of the patch of lower megabreccia exposed in the west wall of Split Mountain Gorge), and may represent a paleobathymetric depression related to the evacuation or mobilization of alluvial fan sediment by the megabreccia. In this location, ~12 m of amalgamated channelized Lycium member turbidites rest on top of alluvial fans and a debris flow that may be equivalent to the lower megabreccia to the southeast (Fig. 27 A). This Lycium member outcrop is the largest amalgamated turbidite channel outcrop in the study area. In Cairn Canyon, the upper surface of the lower megabreccia and the contact with the overlying gypsum is highly undulatory, with relief on the order of ~5 m

(Fig. 18 A). In the deepest paleobathymetric / paleotopographic lows, ~2 m of the coarse sand facies newly presented in the study lies between the lower megabreccia and the gypsum.

The most striking examples of MTD-related paleobathymetry occur with the upper megabreccia. The top surface is undulatory on many scales (Fig. 28). The large protruding boulders at the top of the upper megabreccia deposit or small mounds of megabreccia creates relief on the order of 1 – 2 m, and there are numerous instances where overlying Wind Caves and Stone Wash member turbidites lap onto these features. The top surface of the upper megabreccia is also undulatory on the scale of 5 – 10 m, as evidenced by the numerous discrete patches of megabreccia outcrop and onlapping turbidites that are commonly exposed in bisecting canyons (Fig. 27 B, C and D). In Oyster Shell Wash #3, the top surface of the upper megabreccia drops down >10 m and is filled by ~1 – 2 m beds of Wind Caves member turbidites (Fig. 20). Many of the channelized turbidites that fill the paleobathymetry contain ~0.5 – 1 m rounded boulders within channel axes.

Figure 27. Channelization impact of turbidites on megabreccia. (A) Amalgamated channels of Lycium member turbidite at edge of lower megabreccia in Oyster Shell Canyon #1. (B) Stone Wash member on top of upper megabreccia in Lycium Canyon.

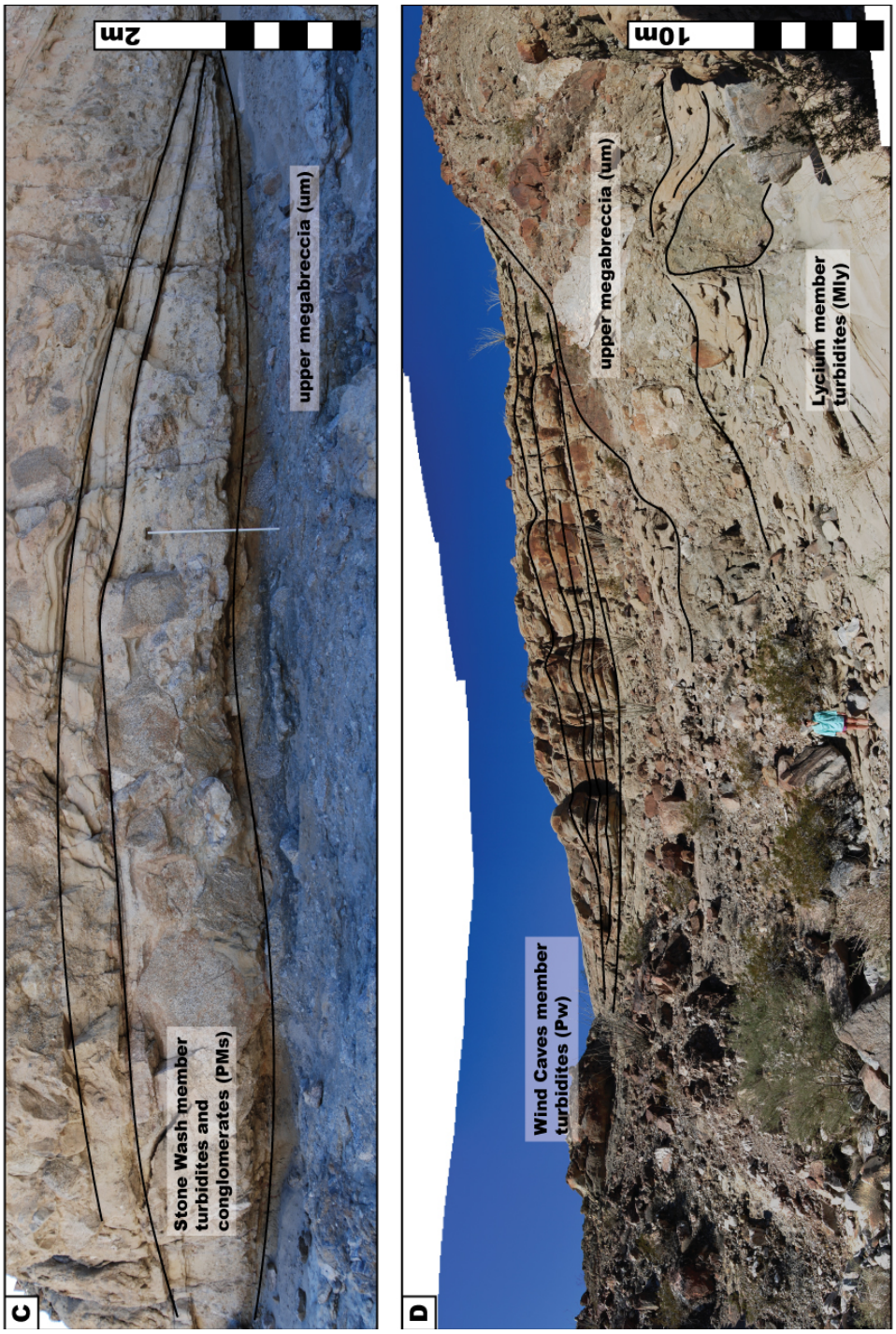

Figure 27 (cont.). Channelization impact of turbidites on megabreccia. (C) Stone Wash member on top of upper megabreccia in Lycium Canyon. (D) Wind Caves member turbidites on top of upper megabreccia near the entrance to Oyster Shell Canyon #2.

MTD Impact on Sandstone Lateral Continuity

Mass transport deposit impact on the lateral continuity of overlying and underlying sandstones occurs at multiple scales. Where relief on the upper surface of the upper megabreccia is a result of protruding boulders or small mounds, ~1 – 2 m of turbidites pond and onlap onto these paleohighs (Fig. 28). Larger-scale paleobathymetry linked to the undulatory upper megabreccia top surface creates turbidity current conduits where channelized Wind Caves and Stone Wash member turbidites fill >10 m of relief (Figs. 27 and 28). Had the Fish Creek – Vallecito Basin included periods of finer-grained sedimentation during this time interval, capping shales could have effectively cut off any lateral connectivity between adjacent depositional fairways.

The upper megabreccia has the greatest impact on the lateral continuity of sandstones through its interaction with the underlying Lycium turbidites. As discussed previously, there are many instances where tongues of upper megabreccia penetrate 30 m or more into the Lycium turbidites and cause >30 m of folding (Figs. 25 and 28). This incision and deformation significantly disrupts what were once contiguous sandstone beds and results in the partitioning of the sandstones into isolated packages.

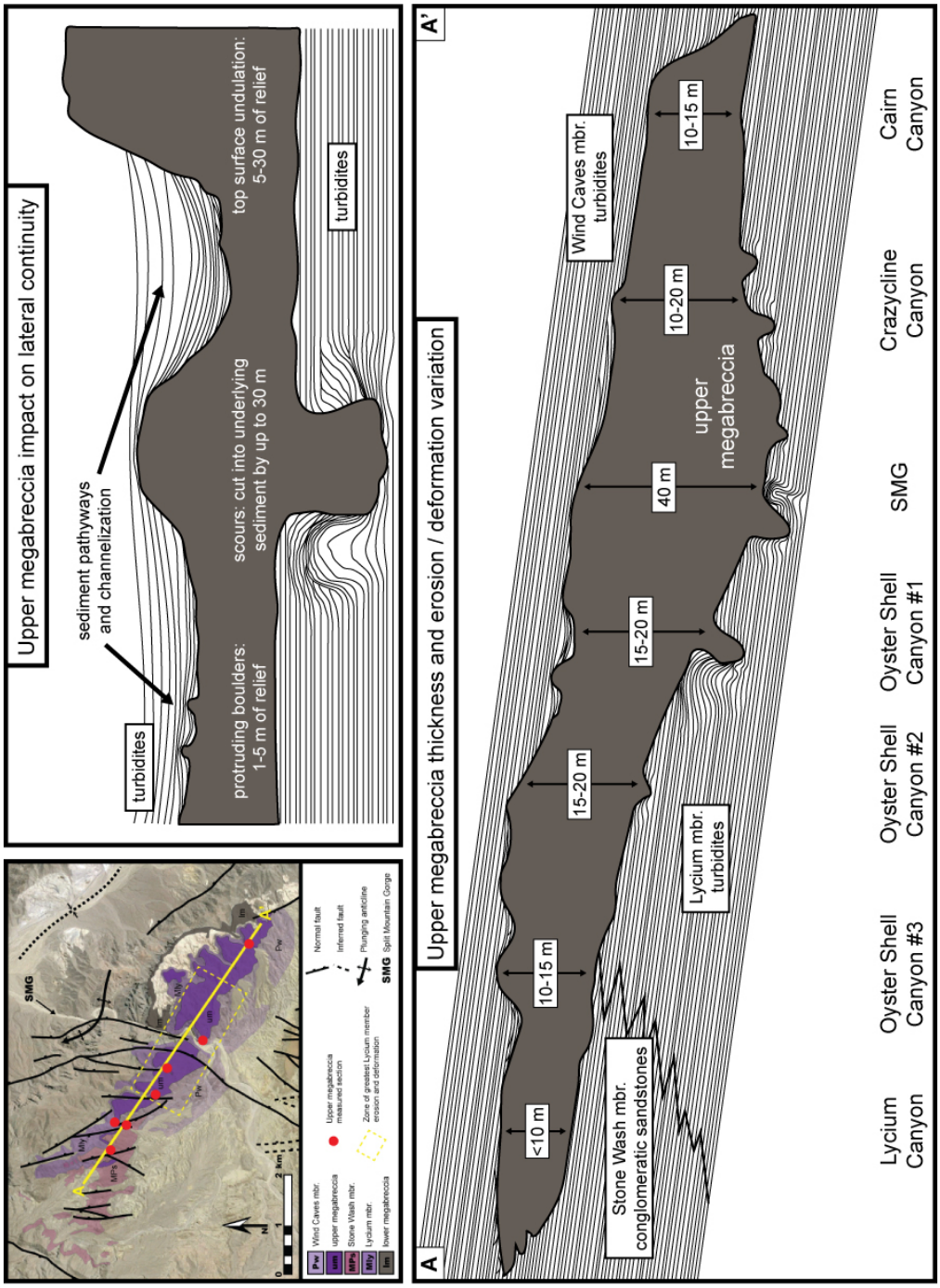

Figure 28. Upper megabreccia thickness variation, degree of underlying sediment erosion and deformation variation, and upper megabreccia impact on lateral continuity of overlying and underlying sediment.

Discussion

Fish Creek – Vallecito Basin Paleogeographic Reconstruction

A valid paleogeographic reconstruction in the Fish Creek – Vallecito Basin must honor the topographic lows suggested by the earliest rift-related deposits, lateral facies transition representing proximal and distal locations, laterally equivalent facies especially between the Split Mountain Gorge area and the Coyote Mountain area, periods of non-deposition or non-Split Mountain Gorge-related deposition south of the Fish Creek Mountains and north of the Coyote Mountains, and on-lap and pinch-out onto basement exposures. It also requires recognition that the West Salton detachment fault was likely closer to the Split Mountain Gorge area in the late Miocene, and that now-buried synthetic normal faults may have existed to the east of the detachment fault. The resulting paleogeographic reconstruction is the first to integrate the above evidence to chronicle a detailed history of the Fish Creek – Vallecito Basin that covers its two most defining events: the sudden transition from subaerial to marine deposition, and the arrival of the Colorado River delta margin.

It is important to note that there has been ~35˚ of clockwise rotation of the basin that has occurred over the past ~1 Ma (Winker and Kidwell, 1996). The following paleogeographic reconstruction references cardinal direction based on the present day orientation of the basin.

During late Miocene Elephant Trees Formation lower conglomerate member and lower sandstone member deposition (Fig. 29 A), paleocurrent direction in the alluvial fan conglomerate was dominantly to the east-northeast. A monomictic clast composition similar to that of the present day Vallecito Mountains requires a source to the southwest of Split Mountain Gorge. Minimal early slip on the West Salton detachment fault and/or the presence of synthetic normal faults provides an appropriate source location and clast

lithology for the alluvial fan sediment. The lower sandstone member, representing distal alluvial fan and braided stream deposits, occupied the deepest part of the basin and flowed to the north. At this time, there was little to no deposition in the area between the Fish Creek Mountains and the Coyote Mountains. Exposed in this elevated area were mid-Miocene volcanics and sandstones of the Alverson and Red Rock formations, which are considerably older (~14 – 24 Ma) than the ~6.3 – 8 Ma Elephant Trees Formation.

The transition from subaerial deposition to subaqueous deposition and first influx of marine water from the Gulf of California is a brief, but important period of time in the basin's history from ~6.57 Ma to 6.27 Ma (Fig. 29 B). Failure of Vallecito Mountain basement rock triggered the collapse of a basin wall and the emplacement of the lower megabreccia. Stratigraphic relationships and the absence of the lower megabreccia northwest of Split Mountain Gorge suggests that the lower megabreccia primarily came to rest on top of the distal alluvial fans and braided stream deposits of the lower sandstone member in the deepest part of the basin. Soon after, a small amount of marine water entered a deep basin that was already significantly below sea level. Evaporation and occasional recharge of marine water resulted in the deposition of the Fish Creek gypsum.

It is unclear from what direction the marine water entered. Given the lack of marine deposition in the area between the Coyote and Fish Creek mountains at this time, and evidence in the gypsum deposits suggesting deep basin – shallow water deposition, flow to the north over the Coyote Mountains is unlikely. Winker (1987) referred to the Fish Creek Gypsum as "pre-marine" evaporites, and suggested that the evaporite basin could have been connected to the advancing Gulf of California by a permeable sill or narrow passage. Dean (1996) determined that the thickest gypsum was originally located in the northwest-trending wash adjacent to the U.S. Gypsum company quarry, which

would have been the deepest part of the basin at the time and again corresponds to the location of the distal alluvial fan and braided stream deposits. The gypsum pinches out near northern entrance of Split Mountain Gorge, where it interfingers with the transitional alluvial fan / turbidite facies. This may suggest that marine water entered the basin from the northeast, but infiltration from the southwest, possibly along the West Salton detachment fault or related faults, is more likely.

Full flooding of the already deep basin and deposition of Lycium member marine turbidites in water depths >150 m, two key facts that are new to this study, occurred ~6.27 Ma (Fig. 29 C). Paleocurrent direction indicates deposition from the west-southwest, the same as the alluvial fans. The basin configuration remained the same, with proximal Elephant Trees Formation alluvial fan and Stone Wash member shallow marine conglomerates abutting the basement highs and ringing the basin. The thickest and sandiest Lycium turbidites exposed in outcrop are found in the area of Split Mountain Gorge. The entire turbidite package thins dramatically, and individual beds become thinner and finer-grained in the vicinity of Cairn Canyon. These facies relationships suggest that, as was the case with alluvial fan, lower megabreccia, and gypsum deposition, this area represents the deepest, most distal basin portion of the basin at the time. In the Fish Creek and Coyote mountain areas, Garnet Formation conglomerates, highly fossiliferous Andrade member sandstones, and an Andrade carbonate platform were deposited. These units are distinct from the Stone Wash and Lycium member deposits deposited in the area of Split Mountain Gorge.

The rapid lateral facies changes around the Split Mountain Gorge area may be attributed to steep slopes and complex paleogeography within a small basin, perhaps only a sub-basin within the larger Fish Creek – Vallecito Basin at late Miocene time (Winker and Kidwell, 1996; Dorsey et al., 2011). The transition from subaerial to subaqueous

deposition, however transitional, is a dramatic one because base level rose significantly due to great water deepening. Irrespective of microfossil-based paleobathymetric estimates of relatively shallow (inner neritic) water, the Lycium member turbidites require >150m water depth. This and other evidence suggests that the dramatic deepening was caused by marine infiltration through a sill breach or other catastrophic breach into an already topographically deepened landscape.

A second collapse of basin walls trigger the emplacement of the upper megabreccia (Fig. 29 D). Based on clast lithology and an inferred paleoflow direction to the north, a Vallecito or Fish Creek mountain source area is unlikely. The Stone Wash member conglomerates closest to the Vallecito Mountains retain a monomictic clast lithology, but those further away are polymictic and contain metamorphic clasts not present in the Vallecito Mountains. Therefore a now-buried basement exposure directly to the south that contained abundant metamorphic lithologies is the favored source location for the upper megabreccia. Again the bulk of the upper megabreccia was deposited close to the deepest part of the basin, although there is evidence that the flow traveled up the northwestern paleoslope and came to rest on the proximal shallow water Stone Wash member conglomerates.

Reversal of paleoflow to the south and the arrival of the first Colorado River-derived sediments occurred ~5.3 Ma (Fig. 29 E). Wind Caves member turbidites enter the basin from the north, and the Split Mountain Gorge area remains distinct from the continued deposition of the Garnet Formation conglomerate and Andrade member sandstones in the area north of the Coyote Mountains.

Full integration of the Fish Creek – Vallecito Basin with the larger Salton Trough occurs ~5.1 Ma, signaled by the arrival of the Colorado River deepwater slope sediments of the Deguynos Formation Mud Hills member (Fig. 29 F). The Mud Hills member

mudstones and rhythmites completely filled bathymetric lows, and are the first marine sediments to cover the Fish Creek Mountains basement high and the Andrade member sandstones in the vicinity of the Coyote Mountains. Alluvial fan and proximal shallow marine conglomeratic facies were most likely always present at the basin margins. In this reconstruction, the coarse proximal Split Mountain and Imperial group facies give way to Canebrake Conglomerate-equivalent facies. Most importantly, the southward advancing Colorado River margin entered the deeper water of the Fish Creek – Vallecito basin as a spectacular ~500 – 800 m high sedimentary prism, represented by the Mud Hill member at its base to the sandy shelf and fluvial sediments of the Camels Head member and the Arroyo Diablo Formation. Many previous workers failed to recognize the significance of the Mud Hills, Camels Head, and Arroyo Diablo members as contemporaneous facies of a southward-advancing Colorado River delta margin clinoform that likely extended laterally, albeit irregularly, to the eastern basin margin.

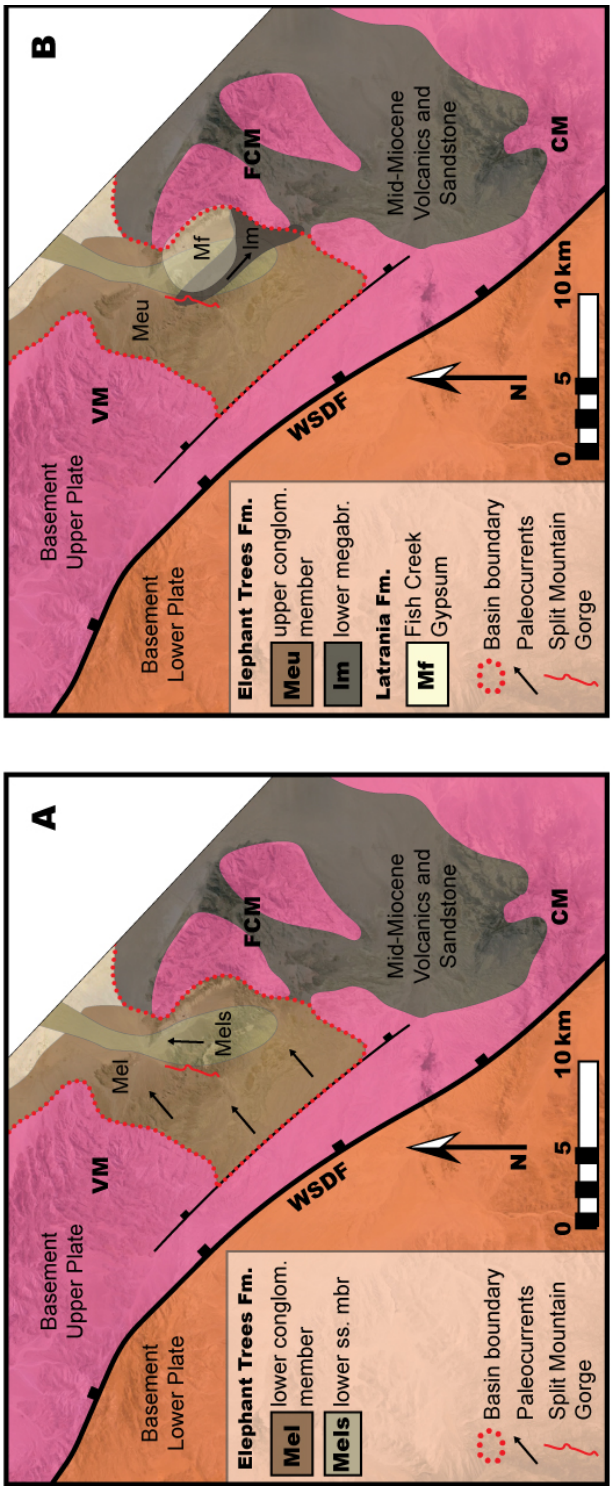

Figure 29. Paleogeographic reconstruction of the Fish Creek – Vallecito Basin. See text for full description.

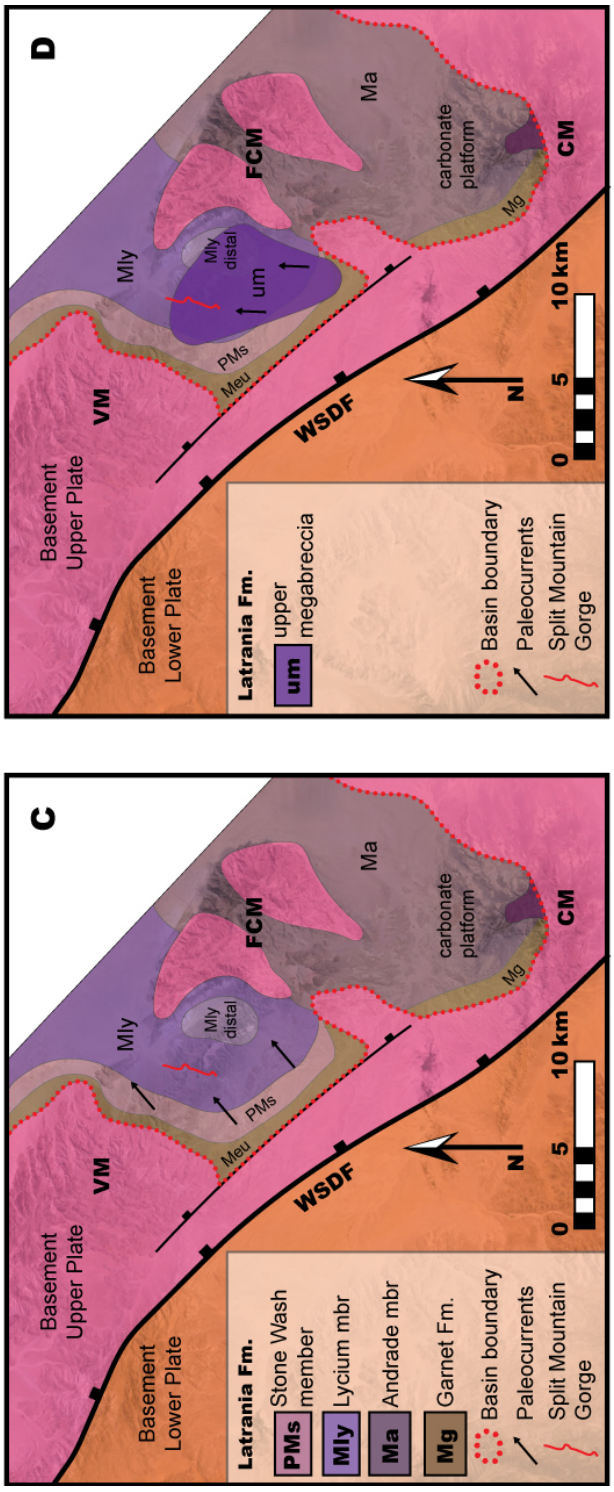

Figure 29 (cont.). Paleogeographic reconstruction of the Fish Creek – Vallecito Basin. See text for full description.

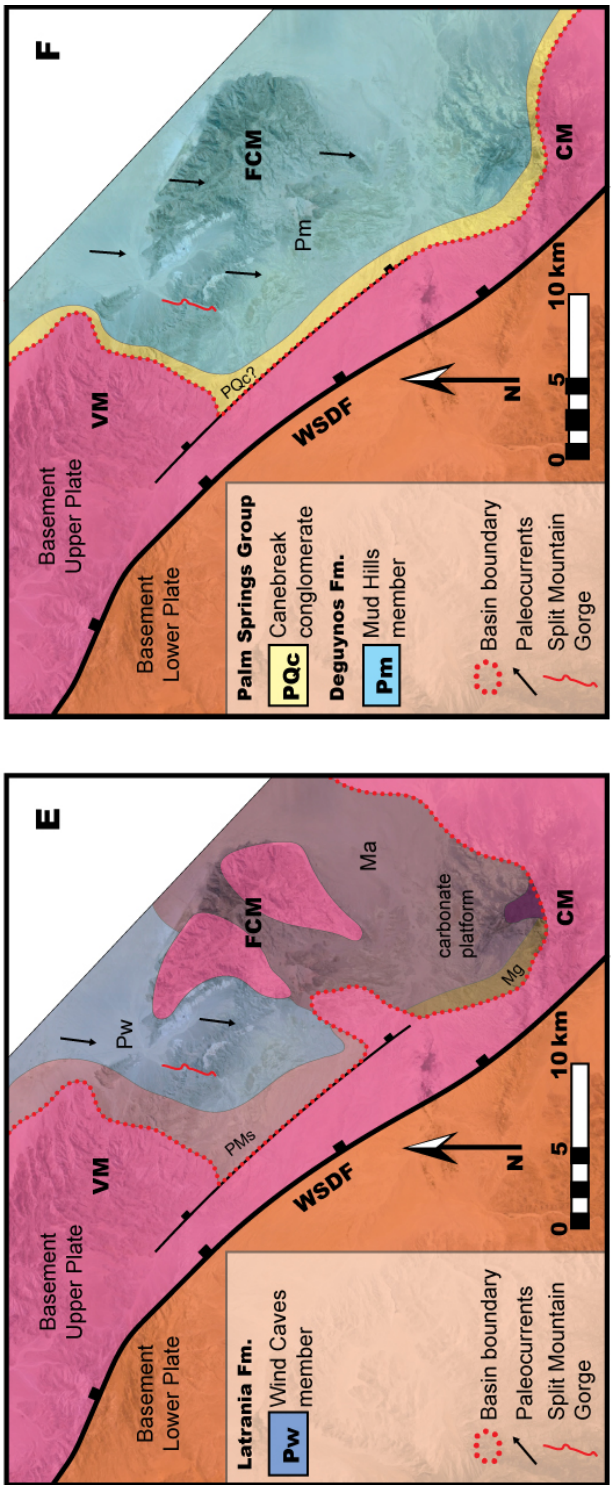

Figure 29 (cont.). Paleogeographic reconstruction of the Fish Creek – Vallecito Basin. See text for full description.

STURZSTROM EMPLACEMENT MECHANISMS

The emplacement mechanism that can explain the variety of feature and flow observations associated with sturzstroms, such as their long run-out, jigsaw-puzzle fabric, and compositional zoning, is still a matter of debate. Sturzstroms are excessively mobile, traveling farther than predicted by a simple frictional sliding model. Their run-out approximately increases in proportion to the flow volume (Legros, 2002; Hungr and Evans, 2004). Based on eyewitness accounts, sturzstroms flow at speed in excess of 50 m/s as if a torrential river of rock. All show great degrees of comminution, and little evidence of mixing as a turbulent flow. There is also evidence that sturzstroms dilate during emplacement, with a ~20 – 30% volumetric increase. Irrespective of their variability in lithologic composition (crystalline igneous rock, volcanic rocks, and carbonates) and depositional environment (subaerial, subaqueous, and even on Mars), sturzstroms share these common characteristic elements, and most likely a common mechanism of motion and emplacement (Bowman et al., 2012). Legros (2002), Hungr and Evans (2004), and Hungr (2006) provide detailed reviews and criticisms of proposed hypotheses that attempt to explain the mobility of long-runout landslides. Included here is only a brief summary of the main emplacement mechanism hypotheses.

Many hypotheses involve a fluidizing medium to explain sturzstrom mobility. Based on study of the Elm, Frank, and Blackhawk landslides, Shreve (1968) proposed that early in a rock avalanche flow it is able to override and entrap a substantial volume of air by launching over irregular topography. This easily sheared air cushion provides lubrication and enables the sturzstrom to slide, rather than flow, resulting in high emplacement velocities and longer run-out distances. Leakage of the trapped air causes the slide to come to an abrupt stop, and creates the lateral and transverse ridges, imbricate thrusts, and the hummocky upper surface common to many sturzstroms. The

comminution and jigsaw-puzzle fabric is created by the fracturing of clasts by the impact, which remain um-mixed because of the lack of further movement. De Blasio (2008) noted that the high shear rates at the base of flows could produce frictional heat that may cause any water present to quickly be brought to a boil. This production of a lubricating vapor combined with low permeability within the flow could cause increased vapor pressure and a reduction in the co-efficient of friction.

Other emplacement hypotheses invoke granular flow models where fluid sturzstrom motion is caused by stress transmitted from grain-to-grain collisions, referred to by Bagnold (1954, 1956) as cohesionless grain flow. Kinetic energy is transferred by these collisions and is dissipated by friction (Hsü, 1975). Hsü (1975) believed that Shreve's sliding model was incorrect, and that sturzstroms did flow as a mass of cohesionless grains. He proposed that pulverized rock dust distributed throughout the flow provided dispersive stress that effectively reduced the co-efficient of friction. Melosh (1979) proposed that acoustic fluidization, or the reduction of inter-particle friction by acoustic-frequency vibrations at the base of the flow, could account for the long run-out distances of sturzstroms.

Mechanical fluidization, a process of spontaneous reduction of friction at high rates of shearing due to dispersive pressures present within the flow, is a model favored by Davies (1982), Davies and McSaveney (1999), Hungr and Evans (2004), and Davies and McSaveney (2009). Despite the wide range of conditions in which high mobility sturzstroms occur, an intense comminution of debris is always present. These workers proposed that very high local pressures are created when grains within the flow fragment and collide, which reduces intergranular effective stress and the frictional resistance to shear, and results in an increase in landslide velocity and travel distance. Additionally, shear distributed throughout a significant depth of a flow will generate dispersive

pressure that causes dilation of the flow. This dynamic fragmentation increases the areal dispersion of debris and also contributes to greater sturzstrom run-out.

That sturzstroms could slide over a thin layer of rock melted by the intense friction at their bases was proposed by Erismann (1979), Heuberger et al. (1984), Masch et al. (1985), Legros et al. (2000), and De Blasio and Elverhøi (2008). Concentration of shear at the base of the slide produces sufficient frictional heat to induce melting in non-carbonate rocks, referred to as frictionite or hyalomylonite, which is similar to pseudotachylites found in tectonic shear surfaces. There are currently three documented instances of melting at the base of sturzstroms: rock avalanches of crystalline and metamorphic rocks at Koefels in Austria and Langtang in central Nepal, and the Arequipa volcanic landslide in Peru. Masch et al. (1985) conducted transmission electron microscopy (TEM) analysis of the Koefels and Langtang slides, found that the glassy matrix formed by the partial to almost complete melting of the granitic to granodioritic host rocks, and estimated minimum temperatures of 1520° C based on the presence of partially melted quartz grains. Legros et al. (2000) observed that frictionite only occurs at the base of the thickest (~300 m) central part of the Arequipa landslide deposit and below landslide deposits that are several hundred meters thick at Koefels and Langtang. Landslide deposits less than 100 m thick do not possess a melted basal surface, which suggests that the thickness of sturzstrom deposits is an important variable controlling the formation of frictionite at their base. Hungr and Evans (2004) cautioned that while rock melting may occur in some cases, where a rockslide is unusually thick, it might not be a widespread phenomenon due to the paucity of examples reported in the literature.

Pertinent to the contemplation of sturzstrom emplacement mechanisms is the distribution of shear. As we can glean from the assorted hypotheses presented above,

there is no consensus as to whether sturzstroms travel as a plug overriding a surface of intensely focused shear, or if they flow as a result of distributed shear with the body.

Bowman et al. (2012) suggested that there is relatively little shearing within the body of a sturzstrom. Davies and McSaveney (2009) reported that shear in grain flows has been shown to often be concentrated in 5-to-10-grain-deep shear localizations or shear bands, which may develop ephemerally at all locations in the flow. In this scenario the entire grain mass would experience shear, but shear would not be continuous at any one location. While shear banding is commonly reported in deposits of comminuting grain flows, such as deposits of volcanic debris avalanches and in the shear zones of earthquake faults, it is not typically observed in rock avalanches as there is little evidence of shear localization. In a study of Koefels and Langtang frictionite, Masch et al., (1985) attributed inclusions containing microstructures typical of plastic deformation at high temperatures as features inherited from previous tectonic events.

According to Crosta et al. (2007), however, both sliding and internal deformation contribute to the motion and deposition of sturzstroms. Calculations by Legros et al. (2000) showed that, of the total energy released during sturzstrom emplacement, only a small portion would be used to melt the base of the flow. Sturzstrom emplacement may therefore be dominated by stresses that affect the entire flow body and not those concentrated in only a thin basal layer.

Micro-scale fabrics present in both the subaerial lower megabreccia and the subaqueous upper megabreccia in the Fish Creek – Vallecito Basin (Fig. 23) suggest that some degree of shear is accommodated within the flow. Zones of coalesced mica and highly comminuted mineral grains and lithic fragments form countless shear planes. Sliding on the phylosillicate laminae and the fracturing, rotation, and frictional sliding of the more competent grains did accommodate movement and displacement within at least

the basal 5 m of the flow and within tongues of upper megabreccia injected into underlying turbidites.

Internal movement was sufficient to produce a cataclasite that resulted in meters to perhaps tens of meters of displacement within the sturzstrom (Behr pers. comm., 2015). On the whole, however, it appears that the bulk of the shear and displacement was accommodated at the base of the flow, and not within the flow itself. A combination of plug flow on an intensely focused zone of shear at the base of sturzstroms (in some rare occasions resulting in melting and frictionite production) and mechanical fluidization and distributed shear within the flow (perhaps as ephemeral shear localizations throughout the flow) is likely responsible for the macro-scale fabrics, long run-out distances, and high emplacement velocities common to all sturzstroms.

MTD-Turbidite Interaction

MTDs and MTCs can represent a significant portion of slope and basin floor deposition and significantly modify existing slope and basin bathymetry through the evacuation of the failed sediment and their erosive power during flow. MTDs and MTCs create new bathymetry on their surfaces that may reorganize sediment pathways and influence subsequent sediment deposition. They may also significantly impact the lateral continuity of underlying deposits through irregular erosion and injection along their basal surface. Exposures in the Fish Creek – Vallecito Basin of upper megabreccia interaction with underlying and overlying turbidites provide useful outcrop analogs to similar features present in seismic data, and highlight the near ubiquitous erosion, deformation, and accommodation space creation that is present in such systems but remains undetectable at scales below seismic resolution.

The basal surfaces of MTDs are variable in the degree of erosion and in the geometry of the surface. Some MTD and MTC basal surfaces imaged through seismic-reflection data are planar and show little evidence of erosion. Using the Fish Creek – Vallecito Basin upper megabreccia as an outcrop analog, this study shows that significant erosion and deformation of underlying sediment during MTD flow nevertheless may have taken place, albeit at a scale that is undetectable in seismic-reflection.

With their ability to image extensive volumes of rock over several kilometers, seismic studies have an advantage of scale. Limited outcrop exposures may make it difficult to determine how much removal of underlying sediment had occurred, however. Weimer and Shipp (2004) described a as a common feature of MTDs and MTCs a stair-step basal surface profile where, from one side of the debris flow to another, the degree of erosion varies and the basal decollement is located at different depths. An outcrop analog to this broad spatial variability in erosion imaged in seismic data is found in the Fish Creek – Vallecito Basin study area. The greatest degree of erosion and deformation of the underlying Lycium member turbidites by the upper megabreccia occurred in the vicinity of Spilt Mountain Gorge and the Fish Creek Wash (Fig. 28). In these locations the upper megabreccia reaches its maximum thickness and the turbidites are thickly bedded, coarse-grained, and channelized. Significantly less erosion and deformation of the turbidites occurred to the northwest and southeast, where the turbidite facies are proximal conglomeratic debris flows and distal thin-bedded and finer-grained basin floor deposits respectively.

It has been suggested that where sea-floor topography acts to confine the flow, erosion of the underlying sediments may be the greatest, and that differences between the axial and peripheral parts of the MTC may also be linked to flow confinement control over the degree of basal incision. While this study does not contradict the assessment that

flow confinement could result in increase erosion of underlying sediments, it does offer an additional factor that may influence the degree of erosion produced. As discussed previously, the greatest amount of erosion and deformation seen in the study area occurs in >0.5 – 1 m thick beds of sandy Lycium turbidite facies. Proximal conglomeratic facies and distal muddy facies appear to have been significantly less eroded and deformed. The weight of the megabreccia over thick sandy turbidites may have resulted in the overpressure of interstitial fluid, making erosion and deformation more likely. Therefore both the thickness of the debris flow and the characteristics of the underlying sands may impact the degree of erosion and deformation that occurs.

Another feature common to the basal surfaces of MTDs and MTCs are the significant linear grooves or megascours, often more than 30 m deep, reported in seismic studies by Moscardelli et al. (2006), Ortiz-Karpf et al. (2015) and other workers. Although a linear nature could not be confirmed due to a patchwork of exposures, there is ample outcrop evidence of erosion at similar scales in the Fish Creek – Vallecito Basin, especially in the vicinity of Split Mountain Gorge (Fig. 25) and Oyster Shell Wash #2 (Fig. 24 B). The creation of these megascours has been attributed to blocks or clasts transported by the flow (Weimer and Shipp, 2004). Outcrop exposures of highly erosive penetrating upper megabreccia tongues or lobes do not contain abnormally large clasts relative to the size of the lobes, which suggests that contrary to these seismic studies transported blocks or clasts may not be required to produce erosional lineations or megascours.

Bathymetry created by MTDs and MTCs significantly controls the distribution and overall architecture of overlying deposits (Moscardelli et al., 2006; Armitage et al., 2009; Mulder and Etienne, 2014). The Fish Creek – Vallecito Basin contains numerous

outcrop examples of upper megabreccia modification of available accommodation space that influenced subsequent turbidite deposit distribution and geometry on multiple scales.

Bathymetric lows on the irregular upper megabreccia top surface acted as sediment pathways which resulted in the deposition of thick channelized Wind Cave member turbidite facies. Ponding on the upper megabreccia surface created local, lateral compartmentalization of turbidites at various scales within the study area (Figs. 27 and 28). Given sufficient deposition of finer-grained sediment, entire depositional packages could have been isolated and compartmentalized. These outcrop observations of ponding and compartmentalization are in line with seismic study observations reported by numerous workers (Shor and Piper, 1989; Pickering and Corregidor, 2000; Pickering and Corregidor, 2005; Armitage et al., 2009; Mulder and Etienne, 2014).

Moscardelli et al. (2006) showed in their seismic study of MTCs on the deep-marine margin of eastern offshore Trinidad that the thickness of an overlying turbidite levee-channel system is greatest along the axial trace of the underlying MTC, and attribute this to excess accommodation space in the erosive channel left underfilled by the MTC during flow, erosion, and deposition. A similar relationship between the upper megabreccia and the overlying Wind Caves member turbidites exists in the study area. The thickest, channelized facies of the Wind Caves turbidites are located in an area centered on the Fish Creek Wash. This is also where the upper megabreccia is the thickest and where the greatest degree of erosion and deformation of the underlying Lycium member turbidites had occurred (Fig. 28).

Accommodation created by MTDs and MTCs is a product of an irregular top surface that can often be linked to a complex internal structure generated during flow and emplacement. Olafiranye et al. (2013) documented tens of meters of relief created by the buckling of an upper MTD surface during emplacement of debris flows offshore Angola,

a feature Weimer and Shipp (2004) described as common to MTD and MTC deposits. In the Fish Creek – Vallecito Basin, the irregular upper megabreccia top surface is expressed as numerous discrete patches of megabreccia outcrop and associated onlapping turbidites commonly exposed in bisecting canyons. These outcrops can be linked to the imbricate thrusts and lateral pressure ridges expressed at the distal end of MTD and MTC flows described in seismic by Weimer and Shipp (2004), and to the same features present on the Blackhawk landslide sturzstrom studies by Shreve (1968).

Outcrop exposures in the Fish Creek – Vallecito Basin also compare favorably to other outcrop analogs described in previous MTC and MTD studies. Pickering and Corregidor (2005), in their investigation into MTC-created accommodation space in confined basin-floor submarine fan outcrops in the south Spanish Pyrenees, reported ~35 m of paleobathymetry which influenced turbidity current flow and turbidite depositional morphology. Paleobathymetry created by the upper megabreccia in the study area is similar in scale.

The architectural evolution of the Wind Caves member turbidites deposited on top of the upper megabreccia is similar to that described by Armitage et al. (2009) in the Cretaceous Magallanes foreland basin of southern Chile. In both instances, the initial sandstone beds deposited on the irregular debris flow surface filled any paleobathymetric lows and pinched out onto the relative paleobathymetric highs. As sedimentation progressed, the irregular surface of the debris flow deposit was smoothed, confinement was decreased, and deposited sands became more laterally continuous. Armitage et al. (2009) developed a MTD surface-topography model containing a hierarchy of three fundamental tiers of upper surface relief defined by the maximum values of the horizontal (x) and the vertical (y) dimensions relative to local elevation. Each tier of surface relief is distinguished from the next by approximately one order of magnitude

difference in both of the two dimensions. Tier 1 MTD surface topography is up to several meters in magnitude in the x and y dimensions. Tier 2 MTD surface topography is 10 meters to several tens of meters in the x dimension and several meters to several tens of meters in the y dimension. Tier 3 MTD surface topography is several hundred meters in both the x and y dimensions. Local pockets of ponded sandstone created by Tier 1 MTD surface topography and discrete packages of sandstone laterally compartmentalized by Tier 2 MTD surface topography are commonly seen in Wind Cave member turbidite deposits on top of the upper megabreccia.

Conclusions

The Fish Creek-Vallecito Basin, part of the larger Salton Trough region of southern California and part of the original Gulf of California before dextral movement on the San Andreas Fault, contains a late Miocene to Pliocene stratigraphic section that records the opening of the rift basin, marine flooding by the Gulf of California, and the arrival of the spectacular ~500 – 800 m high sedimentary prism of the advancing Colorado River deltaic margin. Multiple times during the earliest filling of the basin the unstable alluvial slopes and basin walls collapsed to form fast, far travelling megabreccia landslides or debris flows. The mass transport deposits and other rapid lateral and vertical facies changes are evidence for unstable slopes and variable paleotopography that influenced turbidite deposition in a tectonically active extensional rift basin.

The Fish Creek-Vallecito Basin mass transport deposits have been interpreted as both subaerial and subaqueous debris flows formed at a time when marine water first appeared in the already low-lying basin. The lower Split Mountain Group debris flow megabreccia was deposited subaerially over extensive alluvial fans. Continued extensional subsidence or a catastrophic breaching of the basin walls then led to rapid marine incursion, such that the lower debris flow was immediately and conformably overlain by gypsum, mudstones, and coarse-grained Lycium member turbidites of the Imperial Group. The subaqueous upper debris flow severely deforms, scours, and truncates the underlying Lycium turbidites, and profoundly impacts the routing and deposition of the overlying Wind Caves member turbidites.

Mass transport deposits represent a significant component of modern and ancient deep-water depositional systems. However, geophysical data lack the resolution needed to identify meso-scale (meters to tens of meters) interactions between mass transport

deposits and the underlying and overlying sediment. The rift basin sedimentary deposits of the Fish Creek – Vallecito Basin contain extensive outcrops of subaerial and subaqueous debris flows and coarse-grained turbidites that provide an opportunity to examine the variability related to debris flow emplacement.

This study has shown that debris flow erosion and deformation of underlying sediment can be significant and extensive at a scale below the resolution of seismic-reflectivity data. Paleobathymetry on an irregular debris flow top surface impacts sediment routing and storage, and commonly acts as turbidity current conduits and locations favorable to the ponding of turbidity current deposits. Pinch-out of turbidite beds against bathymetric highs as well as the significant basal scouring of underlying sands by debris flows can significantly impact the lateral continuity of reservoir-quality sandstone deposits. The degree of erosion and deformation of underlying turbidites by a debris flow may be related to debris flow confinement and thickness as well as the characteristics of the turbidites over which it flows. The Fish Creek – Vallecito mass transport deposits are similar to other described debris flow – turbidite interactions, both from outcrop and geophysical data, and can be used as outcrop analogs to deep-water subsurface systems.

The basin also presents the opportunity to study in greater detail the unique sturzstrom megabreccia deposits. Thin section analysis of micro-scale fabrics suggests that shear was widely distributed and not confined to a thin basal zone, which has implications for proposed emplacement mechanism hypotheses that attempt to explain their high flow velocities, long run-out distances, and intense comminution.

References

Abbott, P.L., 1996. Why Sturzstroms? In: Abbott, P.L., Seymour, D.C. (Eds.), Sturzstroms and Detachment Faults, Anza-Borrego Desert State Park, California. Santa Ana, California, South Coast Geological Society, pp. 149-163.

Abbott, P.L., Kerr, D.R., Borron, S.E., Washburn, J.L., Rightmer, D.A., 2002. Neogene sturzstrom deposits, Split Mountain area, Anza-Borrego Desert State Park, California. In: Evans, S.G., DeGraff, J.V. (Eds.), Catastrophic Landslides: Effects, Occurrence, and Mechanisms. Geol. Soc. Am., Rev. Eng. Geol. 15, pp. 379-400.

Armitage, D.A., Romans, B.W., Covault, J.A., Graham, S.A., 2009. The Influence of Mass-Transport-Deposit Surface Topography on the Evolution of Turbidite Architecture: The Sierra Contreras, Tres Pasos Formation (Cretaceous), Southern Chile. J. Sed. Res. 79, 287-301.

Axen, G.J., Fletcher, J.M., 1998. Late Miocene–Pleistocene extensional faulting, northern Gulf of California, Mexico and Salton Trough, California. Int. Geol. Rev. 40, 217–244.

Bagnold, R.A., 1954. Experiments on a gravity-free dispersion of large solid spheres in a Newton fluid under shear. Proc. Royal Soc. Lond. A: Mathematical, Physical and Engineering Sciences 225, 49-63.

Bagnold, R.A., 1956. The flow of cohesionless grains in fluids. Proc. Royal Soc. Lond. A: Mathematical, Physical and Engineering Sciences 249, 235-297.

Bateman, S., (2015). Earliest turbidites emplacement (6.3-5.6 Ma) into the Miocene Gulf of California (Fish Creek – Vallecito Basin). M.S. Thesis, Austin, Texas, The University of Texas at Austin.

Bowman, E.T., Take, W.A., Rait, K.L., Hann, C., 2012. Physical models of rock avalanche spreading behaviour with dynamic fragmentation. Can. Geotech. J. 49, 460-476.

Butler, R.W.H., McCaffrey, W.D., 2010. Structural evolution and sediment entrainment in mass-transport complexes: outcrop studies from Italy. J. Geol. Soc. Lond. 167, 617-631.

Callot, P., Sempere, T., Odonne, F., Robert, E, 2008a. Giant submarine collapse of a carbonate platform at the Turonian–Coniacian transition: the Ayabacas Formation, southern Peru. Basin Res. 20 (3), 333-357.

Callot, P., Odonne, F., Sempere, T., 2008b. Liquification and soft-sediment deformation in a limestone megabreccia: the Ayabacas giant collapse, Cretaceous, southern Peru. Sediment. Geol. 212 (1), 49-69.

Campbell, C.S., Cleary, P.W., Hopkins, M., 1995. Large-scale landslide simulations: global deformation, velocities and basal friction. J. Geophys. Res. 100, 8267–8273.

Cassiliano, M.J., 1999. Biostratigraphy of Blancan and Irvingtonian mammals in the Fish Creek–Vallecito section, southern California, and a review of the Blancan-Irvingtonian boundary. J. Vertebr. Paleontol. 19, 169–186.

Cloos, M.E., 2014. Detrital zircon U-Pb and (U-Th)/He geo-thermochronometry and submarine turbidite fan development in the Mio-Pliocene Gulf of California, Fish Creek-Vallecito Basin, southern California. M.S. Thesis, Austin, Texas, The University of Texas at Austin.

Crosta, G.B., Frattini, P., Fusi, N., 2007. Fragmentation in the Val Pola rock avalanche, Italian Alps. J. Geophys. Res. 112, F01006.

Cruden, D.M., Hungr, O., 1986. The debris of the Frank Slide and theories of rockslide-avalanche mobility. Can. J. Earth Sci. 23, 425-432.

Dakin, N., Pickering, K.T., Mohrig, D., Bayliss, N.J., 2013. Channel-like features created by erosive submarine debris flows: Field evidence from the Middle Eocene Ainsa Basin, Spanish Pyrenees. Mar. Pet. Geol. 41, 62-71.

Davies, T.R., 1982. Spreading of Rock Avalanche Debris by Mechanical Fluidization. Rock Mech. 15, 9-24.

Davies, T.R., McSaveney, M.J., 1999. Runout of dry granular avalanches. Can. Geotech. J. 36, 313–320.

Davies, T.R., McSaveney, M.J., 2009. The role of rock fragmentation in the motion of large landslides. Eng. Geol. 109, 67-79.

Dean, M.A., 1996. Neogene Fish Creek Gypsum and Associated Stratigraphy and Paleontology, Southwestern Salton Trough, California. In: Abbott, P.L., Seymour, D.C. (Eds.), Sturzstroms and Detachment Faults, Anza-Borrego Desert State Park, California. Santa Ana, California, South Coast Geological Society, pp. 149-163.

De Blasio, F.V., 2008. Production of frictional heat and hot vapour in a model of self-lubricating landslides. Rock Mech. Rock Eng. 41, 219-226.

De Blasio, F.V., Elverhøi, A., 2008. A model for frictional melt production beneath large rock avalanches. J. Geophys. Res. 113, F02014.

Dorsey, R.J., Fluette, A., McDougall, K., Housen, B., Janecke, S.U., Axen, G.J., Shirvell, C.R., 2007. Chronology of Miocene–Pliocene deposits at Split Mountain Gorge, Southern California: A record of regional tectonics and Colorado River evolution. Geol. 35 (1), 57-60.

Dorsey, R.J., Housen, B.A., Janecke, S.U., Fanning, C.M., Spears, A.L.F., 2011. Stratigraphic record of basin development within the San Andreas fault system:

Late Cenozoic Fish Creek –Vallecito basin, southern California. Geol. Soc. Am. Bull. 123 (5-6), 771-793.

Erismann, T. H., 1979. Mechanisms of large landslides. Rock Mech. 12 (1), 15-46.

Festa, A., Pini, G.A., Dilek, Y., Codegone, G., 2010a. Mélanges and mélange-forming processes: a historical overview and new concepts. In: Dilek, Y. (Ed.), Alpine Concept in Geology. Int. Geol. Rev. 52 (10–12), pp. 1040–1105.

Festa, A., Pini, G.A., Dilek, Y., Codegone, G., Vezzani, L., Ghisetti, F., Lucente, C.C., Ogata, K., 2010b. Peri-Adriatic mélanges and their evolution in the Tethyan realm. In: Dilek, Y. (Ed.), Eastern Mediterranean Geodynamics (Part II). Int. Geol. Rev. 52 (4–6), pp. 369–406.

Festa, A., Dilek, Y., Pini, G.A., Codegone, G., Ogata, K., 2012. Mechanisms and processes of stratal disruption and mixing in the development of mélanges and broken formations: redefining and classifying mélanges. Tectonophysics 568–569, 7–24.

Fisher, R.V., 1971. Features of coarse-grained, high-concentration fluids and their deposits. J. Sed. Res. 41 (4), 916-927.

Goguel, J., 1978. Scale-dependent rockslides mechanisms, with emphasis on the role of pore fluid vaporization. In: Voight, B. (Ed.), Rockslides and Avalanches. 1. Natural Phenomena. Elsevier, Amsterdam, pp. 693–705.

Habib, P., 1975. Production of gaseous pore pressure during rock slides. Rock Mech. Rock Eng. 7 (4), 193-197.

Hackbarth, C.J., Shew, R.D., 1994. Morphology and stratigraphy of a mid-Pleistocene turbidite leveed channel from seismic, core and log data, northeastern Gulf of Mexico. In: Submarine Fans and Turbidite Systems, SEPM, Gulf Coast Section, 15th Annual Research Conference, pp. 127-133.

Hampton, M.A., 1975. Competence of fine-grained debris flows. J. Sed. Res. 45 (4), 834-844.

Hampton, M.A., 1979. Buoyancy in debris flows. J. Sed. Res. 49 (3), 753-758.

Heuberger, H., Masch, L., Preuss, E., Schröcker, A., 1984. Quaternary Landslides and Rock Fusion in Central Nepal and in the Tyrolean Alps. Mt. Res. Dev. 4 (4), 345-362.

Hewitt, K., 1999. Quaternary Moraines vs Catastrophic Rock Avalanches in the Karakoram Himalaya, Northern Pakistan. Quat. Res. 51, 220-237.

Hsü, K.J., 1975. Catastrophic Debris Streams (Sturzstroms) Generated by Rockfalls. Geol. Soc. Am. Bull. 86, 129-140.

Hungr, O., 2006. Rock avalanche occurrence, process and modelling. In: Evans S.G., Mugnozza, G.S., Strom, A., Hermanns, R.L. (Eds.), Landslides from Massive Rock Slope Failure. Springer Netherlands, pp. 243-266.

Hungr, O., Evans, S.G., 2004. Entrainment of debris in rock avalanches: An analysis of a long run-out mechanism. GSA Bull. 116 (9/10), 1240-1252.

Johannessen, E.P., Steel, R.J., 2005. Shelf-margin clinoforms and prediction of deepwater sands. Basin Res., 17 (4), 521-550.

Johnson, B., 1978. Blackhawk landslide, California, U.S.A. In: Voight, B. (Ed.), Rockslides and Avalanches. 1. Natural Phenomena. Elsevier, Amsterdam, pp. 481–504.

Kastens, K.A., Shor, A.N., 1985. Depositional processes of a meandering channel on Mississippi Fan. AAPG Bull., 69 (2), 190-202.

Kerr, D.R., 1982. Early Neogene Continental Sedimentation, Western Salton Trough, California. M.S. Thesis, San Diego, California, San Diego State University.

Kerr, D.R., 1984. Early Neogene Continental Sedimentation in the Vallecito and Fish Creek Mountains, Western Salton Trough, California. Sediment. Geol. 38, 217-246.

Kerr, D.R., Abbott, P.L., 1996. Miocene subaerial sturzstrom deposits, Split Mountain, Anza-Borrego Desert State Park. In: Abbott, P.L., Seymour, D.C. (Eds.), Sturzstroms and Detachment Faults, Anza-Borrego Desert State Park, California. Santa Ana, California, South Coast Geological Society, pp. 149-163.

Kerr, D.R., Kidwell, S.M., 1991. Late Cenozoic sedimentation and tectonics, western Salton Trough, California. In: Walawender, M.J., Hanan, B.B. (Eds.), Geological Excursions in Southern California and Mexico. San Diego, California, Department of Geological Sciences, San Diego State University, pp. 397–416.

Legros, F., 2002. The mobility of long-runout landslides. Eng. Geol. 63, 301-331.

Legros, F., Cantagrel, J-M., Devouard, B., 2000. Pseudotachylyte (Frictionite) at the Base of the Arequipa Volcanic Landslide Deposit (Peru): Implications for Emplacement Mechanisms. J. Geol. 108 (5), 601-611.

Lucente, C.C., Pini, G.A., 2003. Anatomy and emplacement mechanism of a large submarine slide within a Miocene foredeep in the Northern Appennines, Italy: a field perspective. Am. J. Sci. 303, 565–602.

Masch, L., Wenk, H.R., Preuss, E., 1985. Electron Microscopy Study of Hyalomylonites – Evidence for Frictional Melting in Landslides. Tectonophys. 115, 131-160.

McDougall, K., 2008. Late Neogene marine incursions and the ancestral Gulf of California. Geol. Soc. Am. Spec. Pap. 439, 355-373.

McGilvery, T.A., Cook. D.L., 2003. The influence of local gradients on accommodation space and linked depositional elements across a stepped slope profile, offshore Brunei. In: Shelf margin deltas and linked down slope petroleum systems: Global significance and future exploration potential. Gulf Coast Section SEPM 23rd Annual Research Conference, pp. 387-419.

Melosh, H.J., 1979. Acoustic fluidization - a new geologic process? J. Geophys. Res. 84, 7513–7520.

Middleton, G.V., Hampton, M.A., 1976. Subaqueous sediment transport and deposition by sediment gravity flows. In: Stanley, D.J., Swift, D.J.P. (Eds.), Marine Sediment Transport and Environmental Management. Wiley, New York, pp. 197-218.

Moscardelli, L., Wood, L., Mann, P., 2006. Mass-transport complexes and associated processes in the offshore area of Trinidad and Venezuela. AAPG Bull. 90 (7), 1059-1088.

Mulder, T., Etienne, S., 2014. Discovery of an outcropping Mass Transport Deposit (MTD) in the Palaeogene subalpine synclines of southeastern France: Implications on flexural sub-basin deformation. C. R. Geosci. 346, 37-44.

Nemec, W., Steel, R.J., 1984. Alluvial and coastal conglomerates: their significant features and some comments on gravelly mass-flow deposits. In: Koster, E.H., Steel R.J. (Eds.), Sedimentology of Gravels and Conglomerates — Memoir 10. Canadian Society of Petroleum Geologists, Calgary, Alberta, Canada, pp. 1-31.

Ogata, K., Mountjoy, J.J., Pini, G.A., Festa, A., Tinterri, R., 2014a. Shear zone liquefaction in mass transport deposit emplacement: A multi-scale integration of seismic reflection and outcrop data. Mar. Geol. 356, 50-64.

Ogata, K., Pogačnik, Ž., Pini, G.A., Tunis, G., Festa, A., Camerlenghi, A., Rebesco, M., 2014b. The carbonate mass transport deposits of the Paleogene Friuli Basin (Italy/Slovenia): Internal anatomy and inferred genetic processes. Mar. Geol. 356, 88-110.

Olafiranye, K., Jackson, C. A.-L., Hodgson, D.M., 2013. The role of tectonics and mass-transport complex emplacement on upper slope stratigraphic evolution: A 3D seismic case study from offshore Angola. Mar. Pet. Geol. 44, 196-216.

Ortiz-Karpf, A., Hodgson, D.M., McCaffrey, W.D., 2015. The role of mass-transport complexes in controlling channel avulsion and the subsequent sediment dispersal patterns on an active margin: the Magdalena Fan, offshore Colombia. Mar. Pet. Geol.

Pickering, K.T., Corregidor, J., 2000. 3D reservoir scale study of Eocene confined submarine fans, South Central Spanish Pyrenees. In: Weimer, P., Slatt, R.M., Coleman, J., Rosen, N.C., Nelson, H., Bouma, A.H., Styzen, M.J., Lawrence, D.T. (Eds.), Gulf Coast Section Society of Economic Paleontologists and

Mineralogists Foundation 20th Annual Bob F. Perkins Research Conference. Deep water reservoirs of the world, pp. 776–781.

Pickering, K.T., Corregidor, J., 2005. Mass transport complexes and tectonic control on confined basin-floor submarine fans, Middle Eocene, south Spanish Pyrenees. In: Hodgson, D.M., Flint, S.S. (Eds.), Submarine Slope Systems: Processes and Products. Geol. Soc. Lond. Spec. Publ. 244, pp. 51-74.

Posamentier, H.W., Kolla, V., 2003. Seismic geomorphology and stratigraphy of depositional elements in deep-water settings. J. Sediment. Res. 73, 367–388.

Ruisaard, C.I., 1979. Stratigraphy of the Miocene Alverson Formation, Imperial County, California. M.S. Thesis, San Diego, California, San Diego State University.

Shirvell, C., 2006. Pliocene Exhumation along the West Salton Detachment System and Tectonic Evolution of the Fish Creek–Vallecito Supradetachment Basin, Salton Trough, Southern California. M.S. Thesis, Los Angeles, University of California.

Shor, A.N., Piper, D.J., 1989. A large late Pleistocene blocky debris flow on the central Scotian Slope. Geo-Marine Lett. 9 (3), 153-160.

Shreve, R.L., 1968. The Blackhawk Landslide. Geol. Soc. Am. Spec. Pap. 108, 1-48.

Shultz, M.R., Fildani, A., Cope, T.D., Graham, S.A., 2005. Deposition and stratigraphic architecture of an outcropping ancient slope system: Tres Pasos Formation, Magallanes Basin, southern Chile. In Hodgson, D.M., Flint, S.S. (Eds.), Submarine Slope Systems: Processes and Products. Geol. Soc. Lond., Special Publication 244, pp. 27–50.

Spray, J., 2010. Frictional Melting Processes in Planetary Materials: From Hypervelocity Impact to Earthquakes. Annu. Rev. Earth Planet. Sci. 38, 221-254.

Steel, R.J., Olsen, T., 2002. Clinoforms, clinoform trajectories and deepwater sands. In: Armentrout, J. (Ed.), Sequence Stratigraphic Models for Exploration and Production: Evolving Methodology, Emerging Models and Application Histories. Gulf Coast Section SEPM 22nd Annual Research Conference, pp. 367-381.

Straub, S., 2001. Bagnold revisited; implications for the rapid motion of high concentration sediment flows. In: McCaffrey W.D., Kneller, B.C., Peakall, J. (Eds.), Particulate Gravity Currents. Int. Assoc. Sedimentol. Special Publication 31, pp. 91-109.

Takagi, H., Arita, K., Danhara, T., Iwano, H., 2007. Timing of the Tsergo Ri landslide, Langtang Himal, determined by fission-track dating of pseudotachylyte. J. Asian Earth Sci. 29, 466-472.

Voight, B., Sousa, J., 1994. Lessons from Ontake-san: a comparative analysis of debris avalanche dynamics. Eng. Geol. 38, 261 – 297.

Walker, R.G., (1975). Generalized facies models for resedimented conglomerates of turbidite association. Geol. Soc. Am. Bull. 86 (6), 737-748.

Wassmer, P., Schneider, J.L., Pollet, N., Schmitter-Voirin, C., 2004. Effects of the internal structure of a rock–avalanche dam on the drainage mechanism of its impoundment, Flims sturzstrom and Ilanz paleo-lake, Swiss Alps. Geomorphol. 61, 3-17.

Weidinger, J.T., Korup, O., Munack, H., Altenberger, U., Dunning, S.A., Tippelt, G., Lottermoser, W., 2014. Giant rockslides from the inside. Earth and Planet. Sci. Lett. 389, 62-73.

Weimer, P., Shipp, C., 2004. Mass Transport Complex: Musing on Past Uses and Suggestions for Future Directions. Offshore Technology Conference 2004.

Winker, C.D., 1987. Neogene Stratigraphy of the Fish Creek – Vallecito Section, Southern California: Implications for Early History of the Northern Gulf of California and Colorado Delta. Ph.D. Dissertation, Tucson, Arizona, The University of Arizona.

Winker, C.D., Kidwell, S.M., 1986. Paleocurrent evidence for lateral displacement of the Pliocene Colorado River delta by the San Andreas fault system, southeastern California. Geol. 14, 788-791.

Winker, C.D., Kidwell, S.M., 1996. Stratigraphy of a Marine Rift Basin: Neogene of the Western Salton Trough, California. In: Abbott, P.L., Cooper, J.D., (Eds.), Field Conference Guide 1996. Pacific Section A.A.P.G., GB 73. Pacific Section S.E.P.M., Book 80, pp. 295-336.

Woodard, G.D., 1963. The Cenozoic Succession of the West Colorado Desert, San Diego and Imperial Counties, Southern California. Ph.D. Thesis, Berkeley, University of California.

Wynn, R.B., Masson, D.G., Stow, D.A.V., Weaver, P.P.E., 2000. The Northwest African slope apron: a modern analogue for deep-water systems with complex seafloor topography. Mar. Pet. Geol. 17, 253-265.